REFERENCE ONLY

UNIVERSITY OF LONDON THESIS

Degree PhD Year 2005 Name of Author LICHTWARK G.A.

COPYRIGHT

This is a thesis accepted for a Higher Degree of the University of London. It is an unpublished typescript and the copyright is held by the author. All persons consulting the thesis must read and abide by the Copyright Declaration below.

COPYRIGHT DECLARATION

I recognise that the copyright of the above-described thesis rests with the author and that no quotation from it or information derived from it may be published without the prior written consent of the author.

LOANS

Theses may not be lent to individuals, but the Senate House Library may lend a copy to approved libraries within the United Kingdom, for consultation solely on the premises of those libraries. Application should be made to: Inter-Library Loans, Senate House Library, Senate House, Malet Street, London WC1E 7HU.

REPRODUCTION

University of London theses may not be reproduced without explicit written permission from the Senate House Library. Enquiries should be addressed to the Theses Section of the Library. Regulations concerning reproduction vary according to the date of acceptance of the thesis and are listed below as guidelines.

A. Before 1962. Permission granted only upon the prior written consent of the author. (The Senate House Library will provide addresses where possible).

B. 1962 - 1974. In many cases the author has agreed to permit copying upon completion of a Copyright Declaration.

C. 1975 - 1988. Most theses may be copied upon completion of a Copyright Declaration.

D. 1989 onwards. Most theses may be copied.

This thesis comes within category D.

☑ This copy has been deposited in the Library of UCL

☐ This copy has been deposited in the Senate House Library, Senate House, Malet Street, London WC1E 7HU.

The Role of Muscle Tendon Unit Elasticity in Real Life Activities

Glen Lichtwark

This thesis is submitted to the University of London in accordance with the requirements for the degree of Doctor of Philosophy

Structure and Motion Laboratory
Institute of Orthopaedics and Musculoskeletal Science
University College London
Royal National Orthopaedic Hospital
Brockley Hill
Stanmore, Middlesex, HA7 4LP

ProQuest LLC
789 East Eisenhower Parkway
P.O. Box 1346
Ann Arbor, MI 48106-1346

Abstract

The interaction of a muscle and associated tendon during dynamic activities such as locomotion is critical for both force production and economical movement. It is generally assumed that, under sub-maximal conditions, muscle activation patterns are optimised to achieve maximum efficiency of work. Here, I explore the interaction between the contractile component (CC) and the elastic tendinous tissue to understand the relationship between a muscle's power output and efficiency. In this thesis, I examine the interaction of the CE and the elastic tendinous tissue and its effect on power output and efficiency of muscle using both experimental and modelling techniques. In the first chapter, a model of muscle energetics is developed and validated against dynamic muscle contractions of different muscle types. I then used this model to explore how optimal muscle power and efficiency varies with different activation conditions, elastic properties and length change trajectories. The third and forth chapter presents experiments which explore ultrasound measurement techniques for determining the length changes and mechanical properties of the human *gastrocnemius medialis* (GM) muscle fibres and Achilles tendon (AT) respectively. I then used similar techniques to explore muscle-tendon unit (MTU) interaction during gait under different gait conditions. Specifically, I explore how GM power output and efficiency vary with different speeds and inclination and explore how variation in tendinous compliance might influence muscle efficiency. The results suggest that muscles remain highly efficient due to compliant tendons allowing muscle fibres to act at highly powerful and efficient velocities. However variation in power output and particularly muscle function affects the efficiency of muscle. Finally, I determined that the optimal value of tendon stiffness for maximum GM efficiency during walking and running is close to that determined experimentally.

Table of Contents

Table of Figures

Table of Tables

Acknowledgements

In undertaking a doctoral thesis, one also embarks on a journey to both create and absorb as much knowledge from both themselves and their peers. This I understood when my research began, however I did not realise that along with that great knowledge I would gain much more. I have found a passion for science; new life skills; new communication skills; patience; humility; but above all I have found great friendships. Over the course of my study I have met some amazing people, who have helped me no end, and whom I hope I can always call friends. I would like to specifically thank some of those here, whose help is greatly appreciated. My deepest thanks to the following people -

Family and friends. Without the close support and endless encouragement of my family and friends, this wouldn't have been possible. Studying in another country can be difficult at times, but the support I received from all of you, all over the world made all of the difference.

Staff and students at the Structure and Motion Laboratory, Royal Veterinary College. Particularly those whose early encouragement kept me here in the first place - Thomas Witte, Polly McGuigan and Jo Watson. I would also like to thank James Wakeling for his support and discussions in the later stages of my research work, which has both inspired and assisted me towards completion. Finally, I would also like to thank my PhD buddy, Renate Weller whose good humour, friendship and determination helped get me through. Good luck in the future to you all!

Staff at the Motion Analysis Laboratory, Royal National Orthopaedic Hospital. In particular, Tony Christopher and Roisin Delaney were forever gracious in offering

valuable assistance in both experimental work and discussions about the work. Also, I would like to thank Graham Nicholson from ACDS for his technical help. Kostas Bougoulias, a UCL masters student, must be thanked for his tireless help in data collection which forms the basis for Chapter 4.

I would also like to sincerely thank Chris Barclay (Griffith University, Australia), Nancy Curtin (Imperial College London, UK) and Roger Woledge (Kings College London, UK) for graciously providing data and contributing valuable information and advice for the preparation the papers published in the Journal of Experimental Biology and in Chapters 2 and 3 of this thesis.

Professor Roger Woledge, who gave up his time on request and not only assisted me in achieving a lot of the work that I have completed, but also taught me valuable lessons in science, critical and analytical thinking. Your assistance will never be forgotten.

The Royal National Orthopaedic Hospital Trust (RNOHT) and the British Council for financial support. Without it I'd probably be just another Aussie behind the bar.

Dr Alan Wilson. Whose support, encouragement, motivation and determination I could not do without. I came to your laboratory with little expectation, but I can guarantee you that your work has far exceeded anything I could have imagined. All the best in the future, and may our friendship continue on my departure.

Chapter 1: An introduction to the role of muscle-tendon unit elasticity in real-life activities.

Muscle power output vs efficiency: Contractile vs Elastic Elements

The mechanics and energetics of a muscle are often considered separately, although the two are inextricably linked. Muscles primary function is to produce the forces required for movement; a function which comes at the expense of energy. Therefore in considering the function of muscles during movement it is not only beneficial to understand how the forces are produced, but also how the energetic cost influences the production of this force.

A great deal of research in the past has been focussed on both the energetics and mechanics of muscle fibres; that is the contractile component of muscle tendon-unit. Relationships between force production and muscle fascicle length and velocity are well documented, as is the production of heat with respect to these variables (Fenn, 1924; Woledge *et al.*, 1985; Epstein and Herzog, 1998; Herzog *et al.*, 1992b; Hill, 1938; Gordon *et al.*, 1966). Under biological conditions it has been demonstrated that the patterns of shortening that a muscle undergoes are well matched to these properties and that muscles generally operate at velocities favourable to force production and energy expenditure (Wakeling and Johnston, 1998; Lutz and Rome, 1994; Askew and Marsh, 1997).

Recent advances in experimental techniques to measure muscle function have highlighted the importance of elastic structures in both power production and energetic savings. Elastic structures are those structures that undergo a length change in proportion to the applied force, such as tendon, aponeurosis, myosepta and even at the level of the contractile components themselves. Elastic structures can be of two functional forms; series of parallel. Series elastic structures act in series with the contractile component so

their lengths are additive, whereas parallel structures act in parallel so their force is additive. This is best described with the model first proposed by Hill (1938) (Fig 1.1). Different models are adopted at different times depending oln the architecture of the muscle and also on which level the analysis is being undertaken (at whole muscle level or muscle bundle level). Although elastic structures require energy input to be stretched, the majority of this energy is returned to the system once the tendon shortens again (Alexander, 2002; Alexander, 1988). Therefore the storage and return of energy is free from metabolic processes, unlike the contractile component of muscle which requires the consumption of metabolic energy to both produce work and absorb it.

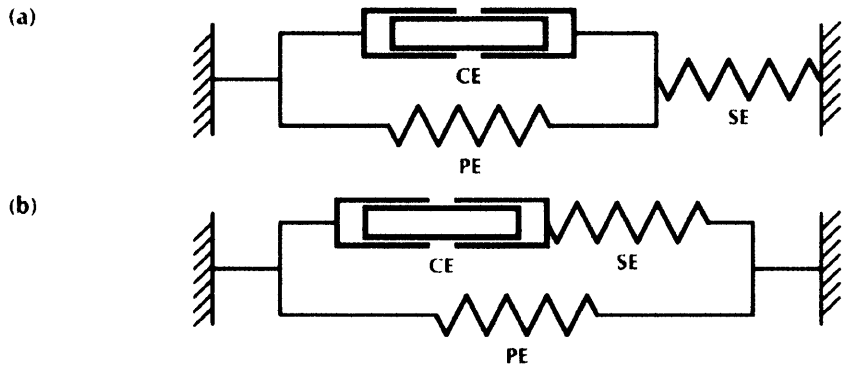

Figure 1.1

Hill type muscle model, demonstrating two alternative organisations of the contractile element (CE), series elastic (SE) element and the parallel elastic (PE) element. A) shows the PE element in parallel to only the CE, whilst it is parallel to both the CE and the SE element in B). Taken from Epstein and Herzog (1998).

The interaction between the contractile component (CC) and the series elastic element (SEE) is therefore key in understanding how the musculoskeletal system produces force and consumes energy during movement. The two components not only influence the others mechanical output, but they can also couple together to enhance or reduce a muscles efficiency. Due to large variation in muscle-tendon unit (MTU) architecture (Bennett *et al.*, 1986; Ker *et al.*, 1988), the relationship between power and

efficiency of a muscle under varying activation conditions is highly variable and has yet to be investigated thoroughly.

Investigating how muscles-tendon units with different properties operate during movements such as locomotion provides us with valuable information with regard to musculoskeletal development and control of movement. Particularly for terrestrial animals, there is a pressure bias towards producing the forces required for locomotion with a high efficiency. Here I present recent experimental findings that have investigated the action of both the CC and the SEE during locomotion in different species and under different conditions. I will also provide evidence that muscle activation is optimised to achieve high power outputs and efficiency.

When considering the mechanics and energetics of a muscle-tendon unit, different features of the muscle should be considered. These are the mechanical contractile properties, the activation/deactivation properties, the series elastic properties, the parallel elastic properties and the energetic cost of each of these. A brief review of each will follow.

Mechanics and energetics of muscle contractile components

Mechanisms of muscle contraction

The molecular mechanisms of muscular contraction can be explained by the cross-bridge theory as first suggested by Huxley (1957). Although this theory has undergone modifications, it essentially suggests that cross-bridges are formed from the thick filaments (myosin) onto the thin filaments (actin) which overlap each other along some length of the muscle sarcomere (see Fig 1.2). Force and movement occur when the cross-bridge heads rotate and pull the thin filament across the think filament towards the middle of the sarcomere. The energy required for this contraction is provided by the hydrolysis of adenosine tri-phosphate (ATP), where one molecule of ATP is split per cross-bridge

cycle. The exact mechanics of cross-bridge cycling within the sarcomere is still an area of extensive research and is under constant refinement; however it is generally the accepted theory of muscle contraction.

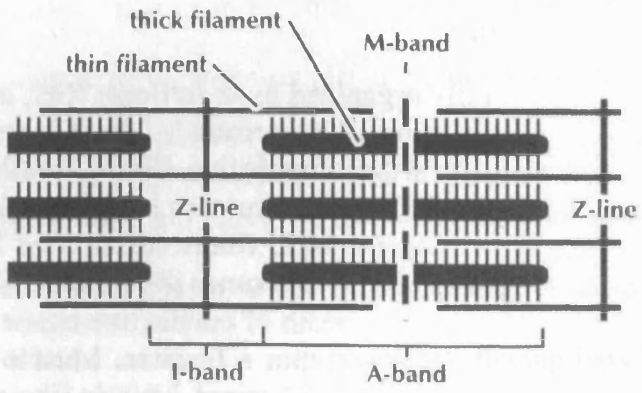

Figure 1.2

Illustration of the basic contractile unit of the muscle as described by Huxley's sliding filament theory. Taken from Epstein and Herzog (1998).

The properties of the CC that result from the mechanisms of contraction have been well documented since the early work of A.V. Hill (1938). Mechanically a muscle can be generally characterised by its force-length and force-velocity relationships. The energetic costs of contracting muscles have also been well documented for various muscle types and general relationships established between length and velocity (Hill, 1938; Fenn, 1924; Woledge *et al.*, 1985). However, consideration should also be given to confounding factors such as excitation-contraction coupling and history dependence of muscular contaction.

Force-length and force-velocity properties of muscle

The force-length and force-velocity properties of muscle are generally defined by the maximal isometric (fixed-end) force a muscle can exert. The maximal isometric force a muscle can exert is primarily a function of the physiological cross sectional area of the muscle, although there is range of physiological values of force that can be produced per

unit cross-sectional area (Epstein and Herzog, 1998). The force length relationship at the sarcomere level represents the amount of overlap of the thick to the thin filaments and has a plateau region which represents the optimal amount of overlap; when the maximum amount of possible cross-bridges can be bound (Gordon *et al.*, 1966) (Fig 1.3a). At the fascicle and whole muscle level, a similar plateu region exists which represents optimal muscle fascicle length (Herzog *et al.*, 1992a). Generally muscle operates around the plateau region of the force-length curve, so that when the joint is at the extremes of its range of motion the muscle is in either the ascending or descending limb of the relationship (Epstein and Herzog, 1998). Experimental finding have however found that the some muscles operate on either side of their plateau regions (Mai and Lieber, 1990), which may be linked to their functional task.

The maximum force a muscle can exert (relative to isometric) also decreases with shortening velocity. A muscle has a maximum shortening velocity, after which no force can be produced (V_{max}). This varies largely between fascicle types and animals, with values ranging from 1.6-24 muscle fascicle lengths per second, however the relationship between force and shortening velocity (relative to V_{max}) is relatively consistent across muscles (see Fig 1.3b). During stretch of muscle, a force greater than that achieved during isometric conditions is attained and this is also a function of the stretching speed. At high speeds of stretching the maximum force attained typically plateaus to around 1.8 times the isometric force in isolated muscle preparations (Fig 1.3b) (Edman *et al.*, 1978), but this value is often less in studies of whole human muscle during contraction (Westing *et al.*, 1990; Webber and Kriellaars, 1997; Ruiter *et al.*, 2000; Westing *et al.*, 1988). The force-velocity relationship of the CC of a muscle also dictates at which speed the optimal power output of the muscle can be achieved, as this is merely a function of force and

velocity. As a result, maximum power output of the CC is generally achieved somewhere around one-third of the maximum shortening velocity (Woledge *et al.*, 1985).

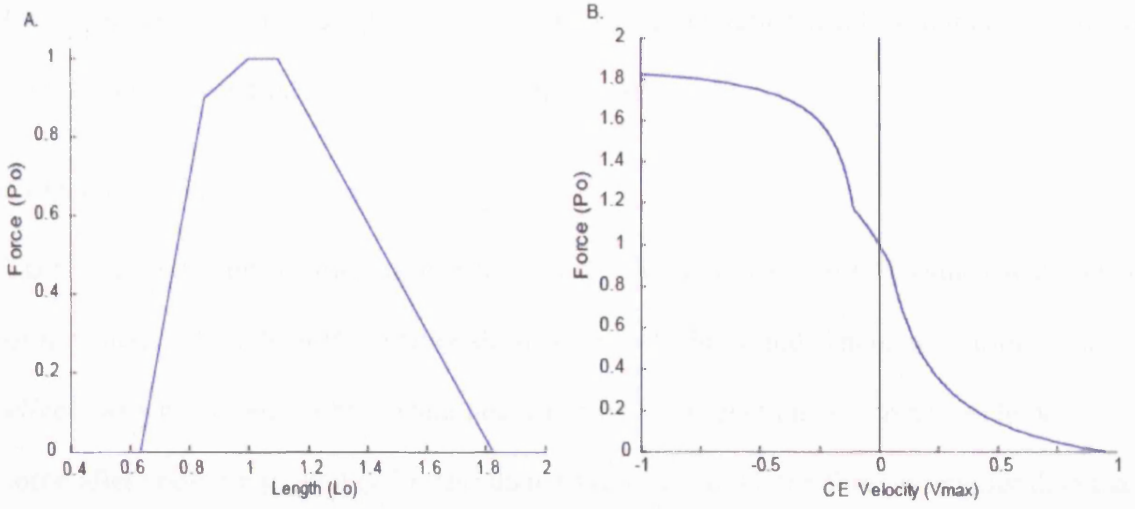

Figure 1.3

A. Example force-length relationship for a sarcomere relative to the optimal length (L_o). A similar relationship is evident in muscle fibres and whole muscles (adapted from Gordon *et al*, 1966). **B.** Example force-velocity relationship of muscle expressed as a function of maximum isometric force (P_o) and maximum shortening velocity (V_{max}) (adapted from Curtin *et al*, 1998).

Muscle Activation

For a muscle to achieve its maximum isometric state, full activation must be achieved. When a muscle is stimulated, calcium (Ca2+) is released from the sarcoplasmic reticulum and is allowed to bind to part of the myosin heads; troponin C. Once Ca2+ binds to troponin C, ATP is hydrolysed and the myosin head is allowed to rotate relative to the actin chain. However, full activation, when the rate of Ca2+ binding to troponin C is equal to the rate that it is leaving, is not achieved instantaneously. Instead there is an exponential rise in activation as the binding sites begin to get saturated (Curtin *et al.*, 1998). Once stimulation is stopped, the calcium is continued to be removed, however it is still allowed to bind to troponin until it is fully cleared, therefore there is a period after the completion of stimulation when force is still produced by the muscle. Therefore the

relationship between stimulation and activation (and hence force production) is complicated by the kinetics of activation. The relationship between the binding rate of Ca2+ and force production (which is effectively the activation level, or number of bound cross-bridges) was first characterised by Hill (1949).

Confounding factors to muscle contraction

There are some confounding factors to force production that aren't explained with either of the Huxley models or the relationships previously described. There are various history effects which can both enhance and potentiate force production. When a muscle develops force after shortening quickly (in less than 10 milliseconds), the force is smaller than that if the muscle were to only contract isometrically. This force depression is related to the speed of shortening (Abbot and Aubert, 1952; Sugi and Tsuchiya, 1988). In contrast, if a muscle is stretched, then the force after the stretch is greater than the isometric force at the same length (Abbot and Aubert, 1952). These history dependent effects of stretching and shortening are yet to be explained thoroughly, however they will have a small affect on a muscles performance during a stretch-shorten cycle because such abrupt changes in muscle length rarely happen in these movements.

Energetics

There is also an energetic cost of producing force that can be characterised by how the muscle is shortening and activating. There is an energetic cost associated with activating the muscle, producing force and also shortening the muscle. The minimum energetic cost for a 100% efficient muscle must equal the work done by a muscle (force x distance shortened). However, when a muscle contracts it also produces heat due to the chemical reactions producing the contraction. Therefore the total energetic cost is equal to the work plus the heat produced. By measuring the heat of contraction it has been found that

muscles not only produce heat when producing force, but produce heat at a greater rate when also shortening (Fenn, 1924). This phenomenon was first discovered in 1929 and has been termed the Fenn effect after the first person to describe it. The cost of activating a muscle, lengthening a muscle and producing forces at different lengths have previously been established for various muscle types and found to all effect energetic cost (Woledge *et al.*, 1985; Lou *et al.*, 1997). Muscle efficiency (work/total cost of work) has been found to range from 10 and 43% in various muscle types (Woledge *et al.*, 1985).

Mechanics and energetics of elastic structures

Mechanical properties of tendon

Elasticity mainly presides in connective tissues such as tendon and aponeurosis. These structures exhibit relatively linear force-length characteristics, whereby the force they produce is linearly proportional to the length change they experience. The elastic properties of tendinous material are due to the compounds that it is made of, primarily collagen and elastin (Alexander, 1988). When the tissue is lengthened it will not begin to exert a force until its length exceeds its 'slack' length. After it exceeds this slack length it will produce force in proportion to the length change. Initially this is not a linear relationship and the force increase is smaller for a given length change. The change in force for a given length change is the stiffness. This stiffness increases in a curvilinear fashion until a relatively linear stiffness prevails. If high enough forces are applied to stretch this elastic material, the length change becomes too great for the tissue which causes rupture; this is known as the failure point (Alexander, 1988).

The force-length properties of a tendon are highly dependent on the architecture of the tendon, however the material properties of tendon have been found to be relatively consistent across different types of tendons from many animal species (Pollock and Shadwick, 1994). The amount of stress (the ratio of force to material cross-sectional area)

a tendon exhibits per unit of strain (ratio of the length change to the slack length) is known as the Young's modulus. A broad survey of this relationship between different bird and mammalian species has demonstrated that there is little variation in tendon material (Bennett *et al.*, 1986; Pollock and Shadwick, 1994). However, other studies have shown that the Young's modulus of a tendon can indeed change with training in guinea fowl (Buchanan and Marsh, 2001). Studies on rat *extensor digitorum longus* have also shown the Young's modulus to be different along the length of both the tendon and the aponeurosis (Ettema and Huijing, 1989).

When a tendon or elastic tissue is loaded (i.e. force is applied to stretch it), then elastic energy is stored in the tendon, which is equivalent to the area under the force-length curve. On release of the tissue the elastic tissue is allowed to recoil, such that the length reduces back to the slack length and the force falls in a similar fashion to that in which it rose. However, some energy is lost on shortening as the force will often fall faster for a given length change at longer lengths than it would for the same length change whilst loading. This loss in energy is called the hysteresis and is basically the area within the force-length curve for a full load-unload cycle divided by the total area stored during loading. The value of hysteresis for elastic tissues such has tendon has been investigated in numerous species and found to vary quite a bit between species. A general value of between 7-30% is accepted for the hysteresis of tendon (Pollock and Shadwick, 1994; Maganaris and Paul, 2002; Alexander, 2002).

Parallel Elastic Structures

Although here I am focussing primarily on the interaction between the CC and the SEE, the structures that act in parallel to a muscle are also significant, particularly at long muscle lengths. It is thought that the primary role for parallel elastic structures is to prevent muscle damage when a muscle is stretched beyond lengths that it can contract

within, i.e. on the descending limb of the force-length relationship. This also helps prevents an inactive muscle from overstretching under external forces. These structures most likely incorporate the muscle fascia, however it is very difficult to quantify their material properties in isolation due to the complex architecture that they present. Nonetheless, the presence of passive force producing structures must be considered when investigating the power and efficiency capabilities of the MTU.

Variation in muscle-tendon unit architectural and mechanical properties

Muscle function

Although muscle (CC) and tendon (SEE) have individual properties that have been determined experimentally, their integrated function defines the role of any specific muscle. This interaction is highly dependent on the specific mechanical and architectural properties of each component. Various studies have investigated the relationships between tendon compliance and muscle architecture (which is a good indicator of the mechanical properties of muscle). These studies suggest that the architecture and mechanical properties of a MTU is highly correlated to its function. For instance muscles with short muscle fibres and long, compliant tendons are often distal limb muscles associated with load bearing during locomotion, or anti-gravity muscles (Biewener and Roberts, 2000). In contrast, muscles with long muscle fibres and short, stiff tendons are generally involved in positional or postural control (Rack and Ross, 1984; Rack *et al.*, 1983), and are also better suited for powerful accelerating movements (Ker *et al.*, 1988; Alexander, 1974; Biewener and Roberts, 2000).

Interaction between muscle and tendon

The relationship between the stiffness of a tendon and the force producing capabilities of the muscle contractile component is critical in the determining how a muscle and tendon

interact during contractions. When a muscle is held constant and stimulated fully, the muscle fibres are allowed to shorten in proportion to the length change of the SEE. The amount of stretch relative to the fascicle length has been coined the 'fixed-end compliance' (Roberts, 2002). Fixed-end compliance represents the capacity of a muscle for shortening, and high values of fixed-end compliance results in the muscle expending a lot of its shortening capacity on stretching the tendon rather than causing movements. A large range of fixed-end compliance has been found in different muscle types and animal species, ranging from 11-35% (Roberts, 2002). A study by Ker and colleagues (1988) found that muscle architecture relates highly to fixed-end compliance, with highly pennate muscles with short fibres often having the highest levels of fixed-end compliance.

Muscle-tendon unit interaction during movement: Optimisation of muscle-tendon unit elasticity

Measurement techniques

Simultaneous measures of both muscle fascicle length changes and tendon length have recently revealed the direct consequence that tendon and aponeurosis strain have on muscle mechanics. In fact, the ability to power movements is influenced as much by the elastic tissue behaviour as it is the contractile component behaviour. The muscle tendon unit interaction can be determined either directly or indirectly. An indirect method involves knowledge of the stiffness of the elastic component and force-length and force-velocity properties of the muscle. By measuring the force in the muscle (or estimating it from inverse dynamics) and having knowledge of the stiffness of the tendon, the length change of the tendon can be approximated (Roberts *et al.*, 1997). Subtracting this length from the length of the whole muscle allows the contractile component length change to be determined. However, this does not necessarily correspond to fascicle length change,

particularly in pennate muscles. Direct *in vivo* measurement of muscle fascicle length has recently become possible using an invasive method known as sonomicrometry or the non-invasive imaging technique of ultrasonography. Sonomicrometry involves embedding ultrasonic crystals into the ends of the muscle fibres and the distance between the two is calculated with knowledge of the speed of sound through the muscle (Biewener, 1998; Gabaldon *et al.*, 2004; Roberts *et al.*, 1997). Ultrasonography allows for direct visualisation of collagenous material, including the tendon, muscle fascia and collagenous material between muscle fibres (Narici, 1999; Narici *et al.*, 1996; Kawakami *et al.*, 1998).

Muscle-tendon interactions during movement

Measures of muscle-tendon unit interaction during movements have revealed much evidence for the important role of muscle elasticity. The compliance of tendons has been shown to expand the operating range of the muscle-tendon unit (Lieber *et al.*, 1992). During locomotion, the relatively compliant ankle extensor tendons of both cats and humans has been found to be uncoupled from the joint movements, where the muscle fibres have been found to shorten or act isometrically while the whole muscle-tendon unit lengthens (Griffiths, 1991; Fukunaga *et al.*, 2001; Fukunaga *et al.*, 2002). This is effectively due to the lengthening of the tendon under load. Additionally the high power outputs required at the ankle for jumping are only possible because of the rapid recoil of tendon which supplements the shortening speed of the muscle (Bobbert *et al.*, 1986).

A series of recent studies on running turkeys by Roberts and colleagues (Gabaldon *et al.*, 2004; Roberts and Scales, 2002; Roberts and Scales, 2004; Roberts *et al.*, 1997) has demonstrated the complex interaction between muscle fibres and compliant tendons under different gait conditions. Specifically, they have shown that the muscles can act in different manners depending on the overall task required. During flat running it was shown that the *lateral gastrocnemius* and *peroneous longus* muscles act relatively

isometrically during force production, which is thought to be highly efficiency (Taylor and Heglund, 1982; Roberts, 2002). However if the external work required by the body is increased or decreased, then the muscles are forced to produce work or absorb it (Gabaldon *et al.*, 2004). This is done by either actively shortening or lengthening the muscle whilst stretching the tendon and producing force. A similar finding has been found for accelerating and decelerating (Roberts and Scales, 2004). Hence the action of a muscle and its interaction with tendinous material can be linked to the required function of the body itself.

Elasticity and muscle activation

A muscle attached to a compliant tendon also requires a different activation pattern to that of a muscle with a stiff tendon to achieve whole muscle power (Ettema, 2001). In general, muscles with compliant tendons activate whilst a muscle is still lengthening (Biewener and Roberts, 2000; Alexander, 1988). In doing so, the contractile component produces a force as it begins to lengthen at a slower rate than the entire muscle tendon unit and hence the tendon stretches. This effectively stores elastic energy in the tendon which is recovered when the tendon overcomes any inertial forces which are acting to stretch the muscle and then shortens rapidly to move the load in the opposite direction. Recently, Ettema (2001) demonstrated that muscles with different tendon compliance could be equally efficient, however muscles with stiffer tendons must be activated during shortening whilst compliant tendons during lengthening of the stretch shorten cycle.

Adaptability and variation in tendon stiffness

Although animals of the same species can generally perform the same tasks, athletic performance varies depending on the activities performed by the individual and other factors such as age. As a consequence the demands on the musculoskeletal system vary

between individuals and muscle-tendons units may be able to adapt to different tasks. For instance strength training has long been known to increase the force power generating capacity of a muscle by increasing the size of the muscle. However, if there are changes in the force generating component of a muscle, then there may also be adaptations by the elastic components that attach to the muscle. Indeed, recently it has been shown that the stiffness of the vastus lateralis tendon in humans may vary depending on althetic performance, with endurance athletes having stiffer tendons than sprinters (Fukunaga *et al.*, 2000). Recent studies also suggest that prolonged bed rest, strength training, the aging process and gender difference may also vary tendon stiffness (Kubo *et al.*, 2000; Kubo *et al.*, 2003; Kubo *et al.*, 2005; Maganaris *et al.*, 2004; Reeves *et al.*, 2003). A training protocol has also been shown to vary the mechanical properties of the Achilles tendon in guinea fowl, where the elastic modulus increased with long-term exercise (Buchanan and Marsh, 2001). Therefore the function of the muscle highly dictates the structure and architecture of tendons.

Aims of Thesis

Muscle-tendon unit elasticity has been shown to be extremely important in producing powerful and efficient movement because it allow for rapid shortening of the muscle-tendon unit and also reduce the work required by the muscle contractile component. However, the relationship between power output and efficiency of a muscle is poorly understood, especially during real life movements. If a muscle is required to produce more power, is this detrimental to the muscles efficiency? Or is the efficiency of a muscle relatively constant? And how does the compliance of a tendon affect the efficiency of a muscle, or its power generating capacity?

To answer these questions it is necessary to first develop our knowledge of how power output and efficiency are affected by the interplay between the contractile component of a muscle and its attached elastic elements. Then it is necessary to examine how muscles interact with the tendinous material in real-life movements and how this changes under different conditions. Then we are able to speculate how changing the muscle-tendon architecture might influence power output and efficiency of muscle and how different roles of muscles will affect their performance.

In this thesis, I will first develop and test theoretical models of muscle contraction which incorporates an energetic component to account for muscle efficiency. Using this model I will explore the relationship between muscle power and efficiency during sinusoidal length changes with varying series elastic compliance and differing activation patterns. I will then investigate methods of measuring human muscle and tendon unit interaction and apply these methods to examine human locomotion under different conditions. I will then apply the models of muscle energetics to critically analyse the relationship between muscle power and efficiency under these different conditions.

Chapter 2: A modified Hill muscle model that predicts muscle power output and efficiency during sinusoidal length changes.

This chapter has been accepted as a paper in the following reference:

Lichtwark, G.A. and Wilson, A.M. (2005). Journal of Experimental Biology, Volume 208, pp2831-2843

All work has been written originally by Glen Lichtwark, with data contributions from Nancy Curtin, Roger Woledge and Chris Barclay as referenced in the chapter.

Introduction

The relationship between the power output of a muscle and the energetic cost of achieving this power output is critical to the locomotory potential of an animal. Power output of a muscle is modulated by changing activation parameters during cyclical length changes. These include the timing of activation (phase of activation) and the period of activation (duty cycle).

It is generally assumed that, under sub-maximal conditions, muscle activation patterns are optimised to achieve maximum efficiency of work. It has been shown in a range of experiments that both the power output and efficiency of a muscle depend on the frequency of oscillation, length change, duty cycle and phase of activation (Curtin and Woledge, 1996; Barclay, 1994; Ettema, 1996b). These studies have demonstrated that a muscle can produce power at a range of efficiencies. For instance, it has been shown that activating the muscle for a longer fraction of the total stretch shortening cycle tends to increase the power output of a muscle, but decrease the efficiency (Curtin and Woledge, 1996). This was due to the excess heat produced during the stretch of muscle. A relatively broad range of activation conditions and length change trajectories would achieve near optimal power output and optimal efficiency, but undertaking sufficient measurements to map these conditions is difficult experimentally.

The reason why the activation conditions for optimum power and optimum efficiency are different is poorly understood. However the series elastic element (SEE) must be accounted for when trying to understand muscle power output and efficiency. The SEE is critical as it can act as an energy storing mechanism, where energy stored during stretching of the SEE can be recovered later in the contraction (Biewener and Roberts, 2000; Alexander, 2002; Roberts, 2002; Fukunaga *et al.*, 2001). This means that the timecourse of the power output of the contractile element (CE) and of the muscle tendon unit (MTU) as a whole can differ during a contraction. It has been suggested that this series elasticity makes muscles more versatile under varying locomotor conditions. For instance, when a muscle accelerates an inertial load from rest, early in the movement the CE contraction velocity is higher than that of the MTU because the SEE is stretching; later in the movement the MTU velocity is higher than the CE velocity because the SEE is shortening (Galantis and Woledge, 2003). This should, theoretically, enable the CE to operate at a velocity concomitant with optimum efficiency or optimum power for more of the movement.

Previously the force and power output of muscle have been accurately predicted during contractions with brief tetani during sinusoidal length changes (Curtin *et al.*, 1998; Woledge, 1998). Cost of contraction can also be derived from Hill-type muscle models that incorporate the SEE (Ettema, 2001; Anderson and Pandy, 2001; Umberger *et al.*, 2003). This is achieved by fitting curves over experimentally derived relationships between energetic cost and power output during contraction. An appropriately validated model of this type makes it possible to explore and map the relationships between power and efficiency of muscle with varying duty cycle, phase of activation and frequency of oscillation, which is difficult to do experimentally. In this chapter:

1. I have adapted the model used by Curtin *et al* (1998) to predict both the power output and the cost of contracting muscles during sinusoidal length changes.
2. I have validated the model's predictions of muscle energy expenditure (heat + work) by comparing the output of my model to data of force output and heat expenditure during sinusoidal length changes with brief tetani from white dogfish muscle (*Scyliorhinus canicula*) and red mouse muscle (*Soleus, Mus domesticus*).
3. I have determined whether the model could account for the differences between optimum power and optimum efficiency conditions by comparison of the resultant power output and efficiency of these muscle types under experimental conditions to the model predictions.

Materials and Methods

Force-Time Predictions

The successful prediction of force production of the *Scyliorhinus canicula* white myotomal muscle during sinusoidal movements, based on a two element Hill-type model, was outlined by Curtin and colleagues (1998). That model used experimentally determined values for series elastic stiffness and force-velocity properties of the muscle and determined suitable activation parameters to produce an accurate representation of the time-course of muscle force production during sinusoidal and ramp length changes. The same relationships were utilised in this study, with the contractile force-velocity relationship and series elastic force-stiffness relationships (and the resultant force-length relationship) illustrated in Fig. 2.1. A detailed description of how these properties are determined is given in Curtin *et al* (1998). The normalised series elastic stiffness is defined with the following equation -

$$S = \left(\frac{SH + SL}{2}\right) + \left[\left(\frac{SH + SL}{2}\right) x \left(1 - e^{(-50x|P - Xo|)}\right) x \left(\frac{(P - Xo)}{|P - Xo|}\right)\right] \qquad (1)$$

where S is the relative SEE stiffness (relative to maximum isometric force divided by optimal muscle fascicle length, Po/Lo), SH is the upper limit to the relative stiffness, SL is the lower limit to the relative stiffness and Xo is the value of force relative to the maximum isometric force (Po) where the stiffness switches between the lower and upper stiffness in an exponential fashion and P is the instantaneous force produced by the muscle. The properties of the bundle of *Scyliorhinus canicula* white myotomal muscle fibres are listed in Table 2.1.

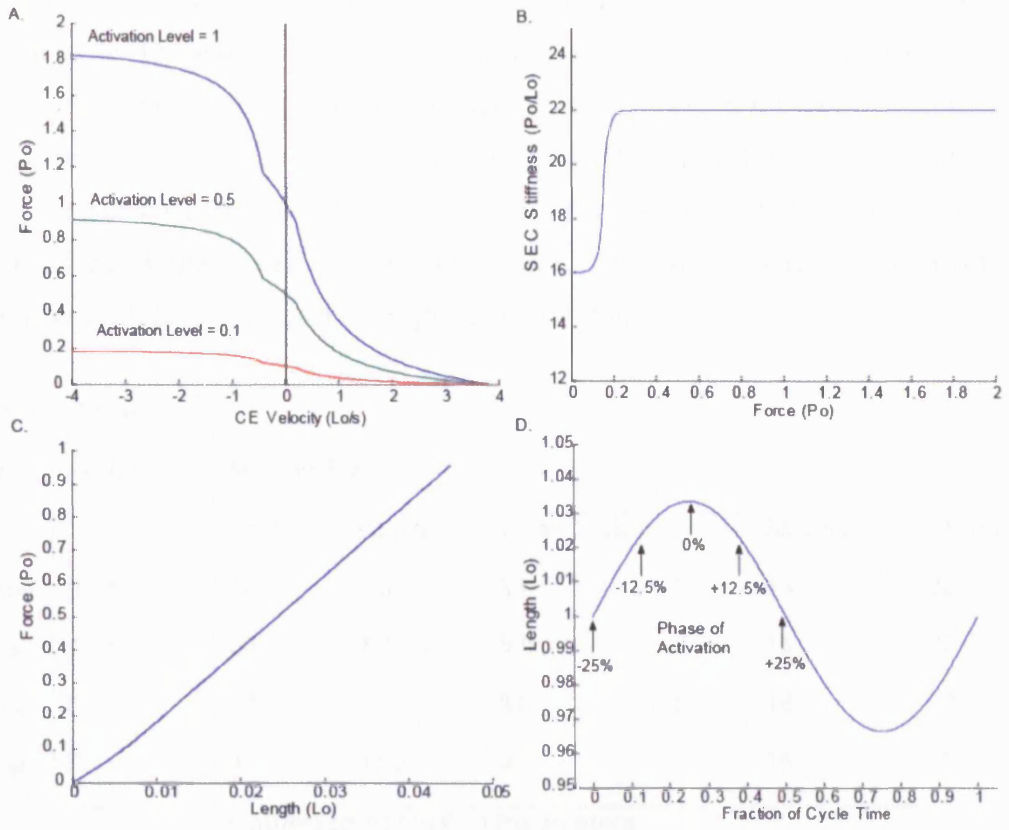

Figure 2.1

Properties of the muscle and definition of terms used in the model. These *Scyliorhinus canicula* white myotomal muscle properties were determined experimentally in the work of Curtin *et al* (1998). A) Force-velocity relationship of the contractile component at different levels of activation. The curve is essentially made up of three curves which include a curve for lengthening, a curve for shortening and these are joined by a curve around zero velocity which represents the 'Edman' region (Edman, 1979). In real-life this curve is more continuous. B) Variation in the SEE stiffness with force and C) the resulting force-length relationship of the SEE. Data has been extrapolated beyond Po (maximum isometric force) as it is not known at which point the elastic structures will yield. This model contains no hysteresis D) Phase of activation is defined as the time between the start of stimulation and the start of shortening expressed as a percentage of cycle duration and is demonstrated with respect to one cycle of length change (a negative value corresponds to activating the muscle whilst the muscle is stretching). Duty cycle is expressed as the fraction of the cycle that the muscle/model is stimulated.

Table 2.1

Properties of the dogfish (*Scyliorhinus canicula*) white myotomal muscle and mouse *soleus* muscle. These parameters are explained in equations 1-3 and 7. Activation parameters (τ_1, τ_2, K and n) were optimised to produce a best fit for the force-time data across a range of activation conditions at each cycle frequency. Po represents the maximum isometric force of the muscle and differs between cycle frequencies due to muscle fatigue in the experimental protocol (see Curtin and Woledge (1996) for details of this procedure). Lo is the optimal length to achieve Po.

Muscle Type	**Cycle Frequency**	**Muscle Properties**						
		Po (N)	*Lo (mm)*	*Vmax (Lo/s)*	*G*	*SL (Po/Lo)*	*SH (Po/Lo)*	*Xo*
Dogfish	0.71	47	7.3	3.8	4	16	22	0.15
Dogfish	1.25	60	7.3	3.8	4	16	22	0.15
Dogfish	5	50	7.3	3.8	4	16	22	0.15
Mouse	3*	48	11.5	4	4	16	22	0.15
		Optimised Activation Parameters						
		τ_1	τ_2		*K*		*n*	
Dogfish	0.71	0.035	0.1		0.16		2.2	
Dogfish	1.25	0.035	0.1		0.19		2.8	
Dogfish	5	0.035	0.1		0.25		6	
Mouse	3	0.045	0.045		0.22		2.69	

In the original model of Curtin and colleagues (1998), a block stimulation was applied, such that during the time period of a train of stimuli pulses the muscle activation level increased to a maximum of 1.0 with an exponential time constant of rise and fall (see Fig 2.2A). This stimulation level can be taken to represent the concentration of free calcium (Ca^{2+}) available to bind to troponin. This stimulation level is in turn related to the activation level, which represents the relative number of attached cross-bridges (*Act*). This relationship is also shown in Fig. 2.2A and is described by Curtin and colleagues (1998).

This model is not very accurate at predicting the time course of force rise and decline during twitch contractions or during deactivation of the muscle (after cessation of stimuli whilst force is still produced). Therefore a new model of stimulation was developed that was designed to respond to each individual stimulus rather than trains of stimuli. This stimulation model was essentially designed to model the rise and fall of activator transients (Ca^{2+} concentration) associated with an individual stimulus (twitch). This can be explained with the following equation -

$$\frac{da}{dt} = \frac{(1-a)}{\tau_1} \quad \text{(during individual stimulus)}$$

$$= \frac{-a}{\tau_2} \qquad \text{(otherwise)} \qquad (2)$$

where a is the activator concentration (Ca^{2+}) and the τ_1 and τ_2 respectively are the time constants dictating the time course of rise and fall of this activator. The individual stimulus can be thought of as a gate opening and allowing an influx of calcium. This gate opens only for a finite period of time, depending on the amplitude and time of the individual stimulus. This model is supported experimentally from measurements of free Ca^{2+} transients (Baylor and Hollingworth, 1998) whereby the activator concentration rises

faster than it falls. This relationship can be seen in Fig. 2.2B where the distinct peaks of activator concentration can be seen in the activator concentration during the twitch.

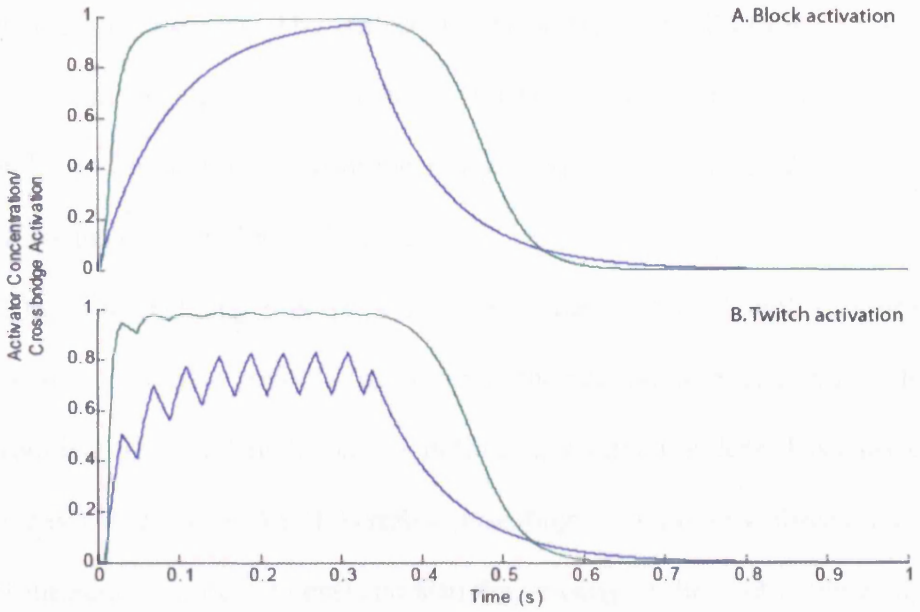

Figure 2.2

The rise and fall of the calcium transients (green) and the resulting activation level (blue) are shown for the original block model (A) and the twitch model (B). Twitches were applied to the model at a frequency of 22Hz, the same as in the experimental design, and each individual stimulus (twitch) lasted 7.5ms. The constants τ_1 (0.03), τ_2 (0.10), K (0.19) and n (2.8) were statically optimised to produce fits to respond to a single stimulus condition (Fig 2.3). A time constant, (d=0.015s), was also required to delay the onset of activation, as was seen in the experimental results. This time constant is thought to be due to the time taken for ATP turnover to proceed and for the calcium signalling to cause a calcium influx.

The crossbridge activation level was modelled in the same way as in Curtin *et al* (1998) where the activation level depends on the free concentration of the activator (a) according to the following equation:

$$Act = \frac{a^n}{\left(a^n + K^n\right)} \qquad (3)$$

where *Act* is the crossbridge activation level, *n* is the Hill coefficient for expressing the co-operativity of binding and K is the value of *a* at which 50% of the crossbridge activation sites are occupied. The time constants for rise and fall of the activator and the binding co-efficients used to calculate the relationship of the activator to the cross-bridge activation level were optimised to fit the response to a single stimulus trial from the raw data used in Curtin *et al* (1996) (Fig 2.3).

If the force-velocity properties of the CE and the force-length properties of the SEE are known, it is also possible to determine the activation level of a muscle fascicle bundle from its force and length changes in time. The activation level basically scales the force-velocity curve (Fig 2.1) and therefore providing one knows the force (and hence the stretch of the series elastic element) and also the velocity of the contractile component, it is possible to estimate the activation level; i.e. the percentage of the total maximum number of cross-bridges bound. This is shown numerically below –

$$Act = \frac{P}{P'} \qquad (4)$$

where P is the instantaneous force produced by the muscle and P' is maximum isometric force scaled for the instantaneous muscle velocity. Therefore an estimated activation level for each experimental condition could be calculated from raw experimental data.

Energetic Model

Efficiency is defined as the work produced by a mechanical system divided by the energetic cost of doing that work; this represents the mechanical efficiency (Ettema, 2001). Efficiency is therefore defined as:

$$Efficiency = \frac{Work}{Heat + Work} \qquad (5)$$

Here I define work as the integral of the force over the change in length of the whole MTU, and heat as the heat produced by the muscle. Positive work is defined as mechanical work produced in shortening the muscle complex, while stretching the muscle complex with an external force is seen as negative work, or work absorbed by the muscle as a whole. If the elongation occurs in the SEE this is elastic deformation and the energy can be recovered with 100% return (no hysteretic damping in this model). If the elongation occurs in the CE this work is converted to heat; this has a small metabolic cost in the model.

The rate of heat production from a muscle is a function (*f*) of crossbridge activation level (*Act*), velocity of the contractile component (V_{CE}), the time relative to the start of the train of stimulation (*t*) and the relative force produced (*P*). For the purpose of this study, where the length of the contractile element remains within the plateau of the force-length relation, length need not be taken into account. The rate of heat production can be further divided into four distinct functions of heat production which sum to give the overall heat rate -

$$\begin{aligned}\frac{dH}{dt} &= \frac{dH_M}{dt} + \frac{dH_L}{dt} + \frac{dH_S}{dt} + \frac{dH_T}{dt} \\ &= f(Act) + f(Act,t) + f(Act,Vcc) + f(P)\end{aligned} \qquad (6)$$

where, H_M has been termed the 'stable' heat, H_L the 'labile' heat, H_S the 'shortening' heat, H_T is the 'thermoelastic' heat (Aubert, 1956; Hill, 1938; Woledge, 1961).

The stable heat rate can be thought of as the minimum heat rate required to produce an isometric force at any given activation state. This includes the heat produced to activate the muscle (transportation of Ca^{2+} to activate muscle) and heat produced to maintain force production at the level of the cross-bridge. Numerous investigators working on a variety of skeletal muscles have found that this stable heat rate can be approximated by a constant in the range of (*a.b)*, the product of Hill's force-velocity

constants (Woledge *et al.*, 1985). When normalised for PoLo units and scaled for activation level:

$$\frac{dH_M}{dt} = Act\left(\frac{a}{P_0}.\frac{b}{V_{max}}.\frac{V_{max}}{L_o}\right)$$

$$= Act\left(\frac{V_{max}}{G^2}\right) \qquad (7)$$

where H_M is the stable heat, a and b are the constants for Hill's force-velocity relation, Po is the normalised maximum isometric force, Lo is the normalised optimum length of the muscle, V_{max} is the maximum shortening velocity and $G = Po/a = V_{max}/b$.

Over the time course of a contraction the heat rate is not completely stable. Aubert (1956) described a phenomenon he termed labile heat production, where if a muscle is contracted over a period of time the maintenance heat rate could fall from a rate of two to three times that of the stable heat rate in an exponentially decaying manner. He termed this extra heat the *labile heat.* Assuming that the stable heat rate is as in equation (5) and using constants to control the rate of decay of the labile heat rate (adapted from data of Linari *et al*,(2003)) we get the equation:

$$\frac{dH_L}{dt} = \left[\left(0.8 \times \frac{dH_M}{dt} \times e^{(-0.72*t)}\right) + \left(0.175 \times \frac{dH_M}{dt} \times e^{(-0.022*t)}\right)\right] \qquad (8)$$

where H_L is the labile heat, t is the time relative to the start of the train of stimulation.

'Shortening' heat rate can be thought of as the extra energetic cost associated with shortening muscle at any given activation level. Once again, numerous investigators have found a relationship between velocity of the contractile component and the heat rate and it has been approximated to a linear relationship with respect to velocity with a gradient of a (Woledge *et al.*, 1985). Normalising for PoLo:

$$\frac{dH_S}{dt} = Act\left(\frac{a}{P_0}.\frac{V_{cc}}{L_o}\right)$$
$$= Act\left(\frac{V_{cc}}{G}\right) \qquad \text{(when } V_{CE} > 0\text{, shortening)} \qquad (9)$$

where H_s is the shortening heat and V_{CE} is the contractile element velocity relative to Lo (units Lo/s). Like the maintenance heat rate, the effective shortening heat rate must also be scaled for activation as it is dependent on the number of bound crossbridges.

Energy output is reduced as a result of active lengthening. Studies by Lou *et al* (1997) have revealed that during an isometric contraction, at least 30% of the heat produced by muscle was the result of activating the muscle (i.e. calcium turnover). Therefore, during active lengthening, the minimum heat rate must be at least 30% of the stable heat rate. Studies by Linari and colleagues (2003) have also found that there is an exponential decay of the rate of energy production as the lengthening velocity increases. This heat rate must also be scaled for activation. During stretch, work done on the contractile component also becomes heat within a short period of time (Linari *et al.*, 2003). This model accounts for this energy. However, it ignores the small time delay. Therefore the heat rate during lengthening can be approximated with the following equation –

$$\frac{dH}{dt} = 0.3\left(\frac{dH_M}{dt}\right) + 0.7\left(\frac{dH_M}{dt}.e^{-8\left(\frac{P}{Act}-1\right)}\right) + P.V_{cc} \qquad \text{(when } V_{CE} < 0\text{, lengthening)} \quad (10)$$

One further factor that is not associated with the contractile component also contributes to the rate of heat production. This is the thermoelastic effect, which causes heat to be absorbed by muscle. This is proportional to the rate of force production and has been characterised by Woledge (1961) with the following relationship:

$$\frac{dH_T}{dt} = -0.014.\frac{dP}{dt} \qquad (11)$$

where H_T is the thermoelastic heat.

The above model of heat expenditure during dynamic contraction can therefore be applied providing the following parameters are known: force; length of contractile component; activation level; Vmax and G. Using experimental measurement of the force output and assuming that the stiffness of the SEE is known, it is possible to calculate the length (and velocity) of the SEE and the CE as follows

$$L_{CE} = L_{MTC} - L_{SEE}$$
$$= L_{MTC} - \left(\frac{P}{S}\right) \qquad (12)$$

where L_{CE} is the length of the CE, L_{MTU} is the length of the MTU, L_{SEE} is the length of the SEE, P normalised force and S is the relative stiffness of the SEE at that force. Therefore, by extracting these data from the experimental results and by predicting the activation level as in equation 4, it is possible to apply the model to experimental results to estimate energetic output.

Comparison to Experimental Data and Analysis

Raw data from the results reported by Curtin and Woledge (1996) was compared to the predicted force and energy outputs (heat + work) with respect to time (Personal communication, Curtin and Woledge, 2003). A subset of varying duty cycles, stimulus phases and frequencies (0.71, 1.25 and 5Hz) of sinusoidal MTU length changes were chosen to compare to the model. The activation parameters (τ_1, τ_2, K and n) were first optimised to minimise the sum of the force differences between the model and the experimental results at each time point for one individual condition (Frequency = 1.25, Duty Cycle = 0.121, Stimulus Phase = 3, from the raw data of Curtin and Woledge, 1996) using the Nelder-Mead simplex (direct search) method (Matlab, Mathworks Inc, Natick, MA, USA). The length change, force, energetic output and activation level were then compared between the model and the experimental results. An estimate of the activation

level was made from the experimental data using equation 4 and an estimate of the CE velocity was made from equation 12. These were input into the energetic model along with the experimentally determined force output to approximate energetic output.

The activation parameters that control the uptake of the activator (K and n) were then optimised to fit force output for each of the individual cycle frequencies (Table 2.1). This was done to account for possible variation in these activation parameters due to shortening speed; a phenomenon known as shortening deactivation. The activation parameters (K and n) were optimised to minimise the sum of the force differences between the model and the experimental results at each time point for three individual conditions at each cycle frequency and the average of these taken as activation parameters for each cycle frequency.

Using the experimentally determined optimal phases for stimulation as published in Curtin and Woledge (1996) for a range of duty cycles, it was possible to use the model to predict the relationship between power output and duty cycle and also efficiency and duty cycle and compare the predicted results to the experimental results across the range of cycle frequencies.

Similarly, the model was fitted with the appropriate values for the mouse *soleus* muscle and the protocol employed experimentally by Barclay (1994) was simulated with the model. This was to ensure that the model could emulate muscle from other species and had not merely been fitted to reproduce the dogfish muscle data. The only parameters that were changed were V_{max} (scaled to Lo/s) and the activation constants (τ_1, τ_2, K and n) and the force data was scaled to F_{max} (Barclay, 1994); these parameters are muscle specific. The appropriate optimal cycle phases, duty cycles and stimulations were applied to the model across a range of frequencies. In this model, it was assumed that the series

elastic element of mouse *soleus* muscle had a similar relative stiffness to that of the dogfish muscle.

Results

Experimental Comparisons

The activation parameters (τ_1, τ_2, K and n) were first optimised to minimise the sum of the force differences between the model and the experimental results at each time point for the following condition; Frequency = 1.25, Duty Cycle = 0.121, Stimulus Phase = 5. A comparison of the model's response to this stimulus is compared to the experimental results in Fig. 2.3. The values of the activation parameters that achieved this fit are given in Table 2.1. It is apparent from the time course of the predicted activation level of the muscle fascicle bundle that the activation parameters used in the model provide a good representation of the activation level

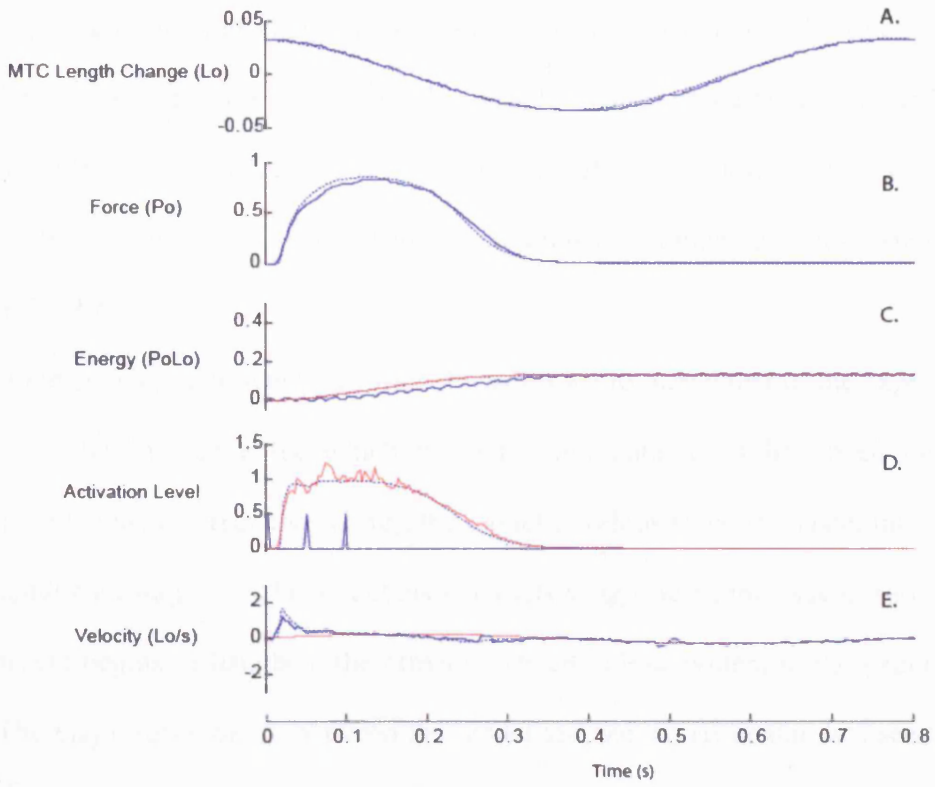

Figure 2.3

Comparison of output of model with that of the experimental results for the single optimised condition (Frequency = 1.25, Duty Cycle = 0.121, Stimulus Phase = 5). The experimental results are taken from raw data used in Curtin and Woledge (1996). A) Length trajectory (relative to Lo) of MTU for the model (dotted line) and experimental results (solid line); B) Force (relative to Po) output for the model (dotted line) and experimental results (solid blue line); C) Energy output (heat+work) for the model (blue dotted line) and experimental results (blue solid line). The experimental results show small amplitude fluctuations as a result of heat measurement from thermopile. The experimental force recordings (Fig 2.3B – solid blue line) and the estimated activation level (Fig 2.3D – red line) were used as inputs into the energetic model to approximate energetic output using the experimental results (red line). D) Activation level (the relative number of attached cross-bridges) predicted by the model (dotted blue line), estimated from the experimental results (red line) and the stimulation pattern from the experiment (solid blue line). E) CE velocity (Lo/s) as predicted by the model (dotted blue line), and as estimated from the experimental results (solid blue line). This is shown in reference to the MTU velocity (red line).

The force-time and energy-time output from the model was then compared to experimental results from a single muscle fascicle bundle preparation (as used in the results of Curtin and Woledge, 1996) across a range of duty cycles, stimulus phases and oscillating frequencies. The results of the simulations are compared to the experimental results in Fig 2.4.

Force development within the model was shown to match that of the experimental examples at the frequency for which the activation parameters had been optimised (1.25Hz). At the fastest frequency (5Hz), the model develops force at a faster rate than the experimental data suggests. The model also predicts a significant increase in force output as the muscle begins to lengthen, the effect of which is less evident in the experimental results. The major discrepancy between the model and the experimental data seems to be due to the time-course of activation level. The model seems to activate at a higher rate than the experimental prediction initially (causing a higher velocity of the CE as the SEE is stretched) and then falls at too slow a rate during deactivation. In contrast, at the slowest frequency of 0.71Hz, the predicted activation level has a slower rate of decline during deactivation, which results in a maintenance of force.

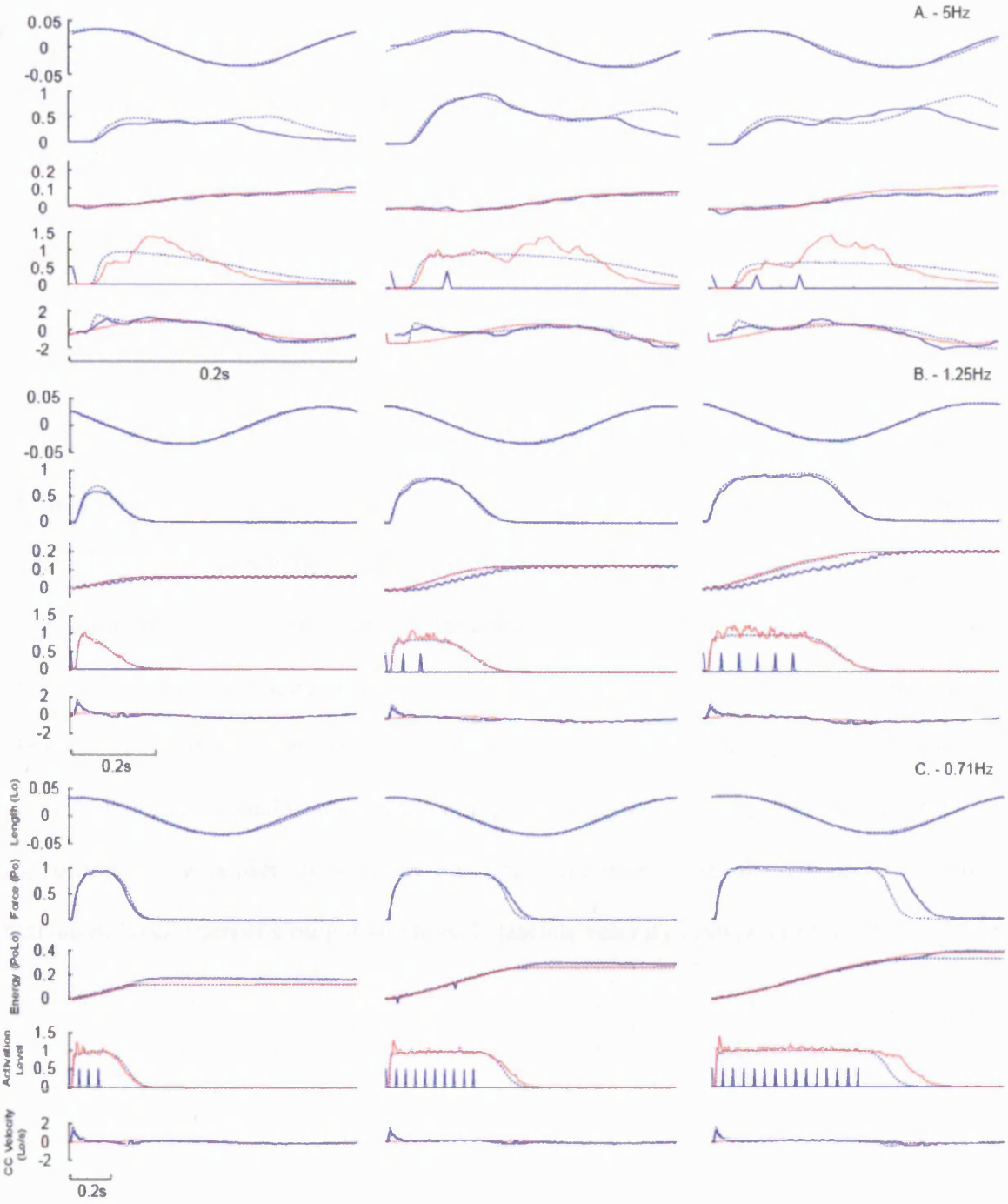

Figure 2.4

Comparison of the model output to the experimental results across a range of stimulation conditions with activation constants optimised to fit a single stimulus condition (Fig. 2.3). Length, force, energetic output, activation and contractile component velocity are compared between the model output (dotted blue lines) and the experimental results (solid blue lines). The convention for these figures is the same as for the single condition in Fig. 2.3, with the red lines indicating the modelled energetic output for the experimental data

(energy plot), the estimated experimental activation level (activation plot) and the MTU velocity (contractile component velocity plot). The comparison is made at three different cycle frequencies, A) 5Hz, B) 1.25Hz, C) 0.71Hz with varying duty cycle and phase.

Activation level changes with shortening speed (a phenomenon known as shortening deactivation). This results in a rapid decline in force if shortening occurs, particularly during deactivation. To account for this I optimised the activation parameters that control the uptake of the activator (K and n) to determine whether this effect could be accounted for at each individual cycle frequencies (Table 2.1). The activation parameters (K and n) were the only parameters optimised to minimise the sum of the force differences between the model and the experimental results at each time point. This was done for three individual conditions at each cycle frequency and the average of these taken as the activation parameters for each cycle frequency. The resultant relationship between the activator concentration and activation level for the optimised activation parameters for each condition is shown in Fig 2.5. A comparison between the model with the optimised activation parameters and the experimental results for force output, activation level, energetic output and muscle fascicle velocity is shown in Fig 2.6.

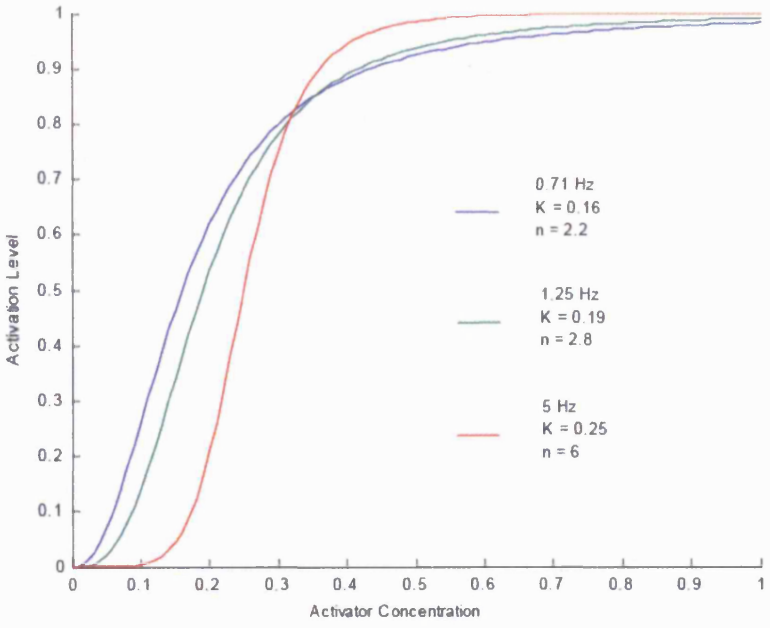

Figure 2.5

The relationship between the activator concentration (Ca^{2+}) and the activation level (the relative number of attached cross-bridges) for each of the optimised values of K and n that produced best fits to the force data at each of the three cycle frequencies (5, 1.25 and 0.71Hz).

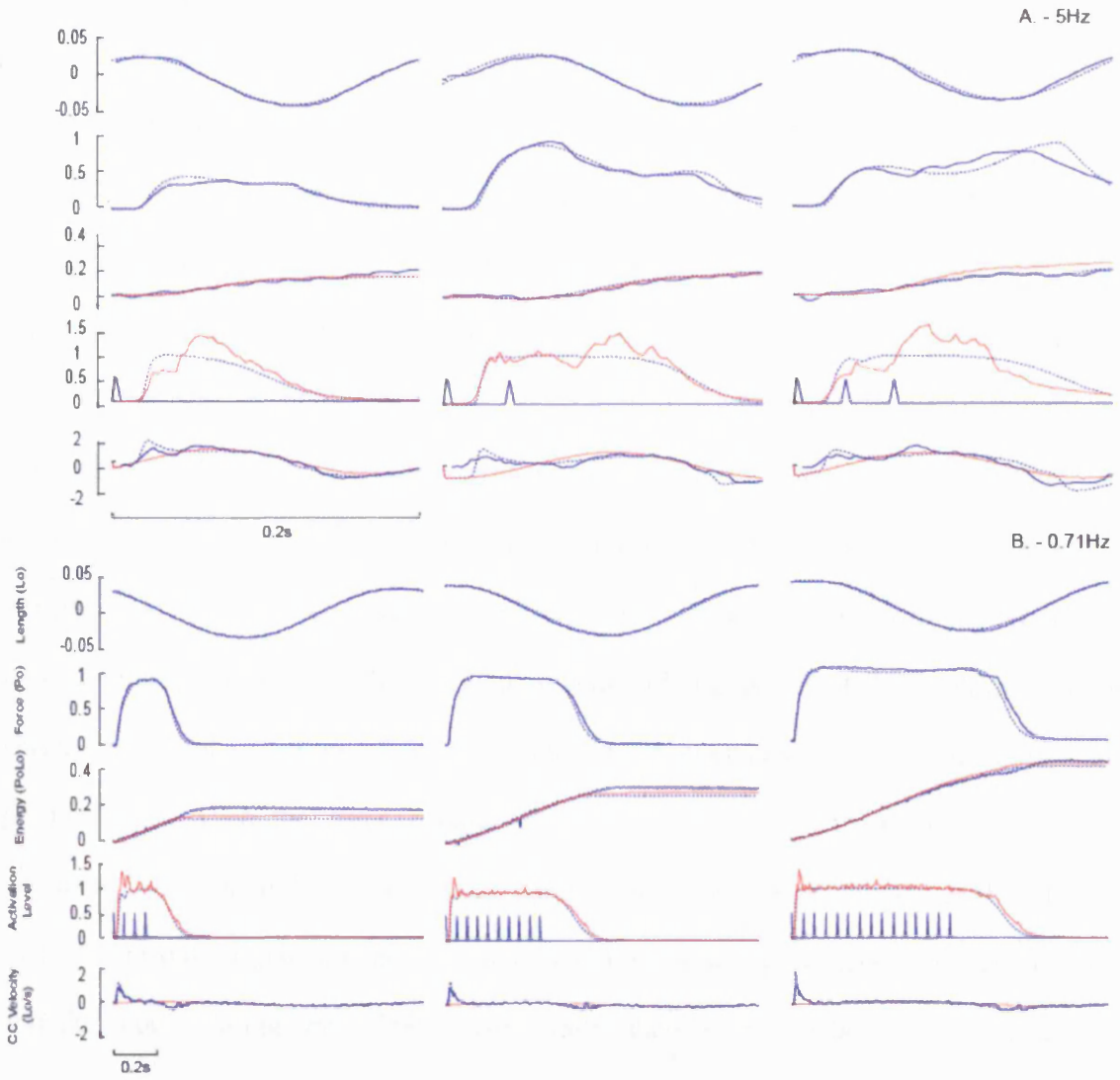

Figure 2.6

Comparison of the model output to the experimental results across a range of stimulation conditions with activation constants optimised to best fit each individual cycle frequency (Fig 2.3). Length, force, energetic output, activation and contractile component velocity are compared between the model output (dotted blue lines) and the experimental results (solid blue lines). The convention for these figures is the same as for the single condition in Fig 2.3, with the red lines indicating the modelled energetic output for the experimental data (energy plot), the estimated experimental activation level (activation plot) and the MTU velocity (contractile component velocity plot).The comparison is made at the frequencies of A) 5Hz and B) 0.71Hz.

A comparison of the energetic output of the muscle and the model (with optimised activation parameters for cycle frequency) suggests that the model makes a reasonable prediction of the experimental energetic output (consisting of work + heat) at all speeds during activation, but does less well during deactivation (the period when the muscle is still producing force while no stimulation is being applied) (Fig 2.4 & 2.5). This is true whether the experimental work output along with the predicted heat output (using the force, CE length and the activation level) is used to calculate the energy, or whether the model's work output is used. The biggest discrepancy between the model and the experimental results occurs during deactivation at 0.71Hz. It is apparent from the experimental results that the there is a continuation of energy output (in the form of heat) shortly after the cessation of force production. In comparison, the model ceases to produce heat when the force reaches zero. Therefore the final energy expenditure predicted by the model is smaller than that of the experimental findings at this speed. There are also discrepancies between the time-course of the experimental energetic output and the model during the 1.25Hz trials, where there seems to be some delay in the between the traces. However the rate of energetic output and the final energetic output compares favourably.

Power and Efficiency

Power output (work/cycle time) and efficiency was also estimated by the model across a range of duty cycles and compared to the average data reported by Curtin and Woledge (1996) (Fig 2.7). These simulations were performed at the optimal stimulus phase for each duty cycle as reported by (Curtin and Woledge, 1996). The optimised activation constants (K and n) for each frequency were used to generate these data (Table 2.1). The model reproduced the experimental relationship between power and duty cycle and also efficiency and duty cycle, and can be used to predict the duty cycles where optimum

power and efficiency occur for all cycle frequencies. The magnitude of power output and efficiency calculated by the model were also accurate for these conditions.

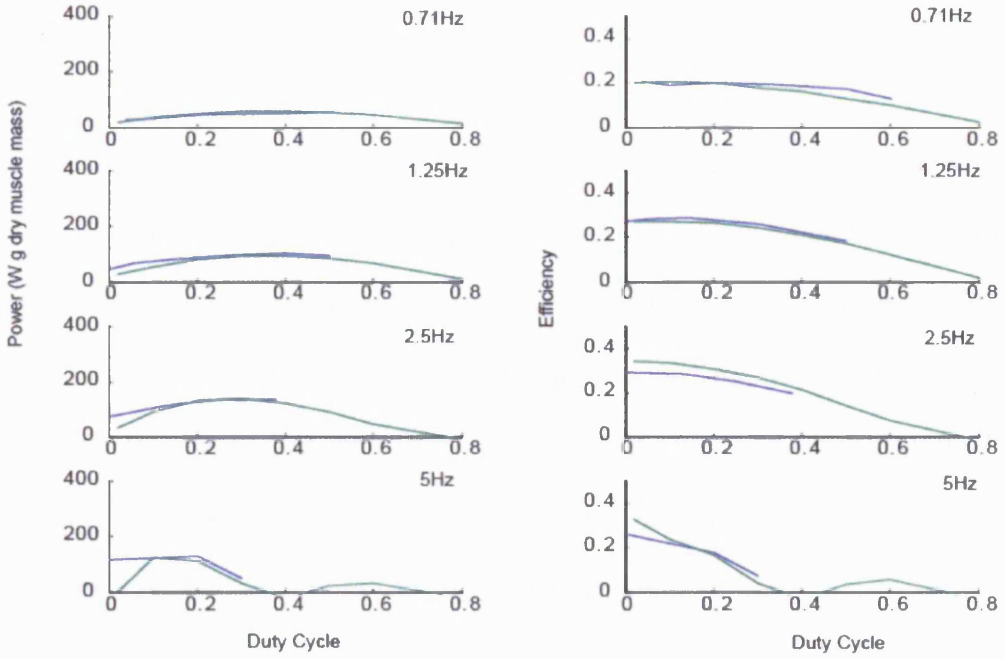

Figure 2.7

Comparison of the experimental (blue) power output (A) and efficiency (B) to the model predictions (green) for a range of cycle frequencies and increasing duty cycle. The same phase of activation was used in each condition. Model results use the optimal activation parameters for each cycle frequency as shown in Table 2.1. Power is defined as the work per cycle time and is scaled up from PoLo/cycle time units based on the properties of the muscle reported by Curtin *et al* (1996).

The force and length data reported by Barclay (1994) were scaled according to the maximum isometric force and the optimal muscle fascicle length. The parameters of the model were kept essentially the same; however; the stimulation rate constants used were τ_1 =0.045 and τ_2 =0.045 and Vmax = 4.0 Lo/second. A comparison of the time course of changes in muscle length, force production and energy output is shown in Fig 2.8a. It is apparent from this figure that there is a reasonable prediction of force and work output across the two cycles although, as for the previous comparisons, the model is less reliable during deactivation. Further discrepancies occurred in the time course of heat output,

where the model shows a higher rate of heat output during the force production, while the experimental data suggests that this heat output continues to rise as the muscle deactivates and force declines. Despite this discrepancy, the absolute value of energy (heat + work) output across whole cycles seems to be very similar.

Fig 2.8B shows the power output and heat rate output (heat/cycle time) of the mouse *soleus* across a range of frequencies for both experimental conditions and model predictions. The results indicate that the relationship between cycle frequency and energy output is predicted well by the model. Again, the heat rate output from the model has a slightly lower magnitude than the experimental data; however, it is always within 25% of the measured values and it is apparent that the model also accurately predicts the optimal frequency of length change for maximising total energy output.

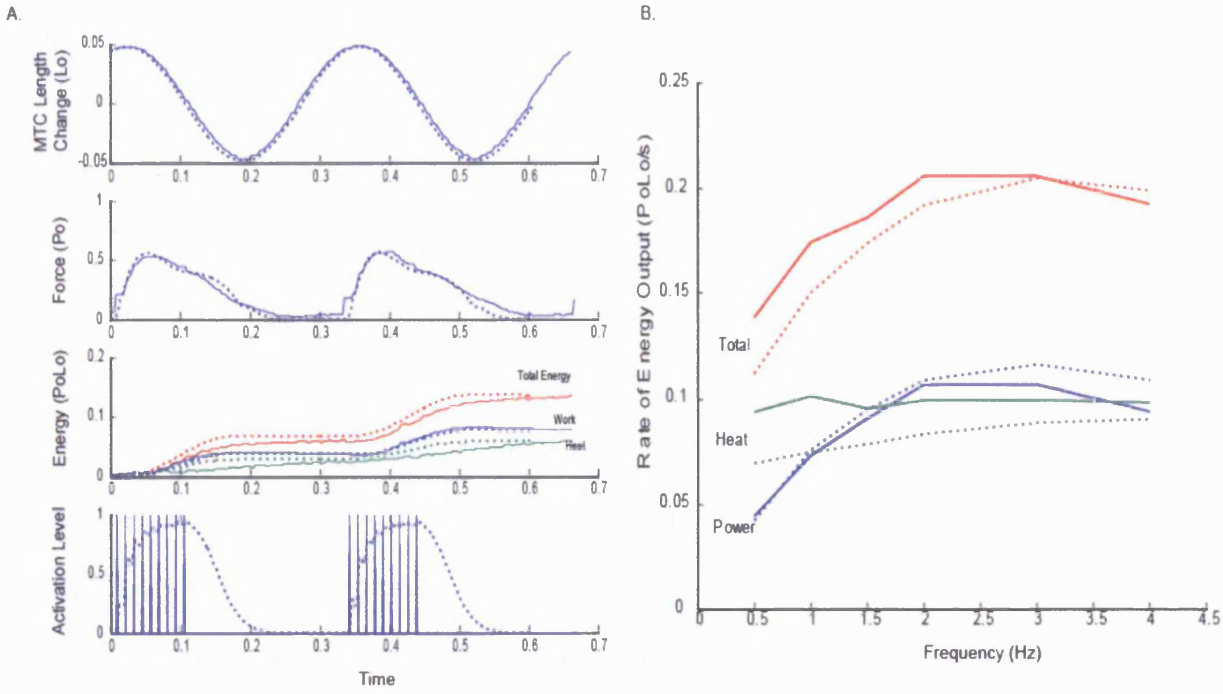

Figure 2.8

A. Comparison of the model (dotted lines) to individual records of length, force, energetic output and stimulation/ activation for an example *soleus* muscle of a mouse (solid lines) as reported in Barclay (1994). Values are scaled according to average data reported by Barclay (1994). **B.** Comparison of model (dotted lines) to experimental (solid lines) power and rate of heat and total energy output (power + heat rate) across a range of frequencies. The stimulation rate constants used were τ_1 =0.045 and τ_2 =0.045 and Vmax = 4.0 Lo/second.

Discussion

A comparison of the time-course of force and energy changes between the model and the experimental condition yielded positive results that are valuable in our understanding of muscle mechanics. It was possible to use a modified Hill-type muscle model, with an energetic component, to reproduce the optimum activation conditions for achieving maximum power output and maximum efficiency of muscle, as per the results of Curtin and Woledge (1996).

The model makes robust predictions for the time-course of the force, energy (heat + work), activation level and contractile element velocity (Fig 2.2) when the activation parameters are optimised for force alone. Although the predicted activation level is based partly on the model itself, it does demonstrate small peaks in the activation level, which correspond to each individual muscle twitch (with a time delay of approximately 0.05s). Providing enough is known about the properties of the muscle in question (force-velocity, force-length and series elastic properties), this technique could be used to estimate the activation level of a muscle in a range of activities where force and length of the muscle (MTU) is directly measured.

Despite the model's ability accurately to predict the timecourse of force production at the 1.25Hz frequency, the results from Fig 2.3 demonstrate that the model is less accurate at 0.71Hz and 5Hz; this is most apparent during *deactivation.* At the fastest frequency, it is apparent that the model maintains a high force level once the real muscle tendon unit begins to lengthen. The experimental results show that the muscle force is low during this period. Analysis of the predicted contractile element velocity from the experimental results suggests that the contractile element needs to be lengthening during the deactivation, rather than shortening which the model predicts. To resolve this problem, the activation parameters need to be changed so that the muscle can deactivate at a faster rate. The opposite effect is required at low frequencies, with a reduction in the deactivation rate required.

Numerous investigators have described a phenomenon termed 'shortening deactivation', whereby at high velocities of muscle shortening, the muscle tends to deactivate and the force trace is depressed (Askew and Marsh, 2001; Josephson, 1999; Leach *et al.*, 1999). The mechanism behind shortening deactivation is not well known. However the results of this study both support its existence and also provide some

information as to how the cycle frequency may influence the activation level. Optimising the activation constants (Tau1, Tau2, K and n) to minimise the sum of the force differences between the model and the experimental results for each of the 9 individual conditions (Fig 2.4) revealed that the constants Tau1 and Tau2 could remain relatively constant and still provide the best fit. By varying just the parameters K and n, it was possible to get good fits between the model and the experimental force-time data for each individual frequency.

The constants K and n can be thought of as representing the rate of binding of the activator (Ca^{2+}) to the troponin which allows for binding and dissociating of the cross-bridges and hence force production. Recent experimental evidence suggests that the off-rate of calcium from troponin increases with the dissociation of the force-generating cross-bridges (which occurs with increasing speed of contraction) (Wang and Kerrick, 2002). Therefore the mechanism behind the phenomenon of shortening deactivation may be the change in affinity of Ca^{2+} to troponin. The predicted change in the relationship between the activator and the activation level demonstrated here provides further evidence that shortening deactivation results from a change in the affinity of the Ca^{2+} to troponin. However, although the optimisation procedure showed that the optimal values of K and n could be characterised across a range of contractions conditions at any given cycle frequency, optimisation under different contraction conditions within the same cycle frequency did show some variation in the activation constants. Therefore the instantaneous speed of contraction is likely to be important, not just the cycle frequency. Further investigation into this area is beyond the scope of this paper and would require a vigorous experimental protocol on live muscle bundles.

The energetic model has been shown to perform relatively well at all frequencies, which is reflected by the ability of the model to predict the duty cycle that produces

optimal efficiency. The rate of energetic output (heat+work) during *activation* in the model provides consistently good agreement with the model. Discrepancies in the onset of the energetic output at 1.25Hz may be due to the experimental setup, where the muscle may have shifted across the thermopile during contraction. However, it is apparent that the same total energy is measured during the period of one cycle. This is not the case in the 0.71Hz contractions, where although the energetic outputs of the experiment and the model match during activation, they do not agree during deactivation and as a result the total energetic output during the cycle is underestimated by the model.

The discrepancies in both force and energetic output during deactivation highlight some possible processes that need further investigation within contraction dynamics of muscle. A common finding in the experimental data is that during the longer periods of activation (>0.2s), the decline in force is associated with a delayed rise in the rate of energetic cost. This is not simulated in the model, which instead predicts a fall in rate of energetic cost once force has declined. This delayed onset of heat production has been cited elsewhere and can partly be explained by the release of heat due to conversion of work by the CE and partly by ATP turnover due to cross-bridge cycling (Curtin and Woledge, 1996; Linari *et al.*, 2003). Another possible source for some of the energy liberation during the fall of the force is hystersis of the elastic tissues. During shortening of the elastic tissues, some of the energy stored in them is lost as heat (Wilson and Goodship, 1994). In biological tissues the range of energy liberated as heat could be as much as 7-30% of total energy stored (Maganaris and Paul, 2000a; Pollock and Shadwick, 1994).

The experimental muscle continues to produce force for a significant time after the cessation of stimulation at 0.71Hz compared to the model, even with the optimised activation constants (Fig 2.5C). This result suggests that cross-bridges are still attached,

either due to continuation of ATP turnover, or perhaps some other passive process. The experimental observation that the rate of energetic cost actually plateaus during this period of force maintenance (before increasing again during unloading; see Fig 2.5c, duty factor = 0.6) suggests that ATP turnover is not responsible for this force maintainence, and instead some other process is involved. The plateau in the force record may also be due to an experimental artefact, however inspection of experimental trials with similar activation conditions suggests that this phenomenon is consistent for a range of conditions. Therefore perhaps some parallel structure at the fascicle level (possibly elastic) is being engaged to produce this force as the force maintenance occurs during muscle lengthening.

The model was highly successful at predicting the various conditions under which the optimal power output and efficiency could occur across two different muscle types. The comparisons to a second set of muscle data, the mouse *soleus* muscle of Barclay (1994), yielded very positive results for the extension of the model to other muscle types. As with the dogfish muscle, the model was particularly successful at mapping the optima for power output and the rate of energy output, despite changing only three parameters from those used in the dogfish model (the activation constants τ_1 and τ_2 and Vmax). The good results may also be assisted by the faster relaxation rate of the mouse muscle, which may hide some of the strange phenomenon that occurs in the dogfish muscle during relaxation.

Accurate modelling of muscle can effectively allow investigators to simulate large amounts of muscle experiments where the conditions of muscle activation and length changes are changed. Experimentation with muscle fibres, bundles or whole muscles is limited by the life of the muscle. Hence, changing the conditions under which contractions are performed, such as duty cycle, phase of activation and frequency, is

difficult without fatiguing/damaging the muscle. Instead, a thorough modelling approach such as that presented here is very useful in determining why muscles function the way they do. More accurate muscle models can also improve simulation of movement with forward dynamics and allow us to determine the effect that varying muscle properties has on muscle mechanics and energetics. Caution should however be used when applying this model of energetics across a broad range of muscle types. Knowledge of the properties of individual muscle types (both of the CE and the SEE) is essential in applying this model. These properties are known to vary greatly across the biological spectrum and care should be taken in determining these properties before applying the model.

Although the model predicts the optimal power output and efficiency conditions, further refinement to the model may improve its robustness under varying conditions. For instance, the current model neglects the force-length relationship of muscle because the amplitude of length change is not believed large enough to exceed the plateau of this relationship. However during animal movement, muscles are often subject to length changes which exceed the plateau and some muscles routinely operate in the ascending limb of the force-length relationship. Therefore, application of the energetic model to biological cases should include a scaling of the energy consumed by this relationship.

Conclusions

In conclusion, it has been demonstrated that a Hill-type muscle model can effectively predict the energetics of muscle contraction (heat + work) for two different muscle types using experimentally determined muscle properties. Using the model, it was demonstrated that the activation parameters for achieving optimal power output and optimal efficiency can be predicted and are in line with experimental data for most conditions. With increases in cycle frequency, it was necessary to vary the activation parameters that control the affinity of the activator (Ca^{2+}) to the force generator (troponin)

in such a way that the off-rate of the activator was increased. This provides further evidence for the phenomenon known as shortening deactivation. The validated model is useful for exploring how activation conditions affect power output and efficiency of a muscle, and how properties of the muscle affect these relationships.

Chapter 3: Effects of series elasticity and activation conditions on muscle power output and efficiency.

This chapter has been accepted as a paper in the following reference:

Lichtwark, G.A. and Wilson, A.M. (2005). Journal of Experimental Biology, Volume 208, pp2845-2853

All work has been written originally by Glen Lichtwark

With a validated model which can predict power output and efficiency of muscle under a range of experimental conditions, it is possible to then do an infinite amount of 'experiments' with the muscle to explore the parameter space and determine how a muscle might be most powerful or efficient. It is possible to vary any of the parameters in the model to determine their effect, however I am most interested in those which can be controlled either neurologically, such as activation conditions, or architecturally, such stiffness of the series elastic element. In this Chapter I will use this technique to examine how these changes might influence power output and efficiency.

Introduction

Muscles generate force under a range of velocity conditions. Muscles can act isometrically (no length change) and perform no net work, or they can shorten or lengthen whilst generating force, which results in performing or absorbing work respectively. The role that an individual muscle performs depends on the activity being performed (Gabaldon *et al.*, 2004; Roberts and Scales, 2002; Roberts and Scales, 2004) and also on the activation conditions of the muscle (Ettema, 1996b). For instance during level running the turkey gastrocnemius muscle fibres remain isometric, whilst on an incline the muscle performs net work by shortening during the stance phase. Individual muscles also

show architectural adaptations depending on their function. Some have long fibres and can shorten over a large length range and at high velocity. Others have shorter fibres, which means that the length change is less but that the cost of force generation and the mass of muscle tissue required to generate force is also less.

The amount of series elasticity present in a muscle, mostly in the aponeurosis and the tendon, can vary depending on its role. Series elasticity has been identified as an advantage in the antigravity muscles of running animals, because the tendon will elongate under load and store elastic strain energy which is subsequently returned later in the movement. For instance, in the wallaby gastrocnemius the muscle fibres are almost isometric and do not change length much during stance, but there is considerable elongation in the series elastic element (SEE) (Biewener *et al.*, 1998). The wallaby muscles however represent one extreme of muscle design and most muscles consist of longer fibres and less significant series elastic tissue. It has been observed that a large amount of series elasticity will enable energy storage at the cost of accurate length change (Alexander, 2002) and it has been predicted that the SEE will increase the versatility of a muscle since the muscle fibres can contract at a different speed from the overall muscle tendon unit (MTU) (Fukunaga *et al.*, 2002; Galantis and Woledge, 2003). It has not been shown how the presence of different amounts of SEE actually influence the economy, power and versatility of muscle under different locomotor conditions, and in particular which activation conditions are optimal.

The relationship between power output and efficiency of a muscle under different contraction conditions has been examined extensively. Experimental comparisons of the optimum activation conditions for power production and efficiency demonstrate that the frequency of oscillation, length change, duty cycle and phase of activation all affect both the power output and the efficiency of muscle (Curtin and Woledge, 1996; Barclay, 1994;

Ettema, 1996b). In those experiments, various combinations of phase, duty cycle, length change and frequency of oscillation achieved optimal power output and efficiency. However, the activation patterns used showed a broad optimum and there did not seem to be a direct relationship between power and efficiency. Hence animal muscle has a range of activation patterns and length trajectories in which they can operate at maximal power or maximal efficiency, or perhaps some combination of the two.

In Chapter 2, I have shown that the activation conditions for optimum power output and efficiency can be reproduced using a Hill-type muscle model that estimates the energetic cost of contacting the muscle. This model was based on experimental data from the white myoseptal muscle of the dogfish and validated using data from the mouse *soleus* muscle. The inclusion of a series elastic element, which is able to store elastic strain energy for subsequent release, changes the time course of power development from that seen in the muscle fascicle bundles themselves. However, muscles that operate with different functions often have a broad range of different elastic tissues (including tendon, aponeurosis, perimyosium and myoseptum) attached both in series and in parallel, and these structures have different levels of compliance. In addition to this, the maximum force generating capacity of a muscle and the muscle fascicle length can vary greatly compared to the compliance of the elastic structures. Therefore the activation conditions and the overall length change of the entire MTU that achieve optimal power output and efficiency should vary greatly between muscles with different architecture and function. It is proposed that the energetic function of a muscle may play an important role in developing the architecture of the MTU (the length of its muscle fibres, the maximum force generating capacity and the compliance of the series elastic tissue) so as to minimise energetic cost during common movements.

Variation in the elasticity of a muscle has been predicted, using a model, to affect its function by altering its work generating capacity and its efficiency under various activation conditions (Ettema, 2001). Although similar power outputs and efficiencies can be obtained with a muscle regardless of the SEE stiffness, these maximums have to be achieved with different activation conditions (i.e. different duty cycles and phases). For instance muscles with a stiff SEE are most efficient when activated during shortening, whereas a compliant SEE would be most efficient when activated during stretch in a stretch-shorten cycle (Ettema, 2001). A stiff SEE is least efficient when activated early in the stretch phase because the contractile element (CE) is forced to absorb work during the stretch phase and then actively generate work at a high energetic cost. However, the amplitude of length change of a muscle will also alter the proportion of length change occurring in the SEE and the CE and this must also be accounted for when determining the influence of SEE stiffness on muscle power output and efficiency. Finally, the level of activation of a muscle may also have an effect on the timecourse of events in a cyclic contraction, particularly power output and energetic cost, and therefore its effect on power output and efficiency should also be explored.

By applying the energetic model of muscle contraction (Chapter 2) it was possible to explore and map the relationship between power and efficiency of muscle with varying duty cycle, phase of activation, amplitude of length change and activation level. This type of protocol is difficult to undertake experimentally on muscle tissue due to muscle fatigue and the difficulty in keeping muscles alive for the duration of these lengthy *in vitro* studies. Applying a validated model allows the experimenter to test across a broader range of conditions and also makes it possible to vary the properties of the muscle to explore how this affects muscle power output and efficiency.

In this Chapter, I hypothesise that activation conditions (timing and duration of activation) exist that elicit a range of powers with near optimal efficiency. Here I will use the model developed in Chapter 2 to demonstrate this and to show that these optimal activation conditions would match those found in experimental data for animals during locomotion. I also hypothesise that the activation conditions required to generate optimum power output and optimum efficiency of a muscle are highly dependent on the stiffness of its series elastic element.

In this chapter I test these hypotheses as follows:

1. I vary the timing and duration of activation in a modified Hill-type muscle model, as described in Chapter 2, to determine the optimum conditions to maximise power output and efficiency. I compare the optimum activation conditions for generating maximum power output and efficiency, and explore how a biological system can approach the optima of both simultaneously.
2. I vary the stiffness of the elastic element and the amplitude of the length change that the muscle undergoes to determine their effect on power and efficiency under different activation conditions.
3. I determine how the stiffness of the series elastic elements might influence the behaviour of a muscle and explore some biological examples which highlight this effect.
4. I determine the effect of changing the level of activation on power output and efficiency of muscle under different activation conditions.

Materials and Methods

I applied the energetic Hill-type muscle model from Chapter 2 to explore how power output and efficiency are affected by the activation conditions, amplitude of length

change and series elastic stiffness during sinusoidal length changes. I first explored the interaction of power output and efficiency under validated conditions using the same model as in Chapter 2 and varying the duty cycle (duration of activation relative to the entire cycle time) and the phase of activation (the time between the start of stimulation and the start of shortening expressed as a percentage of cycle duration). I also performed contractions across a space of duty cycles and stimulus phases to determine the how power and efficiency interact under these conditions. This was done at a frequency of 1.25Hz, where the constants used to determine the rise and fall of activation had been optimised to fit experimental data in Chapter 2. A Nelder-Mead simplex (direct search) optimisation technique was also performed in Matlab (Mathworks Co.) to determine the optimal values of duty cycle and phase of activation maximum power and efficiency.

I then used the same techniques to explore how these results might theoretically vary by changing the series elastic stiffness and also the total length change (amplitude) of the MTU throughout a sinusoidal length change. The model used in Chapter 2 was operated across length changes within the plateau region of the force-length relationship of the muscle. However, in this investigation it is necessary to extend the length change of the MTU such that the muscle fascicle length may affect its force and energy output. Therefore a typical force length relationship of a sarcomere (Gordon *et al.*, 1966) was incorporated to scale the force generating capacity of the muscle fascicle depending on its length (Fig 3.1a). The number of possible cross-bridges attached is related to the relative overlap of the actin and myosin filaments and therefore the maintenance heat rate also needs to be scaled by the force-length relationship in the same way that activation level scales the maintenance heat rate. Although it has been demonstrated that the force-length properties of a sarcomere do not accurately represent those of whole muscles or muscle fascicle bundles (particularly on the descending limb), this model is believed to be

satisfactory in this case because the muscle fascicle length change should not exceed Lo +/- 0.25 Lo (force is always greater than 70% Po).

The muscle model incorporates a SEE stiffness which is represented in normalised form; relative to Po (maximum isometric force) and Lo (optimum muscle fascicle length). This represents the amount of force produced (relative to the maximum force) for any given length change (relative to the muscle fascicle length). Therefore if the absolute stiffness of the SEE was to remain constant, but the muscle optimum muscle fascicle length doubled, then the relative stiffness would also double.

The model was then used to find the optimal activation conditions and length changes for achieving maximum power and efficiency at a stiffness range lower than that measured experimentally, and determined how these optimal conditions change as a result of the lower stiffness. Here, the relative stiffness was reduced from 22 Po/Lo to 4 Po/Lo (with a lower stiffness of 16 and 3 Po/Lo respectively at forces below 0.15Po to account for the toe region of the force length properties of the SEE, see Chapter 2) and the length change was changed from +/- 0.0335 Lo to +/-0.2 Lo. With these values of stiffness and amplitude of length change, the power output and efficiency of the muscle were explored across a space of duty cycles and phases of activations. In addition, a Nelder-Mead simplex (direct search) optimisation technique was used to determine the optimum values of duty cycle, phase of activation and length change to achieve the maximum power and efficiency. The relative stiffness of muscles with similar functions but from a range of species was also determined to compare the findings from the simulations.

Finally, I explored the effect of activation amplitude on power output and efficiency across the range of duty cycles and phases of activations. The activation amplitude here was defined as a simple arithmetic scaling of the activation properties of the muscle. For instance an activation amplitude of 0.5 was equivalent to activating 50%

of the fibres, thereby scaling the activation maximum level of activation by this amount. This relationship is demonstrated in Fig 3.1B. By applying an activation levels at 30%, 50% and 100% I explored how power output and efficiency vary across the space of duty cycles and phases.

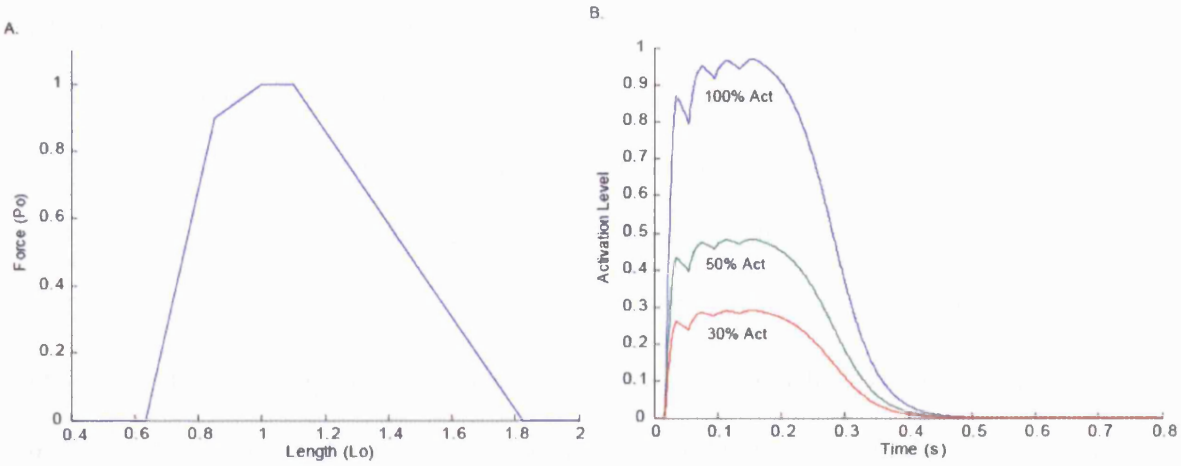

Figure 3.1

A. Force-length relationship used to scale the maximum force output (adapted from Gordon, 1966) by scaling the number of possible cross-bridges that can attach. **B**. Scaling of activation to represent 30%, 50% and 100% of activation levels.

Results

Power and Efficiency – Duty Cycle and Phase of Activation

Using the model, it was possible to explore and map the effect of changing duty cycle and phase of activation on the resultant power and efficiency (Fig 3.2) and also determine the optimum activation pattern to achieve these. Activating the muscle for longer and before the muscle begins to shorten achieves the greatest power output. It is apparent that there is a distinct optimum for both power and efficiency; however there is a relatively large range of duty cycles and phases that can achieve values close to these optimal values. Fig 3.2A demonstrates this by plotting contours at the level of 99, 80, 60 and 40% of maximum power and efficiency as well as the position of the optimal values.

To achieve an optimal power output, the muscle is activated for a relatively long duty cycle (0.368) and be activated whilst the muscle is still lengthening (phase = -5.11). In contrast to this, optimal efficiency was achieved with a shorter duty cycle (0.098) and activation was confined to the shortening phase of the muscle length change (phase = 5.91). The contours achieving both 80% power and 80% efficiency also overlap for a range of combinations of duty cycle and phase of activation. The range of phases of activation for achieving greater than 80% of both maximum power and efficiency was – 15 to 10, while the duty cycle was restricted to between 0.2-0.5.

The workloops of the CE, SEE and the MTU unit to achieve maximum power output and efficiency at a cycle frequency of 1.25 Hz and with a length change of +/- 0.035 Lo are shown in Fig 3.2B. To achieve a maximum power output, the MTU has very little length change as the force rises rapidly to a maximum and remains high while the muscle shortens. Once the muscle deactivates (indicated by the thin portion of the line) the force falls quickly with very little length change in the muscle. This allows the maximum area under the force length curve to be achieved. The CE however shortens (as the SEE is stretched) to produce force and then also lengthens as the force is falls (absorbing small amounts of energy). In contrast, during the maximally efficient contraction, the CE has very little length change (and no stretch) as the force falls. As a result the MTU shortens as the force drops. As there is no hysteresis in the model of the SEE, there is no energy lost here and the area under both the CE workloop and the MTU workloop must be the same.

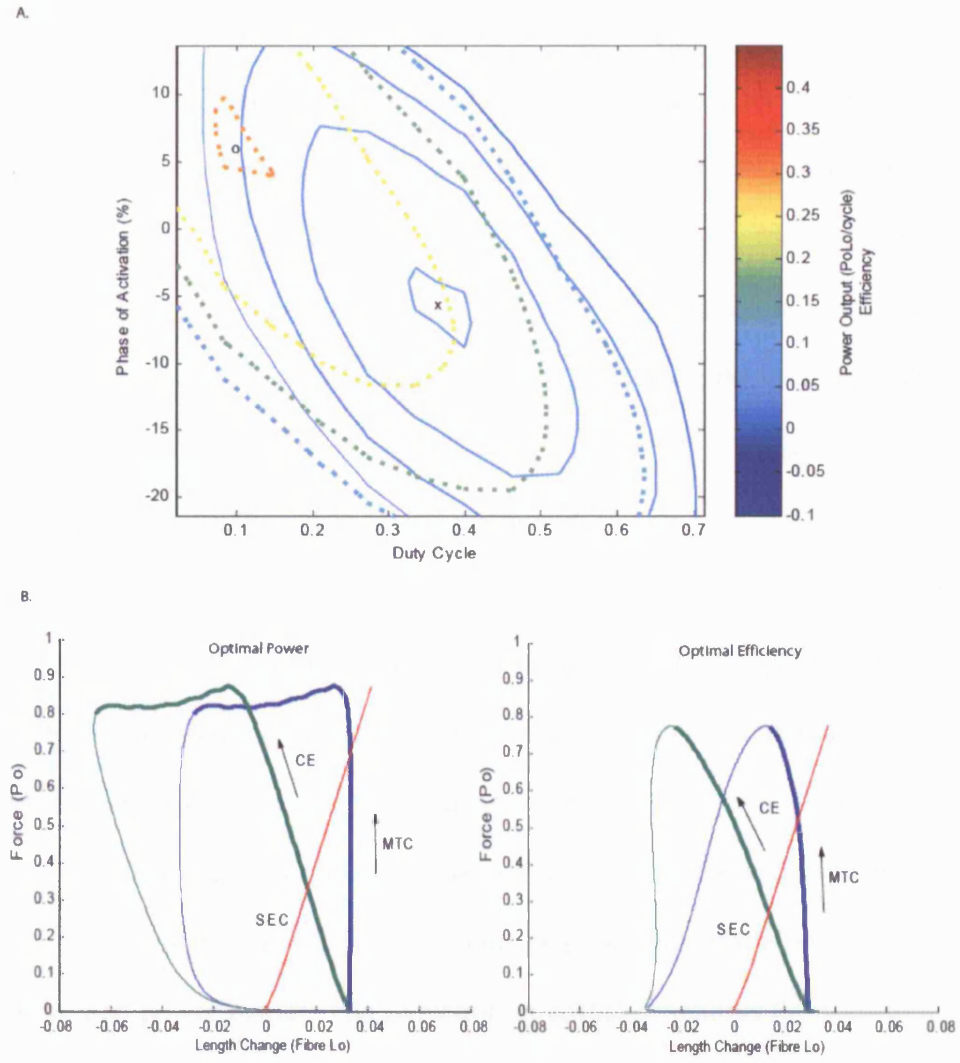

Figure 3.2

A. Contour plot showing the range of duty cycles and phases of activation that can achieve 99%, 80%, 60% and 40% of maximum power output (solid lines) and efficiency (dashed line). The colourbar represents the absolute values for power output (PoLo) and efficiency. The values for achieving optimum power (x) and efficiency (o) are also shown. The frequency of oscillation was 1.25Hz. **B.** Workloops (Force vs Length) for optimal power output and efficiency. The workloop of the contractile element (CE), the series elastic element (SEE) and the muscle tendon unit (MTU) are shown. Positive length changes indicate stretch and the force is the same in the SEE, CE and MTU at any point in time. The duty cycle and phase for optimal power was found to be 0.368 and -5.11 respectively, compared to 0.098 and 5.91 for optimal efficiency. The thick lines indicate the duration of activation.

Power and Efficiency –Series Elastic Stiffness and Length change

The relationship between power output and efficiency with varying series elastic stiffness, amplitude of oscillation and activation parameters (duty cycle and phase of activation) is shown in Fig 3.3. When the relative stiffness was reduced, the maximum power output was achieved with a similar duty cycle, but the muscle needed to be activated further into the stretching cycle of the MTU. This is the case for both the small and large amplitude of length change. A similar relationship holds true for maximum efficiency, although smaller duty cycles are required.

A comparison between the activation conditions that produce maximum power and efficiency output shows that at the low amplitude length change, the muscle needs to be activated earlier (during stretch) and for longer to achieve maximum power output. This relationship holds true for both values of relative stiffness. At the higher (since opposite in lower) amplitude however, the phase can remain very similar to maintain maximum power output and efficiency, and only the duty cycle has to be greater to achieve optimal power output. The reduction in stiffness requires the muscle to activate earlier to achieve both goals at both amplitudes of length change.

At the lower amplitude of length change it is apparent that the maximum power output achievable reduced from 0.067 to 0.051 PoLo/Cycle when the stiffness was changed to the lower stiffness. In contrast, at the high amplitude of length change, the power output was higher for both stiffnesses; however it is higher for the low stiffness condition (0.175) compared to the experimental stiffness (0.156). A similar effect is found for efficiency, where a reduction in stiffness saw the maximum efficiency change from 0.304 to 0.169 at the small amplitude and 0.416 to 0.399 at the large amplitude. When the muscle model has a small stiffness with a large amplitude length change, the activation conditions that achieve maximum power output and efficiency were closest.

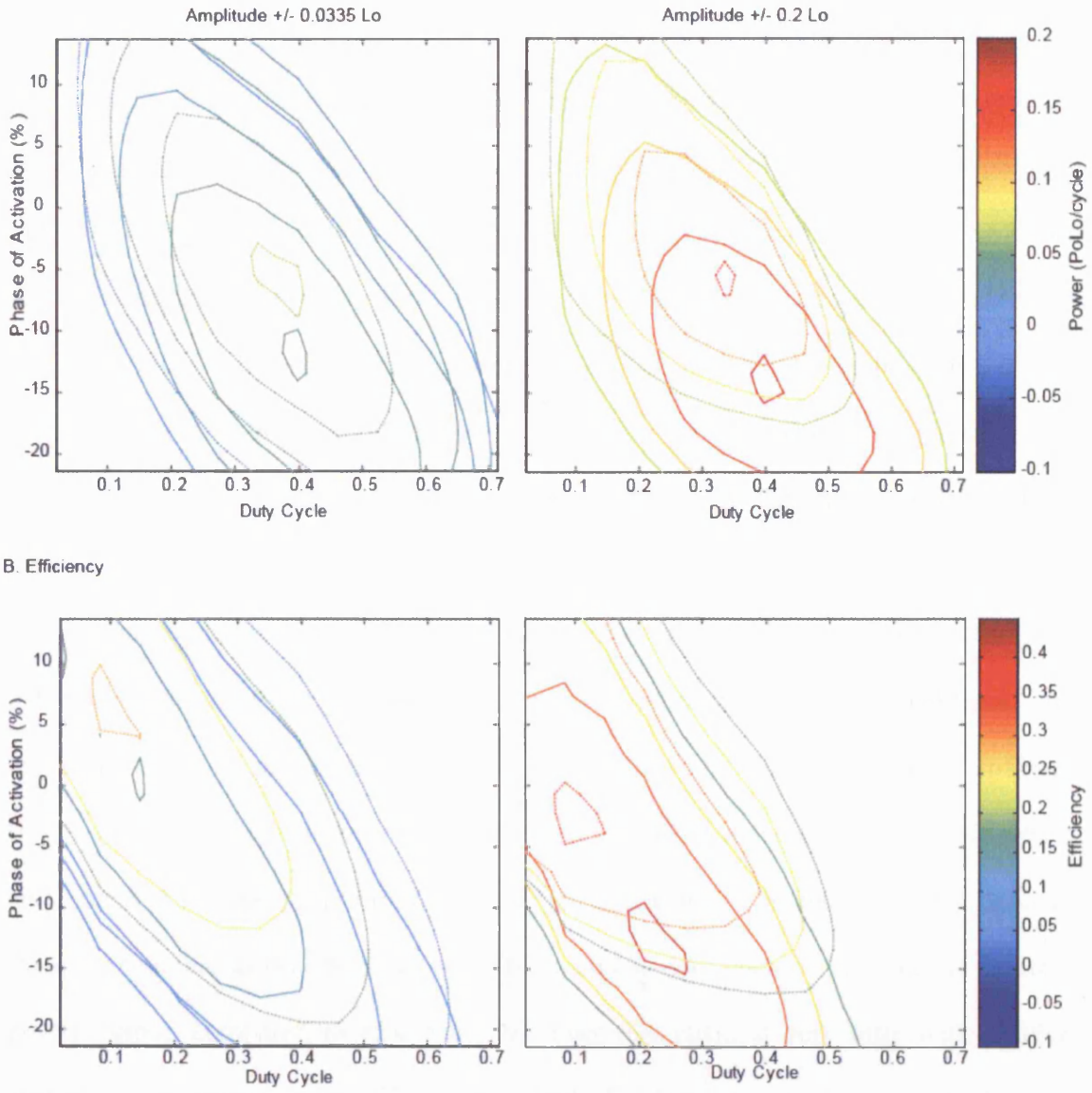

Figure 3.3

Contour plot showing the range of duty cycles and phases of activation that can achieve 99%, 80%, 60% and 40% of maximum power output (A) and efficiency (B) for a compliant relative stiffness (solid lines) and a stiff relative stiffness (dashed line) at two different amplitudes of oscillation. The colourbar represents the absolute values for power (A) and efficiency (B). Compliant relative stiffness = 3-4Po/Lo; Stiff relative stiffness = 16-22Po/Lo (lower stiffness value for forces less than 0.15Po, see Chapter 2).

Maximum Power Output and Efficiency – Effects of Series Elastic Stiffness

Fig 3.4 demonstrates the effect that the relative stiffness of MTU has on maximum power output and efficiency (with optimised activation conditions) at different amplitudes of length change. This shows that a MTU with a higher relative stiffness of the SEE will achieve its optimum power output at a lower amplitude of length change compared to that of its optimum efficiency. However, the simulation with the lower relative stiffness achieved its maximum for both power and efficiency at a similar amplitude of length change. The absolute value of maximum power output and efficiency varied very little with the change in stiffness.

Optimisation of both activation conditions and the amplitude of length change at different relative stiffnesses demonstrated that under the optimal conditions, the maximum values of power output and efficiency don't vary greatly with relative stiffness (Fig 3.4B). However it is apparent that there is a trend of reduced maximum efficiency and increased maximum power with a reduction in stiffness. The conditions that produce these maxima are also plotted in Fig 3.4B. A higher duty cycle is required for optimal power output, compared to efficiency; however this changes very little with relative stiffness. With increases in stiffness, the onset of activation must be later (ie phase of activation must be higher; closer to the beginning of the shortening phase, 0) and this effect is more apparent to achieve optimal efficiency. The opposite is true for the amplitude of length change, where the optimal length change of the MTU reduces with increasing stiffness and must be smaller to achieve maximum efficiency.

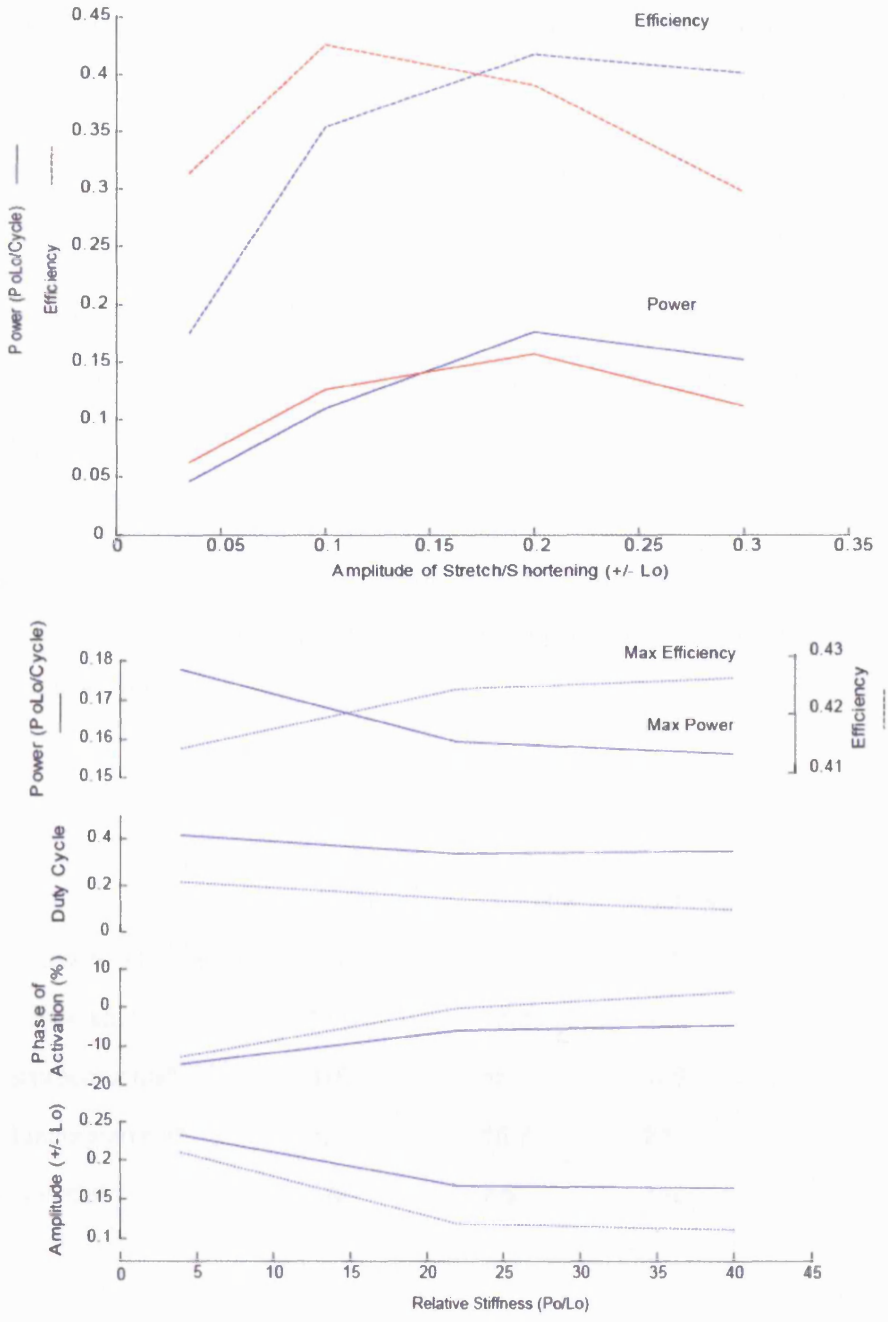

Figure 3.4

A. Maximum power output (solid lines) and efficiency (dashed lines) with changes in the amplitude of stretch/shortening at a low stiffness (blue) and high stiffness (red). **B.** Maximum power output and efficiency and the duty cycle, phase of activation and amplitude of stretch/shortening that achieve that power output with varying relative stiffness. Solid lines represent the values obtained for maximum power output and dashed lines represent those obtained for maximum efficiency.

Table 3.1 lists a number of anti-gravity muscles from animal species ranging from a hopping mouse to a horse and the relative stiffness of each. From this table it is apparent that relative to the length of the fascicle and the maximum force generating capacity, the compliance of the tendon tends to increase (decreasing stiffness) with the size of the animal. The stiffness of the horse SEE is almost an order of magnitude smaller than that of the hopping mouse, however the functions of these muscles are notably different across the different species.

Table 3.1

A range of muscles with similar roles from animals of different size and their properties. The calculated relative stiffness normalised to muscle fascicle length and maximum isometric muscle force.

Muscle Type	Po (N)	Lo (mm)	Stiffness (N mm^{-1})	Relative Stiffness (PoLo)
Hopping Mouse Gastrocnemius*	3.6	7.3	7.7	15.61
Rat Gastrocnemius *	11.3	13.8	15.9	19.41
Human Gastrocnemius^	875	65	150	11.14
Wallaby Gastrocnemius*	135	18.7	21	2.91
Horse Superficial " Digital Flexor	716	7.5	118	1.23

* Data from (Ettema, 1996a)

^ Data from (Maganaris and Paul, 2002)

" Data from (Brown *et al.*, 2003)

Power and Efficiency – Effects of Amplitude of Activation

By varying the amplitude of the activation, which may be thought of as reducing the number of active fibres in a whole muscle or bundle of fibres, it is possible to map the change in power output and efficiency with varying activation conditions. Fig 3.5 shows the variation in power output and efficiency as the result of varying the maximum activation level to be 30%, 50% and 100% (amplitude of length change = 0.0335). It is apparent the optimal activation conditions to achieve maximum power output and maximum efficiency and the actual level of efficiency are very similar regardless of activation level. However the magnitude of the power output is dependent on activation level.

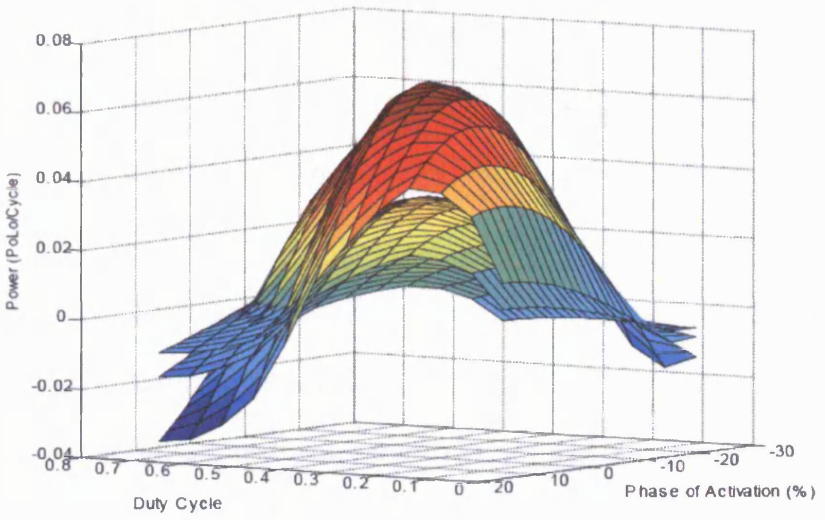

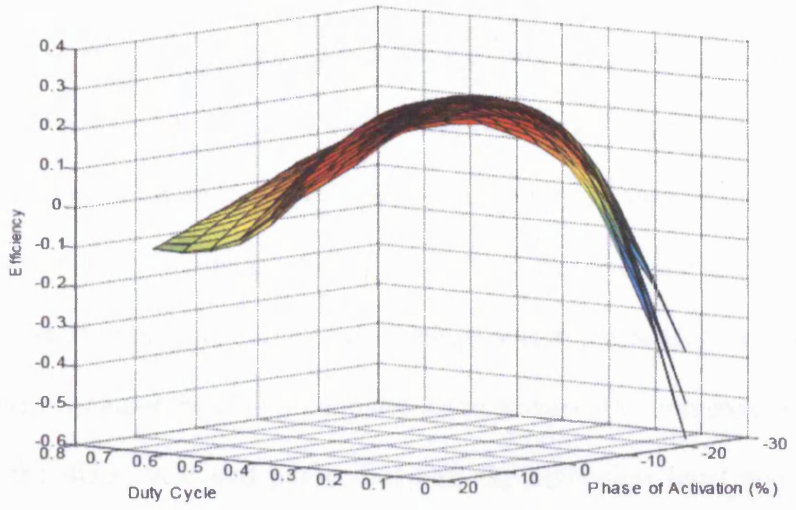

Figure 3.5

Surface plot of variation in power output (A) and efficiency (B) with duty cycle and phase of activation at three different amplitudes of activation levels. Activation levels were scaled to 30%, 50% and 100% of activation.

Discussion

The use of a validated model of muscle mechanics and energetics has allowed us to explore the relationships between activation conditions and power output and efficiency, and also to determine the effect of changing properties of the muscles architecture (SEE stiffness) and function (amplitude of length change). The major difference in the

activation conditions for optimal power as opposed to efficiency (under the experimentally measured conditions of the dogfish white muscle) are that the duty cycle is greater and the phase of activation is earlier for maximising power output. Increasing the relative compliance of the SEE allows a muscle to activate earlier in the stretch shortening cycle and allows for higher power outputs and efficiencies to be achieved than with a stiff muscle. The optimum activation conditions for both maximum power output and maximum efficiency are also closer together for relatively compliant tendons acting with larger amplitude length changes. Therefore I have demonstrated that the SEE has an important effect on activation conditions for power and efficiency.

It was assumed that during animal locomotion that a muscle's power output is constrained by the movement that it wants to perform. If the conditions of locomotion change, for instance if an animal accelerates or runs uphill, some muscles will need to increase their power output to produce the required work on the centre of mass in a limited of period of time (Gabaldon *et al.*, 2004; Roberts and Scales, 2002). To achieve the required power output the activation pattern can be varied in numerous ways, not only by changing the duty cycle and phase, but also the activation level and frequency of stimulation. Therefore there are obviously large, but finite, combinations of activation patterns that can achieve the required power output. It is likely that these activations may also be constrained by pressure towards efficiency. The results of this modelling study suggested that there are indeed activation patterns (at least for the two activation variables altered in this simulation) that achieved a combination of both. For instance, if the animal needed to produce 90% of its maximal power, it is conceivable that it would use a smaller duty cycle and activate at the beginning of shortening of the muscle to achieve the highest efficiency available for that power output (Fig 3.2).

An examination of the workloops arising from activating the muscle for optimal power and efficiency helps demonstrate the importance of the SEE in determining the conditions for optimum power output and efficiency. In maximum power conditions, the work performed by the MTU (area underneath the force-length trace) is maximised for the conditions, and is almost square in shape. For this to occur the contractile component shortens whilst at high force (and activation) and then lengthens during deactivation. This is not the case for achieving maximum efficiency and in fact the CE only lengthens whilst fully deactivated. This is necessary for high efficiencies because work is not then absorbed by the CE and less time shortening at high activation reduces the heat output during the contraction. Therefore there are distinct differences in how the muscle must be activated to achieve either maximum power or maximum efficiency.

Varying the compliance of the SEE will have the effect of altering the timing of the rise and fall of force and also the length change of the CE, therefore this will have a large influence on the relationship between conditions for optimal power or efficiency. This is confirmed in the results in Fig 3.3, which demonstrates that with a significant decrease in the stiffness of the SEE, the phase of activation required to maximise the power and efficiency is earlier than for the high stiffness. Duty cycle for these conditions changes little, except during large length change (+/- 0.2 Lo) where the maximum efficiency can be achieved with a significantly longer duty cycle of 0.22 (compared to approximately 0.1), closer to that of the maximum power. This suggests that relatively compliant tendons may enable a muscle to activate with both high power output and also high efficiency.

The amplitude of the length change of the muscle relative to its stiffness was also shown to be important in influencing the relationship between power output and efficiency. Although similar optimum values for power output and efficiency can be

achieved with muscles, regardless of compliance, the length change of the muscle during the cyclical length change heavily influences the magnitude of the maximum values achievable (under optimal activation conditions). Fig 3.4 demonstrates that longer relative length changes (about 0.2) can achieve the highest power output and efficiency of muscle with compliant SEE, whereas the stiffer SEE would require small amplitude length changes for optimal efficiency and larger length changes for optimal power output.

Whilst considering the design of a muscle, one must also examine the primary function of a particular muscle. It is interesting to note that the optimal duty factors and phases of activation are well within those recorded biologically during repetitive activation in a range of species that employ oscillatory movements. Consistently, investigators of animal locomotion have found that muscles that undergo cyclical length changes will activate before shortening begins (negative phase) and deactivate when the muscle is still shortening (Askew and Marsh, 2002; Griffiths, 1991; Tobalske *et al.*, 2003; Biewener *et al.*, 1998). This is in agreement with my findings that suggest that to have a high efficiency at any given power output, the muscle should be activated just before or after shortening begins, and the muscle should only be activated whilst the muscle is still shortening (smaller duty cycles).

The stiffness of the SEE relative to the CE length places the results of the simulations into context. It was interesting to find such a large change in the relative stiffness with an increase in animal size; however there were only small differences between human and mouse. Therefore, perhaps function of the muscle should also be considered. Fig 3.4 would suggest that the reported range of stiffness differences would not have a great effect on the maximum power output or efficiency of the muscle, however the conditions under which this can be achieved would vary greatly. For instance, MTU's with low relative SEE stiffness are likely to have undergo larger

amplitude length changes relative to the CE length and activate early during the stretch of the muscle to obtain optimal power output and maximum efficiency. This is certainly the case for many large animals, which according to Table 3.1, have low relative SEE stiffness. These muscle often have long tendons and short muscle fibres which is the architecture required for low relative stiffness. Whilst these muscles are not required to achieve high positional control, it is important that they are efficient and powerful. However, the human gastrocnemius has a shorter tendon (relative to its entire MTU length), and because of its more versatile functions may require a reduced relative stiffness, closer to that of the mouse. It is however difficult to generalise over animals who perform different functional tasks and are affected by the laws of scaling.

The timing, amplitude and duration of muscle activation are indeed important for power production and also efficient movement. During cyclical movements such as locomotion, the theoretical power output of many muscles is actually low, but under varying conditions such as acceleration and changes in grade, muscle can be required to produce (or absorb) power (Gabaldon *et al.*, 2004). The current results produce evidence that a muscle can activate with near maximum power output and also near maximum efficiency. However, to vary power output, experimental results suggest that muscles generally change the amplitude of muscle activation (measured from EMG) more so than the timing and duration (Hof *et al.*, 2002a). My simulations which vary the activation amplitude suggest that the same conditions of muscle contraction can produce maximum power output and efficiency at different levels of activation (Fig 3.5). However in changing the activation level the power output invariably drops and the efficiency of the muscle remains consistent. Therefore reducing the activation level and maintaining similar timing and duration of activation is perhaps the best method for modulation of power output in an efficient manner. This finding is supported by the results of (Hof,

2003; Hof *et al.*, 2002b) examining the human *triceps surae*. The effect of the relationship between activation level and fascicle type recruitment is of interest but beyond the scope of this paper.

There are certainly confounding issues in extrapolating these data outside the muscle types for which the model has been validated. For instance each muscle has different properties, including the maximum shortening velocity, the curvature of the force-velocity curve, the rate of activation/deactivation and basic metabolic costs. Indeed each of these factors will either increase or decrease a muscle's power producing capabilities and efficiency. However the relationships between power output, efficiency, optimal conditions of activation, SEE stiffness and amplitude of length change presented here provide an insight into why muscles (including the CE and the SEE) with specific architecture and function activate the way they do.

Conclusions

In summary, here I present a model which can be used to explore the parameter space of activation conditions that can achieve optimal power output and efficiency of muscle, and also a framework for determining the effect of SEE stiffness and length change on these optimal conditions. The results of this study show that a more compliant SEE allows the activation conditions for achieving maximum efficiency closer to that for achieving maximum power output. This is however length change dependent with a compliant SEE requiring greater length change amplitude. This has implications in the design of muscle for its specific function, with muscles with short muscle fibres (in comparison to the length change of the SEE) being more powerful and efficient with proportionately long amplitude length changes. In choosing the activation timing, amplitude and duration, simulations also suggest that biological systems would obtain

greatest benefit by using conditions of optimal efficiency and varying the amplitude of activation to achieve the required power output.

Chapter 4: Muscle fascicle and series elastic element length changes along the length of the gastrocnemius during walking and running.

Some of the work in this chapter has been accepted by the Journal of Biomechanics with co-authors Alan Wilson and Kostas Bougoulias. All work has been written originally by Glen Lichtwark, with contributions from Alan Wilson and Kostas Bougoulias. Data collection was performed by Glen Lichtwark and Kostas Bougoulias.

I have demonstrated that, theoretically, it is possible for a muscle to activate in such way to optimise its power output or its efficiency, and indeed that in some conditions a high value of both is attainable. I have also shown that this can be affected by the amount of compliance in the series elastic element (SEE). However, this has been based on data from bundles of muscle fibres from the dogfish. Does this transfer to whole muscles in larger animals, for instance humans? In this chapter, I will explore methodology which may help to characterise how muscles fascicles actually change length during human locomotion.

Introduction

The interaction of a muscle and associated tendon during dynamic activities such as locomotion is critical for both force production and economical movement. To understand the dynamics of muscle-tendon interaction it is necessary to distinguish the relative length changes of muscle's contractile parts (muscle fibres) from that of the elastic parts (tendons, aponeurosis and other connective tissues). Within animal models it has been possible to measure the length changes of muscle fibres with sonomicrometry (Griffiths, 1991; Roberts and Scales, 2004; Roberts and Scales, 2002). These studies have revealed

that compliant tendons can store and return elastic energy to change the timing and rate of muscular work and allow the contractile components to act nearly isometrically, despite substantial length changes in the muscle-tendon unit. This produces higher forces and reduces the energetic requirements on the muscle fibres. Similar results have been reported for human muscle fibres using ultrasonography (Fukunaga *et al.*, 2002; Fukunaga *et al.*, 2001).

The complex three-dimensional structure of pennate muscles complicates this measurement of muscular function. Most muscles are not homogenous in their architecture, typically comprising of muscle fibres that act at different orientations to the line of action of the muscle; the pennation angle (Epstein and Herzog, 1998; Scott *et al.*, 1993; Wickiewicz *et al.*, 1983; Woittiez *et al.*, 1984; Zuurbier and Huijing, 1993). The additional presence of elastic tissues that act in different directions when stretched, such as aponeurosis and perimyosium, further complicates muscle function (Scott and Loeb, 1995; Van Leeuwen, 1999; Zuurbier and Huijing, 1992). Numerous investigators have attempted to model how pennate muscles contract and change shape in two and three dimensions, and these studies typically find that muscle fibres do not act homogenously along the muscle's length (Otten, 1988; Van Leeuwen and Spoor, 1992). However these models are muscle specific and are not necessarily subjected to the conditions that a muscle undergoes during contraction in a real life activity such as locomotion. These models also do not generally incorporate the interaction of the muscle with other biological structures (e.g. other muscles) that can apply forces to and constrain the shape of a muscle (Maas *et al.*, 2003; Yucesoy *et al.*, 2003).

Muscle fibres may differ in length and orientation along the length of the muscle (Zuurbier and Huijing, 1991). As a result they may also shorten by different amounts and change orientation differently during contractions. This has been demonstrated in the

human biceps brachii muscle, where it was shown that the fibres act non-uniformly along the centreline of the muscle both proximally and distally (Pappas *et al.*, 2002). Similar findings have been found to occur in the rat gastrocnemius muscle (Zuurbier and Huijing, 1993). However an ultrasound study looking at the fascicle length of the *triceps surae* muscle group during graded isometric contractions showed that fibres of each of the three muscles that make up this complex were found to be homogenous in length (Maganaris *et al.*, 1998). No change in ankle angle was allowed during these contractions, whereas muscles typically undergo length changes during movements such as locomotion, which is likely to limit the application of these results in a broader context.

The assumption of muscle fascicle homogeneity during real-life muscle contractions has important implications in the modelling of muscle-tendon unit interaction. The model used by most investigators (Fukunaga *et al.*, 2001; Fukunaga *et al.*, 2002) to calculate the changes in length of the SEE makes the assumptions that the fibres are homogenous and are represented by the action of fibres from the midbelly of the muscle (Fig 4.1A). If the proximal and distal muscle fibres were to shorten or increase pennation angle more than the middle fibres then the actual length change of the muscle would be greater than that predicted from the central fascicle. A recent ultrasonography study on human walking revealed that like many animal models before, the human gastrocnemius muscle acts relatively isometrically during the stance phase, whilst the series elastic element, comprising of both the Achilles tendon and aponeurosis) stretches to store elastic energy, which is released during the take-off phase of the gait cycle (Fukunaga *et al.*, 2001). However this study was performed during very slow walking and assumed muscle homogeneity. It is likely that during faster walking and indeed running that muscle fibres will indeed be required to shorten more, so as to stretch the Achilles

tendon and aponeurosis appropriately to achieve the higher muscle tendon unit (MTU) force.

Using a novel ultrasound probe and setup, I have been able to determine and compare muscle-tendon unit interaction during the real-life activities of both walking and running. Using this technique, I tested the hypotheses that –

1. the *gastrocnemius medialis* (GM) muscle fibres undergo a homogenous length change across three sites along the length of the muscle (distal, middle and proximal) during walking and running;
2. the GM muscle fibres are shorter during running than during walking.

Materials and Methods

6 healthy volunteers (3 male, 3 female) average (mean, +/- SD) age, 31+/- 1.67 years; height, 171 +/- 8 cm; and body mass, 77+/-12 kg gave consent to participate in the study. The study was approved by a local ethics committee (RNOH JREC, 04/Q0506/11). Participants walked and ran on a treadmill at speeds of 4.5km/h and 7.5km/h respectively whilst a variety of measurements were made. A period of 2 minutes warmup was allowed to familiarize participants with the setup.

Joint Kinematics

Active CODA light emitting diodes (LEDs) were attached the following body landmarks: head of the 5th metatarsal, calcaneus, lateral malleolus head of the fibula, lateral epidcondyle of the knee, iliotibial band (halfway betwwn knee marker and greater trochanter) and the greater trochanter. The 3D position of these LEDs was determined with an accuracy of +/- 1mm by using a CODA motion analysis system (Charwood Dynamics, UK) at rate of 100Hz. Sagitall plane knee and ankle angles were determined (plane of the treadmill belt). Knee angle was defined as the angle between the line joining

the lateral epicondyle of the knee and the iliotibial band (upper leg segment) and the line joining the lateral maleolus and the head of the fibula (lower leg segment). Ankle angle was defined as the angle between the lower leg segment the line joining the head of the 5th metatarsal and the calcaneous (foot segment). The markers on the 5th metatarsal and calcaneus were also used to determine the events of the stride cycle, as will be explained later.

Muscle Archictecture

A PC based ultrasound system (Echoblaster 128 , UAB 'Telemed', Vilnius LT-02189, Lithuania) was used to image the *medial gastrocnemius* muscle fibres in the sagittal plane. In this experiment I used a 128-element, linear, multifrequency ultrasound probe at a frequency of 7 MHz and with a field of view of 60mm in B-mode. Images are collected by a PC and recorded in cineloop at 25 frames/second. The images are then saved as a video file for further analysis.

The probe was attached to the GM muscle such that it imaged a sagittal section to the leg (Fig 4.1B). The probe was aligned to the midline of the muscle so that it was approximately in the same plane that the muscle fibres ran. Measurements were made at three levels of the muscle; the midbelly and distally and proximally to this position. The proximal and distal positions were defined as 35mm from the midbelly position which was assessed visually. A fixed distance was used because variation in Achilles tendon length (and hence muscle belly length) amongst the small population prohibited the use of any scaling of position.

Muscle fascicle length was defined as the straight line between the upper muscular fascia and the lower muscular fascia parallel to the lines of collagenous tissue visible on the image (Fig 4.1B). Only one measurement was made in each image because typically only one area could be visualised fully without having to extrapolate out of the field of

view. This measurement was consistently made in the middle of image where the length of the fascicle could be imaged. The pennation angle was defined as the angle made between the upper fascia (the line of action of the tendon) and the direction of the muscle fibres (Fig 4.1B).

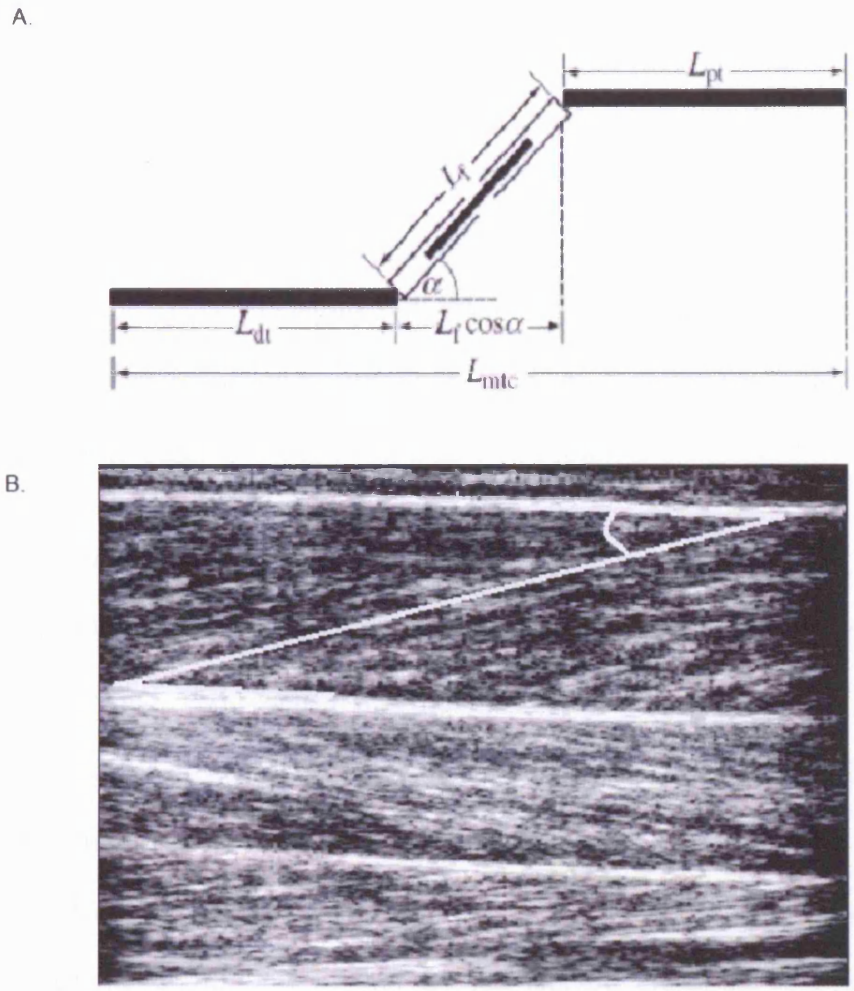

Figure 4.1

A. The musculoskeletal model used by Fukunaga et al (2001) to estimate tendon length changes. In this model, the total change in SEE length (ΔLdt+ΔLpt) is equal to the change in muscle tendon unit length (ΔLMTU) minus the change in muscle fascicle length change in the direction of the SEE (Δ(Lf.cos.α)) which I will call the change in contractile component length (ΔLcc).. This model assumes that ΔLcc can be represented by a single fascicle's action (Δ(Lf.cos.α)). However if we consider multiple fibres along the length of the muscle then ΔLcc is the average length change of each of these fibres in the direction of the tendon (assuming that the fibres are evenly distributed along the length of the muscle). **B.** Ultrasonound image of the *gastrocnemius medialis* muscle in the sagittal plane at the level of the midbelly. Muscle fascicle length was measured as the length of the white line from the upper fascia to the lower fascia and pennation angle was defined as the angle made between the upper fascia (the line of action of the tendon) and the direction of the muscle fibres.

Synchronisation

The motion analysis data was synchronised with the ultrasound data using a digital output signal from the CODA motion analysis system that signified that the system was collecting data. This signal activated a signal generator that fed a 5MHz signal to a sonomicrometry crystal (Sonometrics Ltd, Ontario, Canada) attached to the end of the ultrasound probe. This produced a white signal on the ultrasound picture on the end ultrasound probe crystals.

Determination of Events

The vertical velocity of the calcaneus marker was used to determine when the foot contacted the ground. Foot contact was defined as the time when the vertical velocity crossed from negative to positive. The beginning of swing phase was defined as the time when the calcaneus marker had a postitive vertical velocity and the 5^{th} metatarsal marker changed from a negative horizontal velocity to a positive one. This technique made for a consistent predictor of the time of foot on and foot off under the conditions of both walking and running.

Measures of muscle fascicle length and orientation were made at 0, 20, 40, 60, 80 and 100% of both stance and swing phases (10 measures in all for each cycle). This was done by a spline interpolation of the data measured at 25Hz. In total, three strides for each participant and each condition (gait and probe placement) were analysed and an average at each of the 10 interpolated measurement sites during the stride was found.

The stride was further divided up into the following specific events from the average kinematics: T1-Heel strike; T2 – Foot flat (approximate end of double support for walk), when line of the foot was approximately in line with the horizontal treadmill; T3 – Heel off, when the heel marker left the approximate line of the treadmill; T4 - Toe off; T5

– Heel strike. These times were not validated because they are merely descriptors to aid the description of the results.

Three full stride cycles of ultrasound data were analysed for each participant at both walk and run for each of the three probe sites (proximal, midbelly and distal). A repeated measures analysis of variance (ANOVA) was performed with probe site as a factor and stride time as a repeated measure to determine muscle shortening homogeneity. A univariate ANOVA was also performed at each time interval across the gait cycle to determine where differences in muscle lengths occur due to probe site.

Muscle-tendon length measures

The ankle and knee angles were interpolated to 100 points across the time of a complete gait cycle. These 100 points were then averaged across 5-10 strides (depending on how many occurred during 10 second collection time) for each subject and these were further averaged across all subjects. Length changes of the GM muscle-tendon unit length were estimated for each individual stride from the average joint angle data using the equations derived by Grieve and colleagues (1978). The average shank length of the each of the six subjects (0.361 +/- 0.23 m) was used to determine the absolute length change of the MTU across the gait cycle (Grieve *et al.*, 1978).

To estimate the SEE elongation, muscle fascicle lengths and the pennation angle from the ultrasound images were used along with the whole muscle-tendon length in the same model proposed by Fukunaga *et al* (2001) (see Fig 4.1A). This was done for each of the measures at the proximal, middle and distal measurement sites and then a model combining the average length change of all three measurement sites was used to calculate an approximate tendon length change (described in Fig 4.1A). The length of zero strain (or zero length) was approximated from the length of the tendon at 10% through the swing phase; a time when zero force should be applied through the tendon. This is

supported by the data of Ishikawa *et al* (2005a), who implanted transducers into the tendon and reported that the tendon force was zero briefly after the foot left the ground.

Results

The mean muscle fascicle length and pennation angles at each of the three sites along the muscle (distal, midbelly and proximal) throughout the gait cycle are shown in Fig 4.2. At heel contact in both walking and running, the fibres are at a similar lengths and pennation angles, however their pennation angle varied across measurement sites. The results show that the distal fibres act at a more acute angle throughout the entire gait cycle. With respect to the gait cycle, the muscle fibres first shorten rapidly from heel contact until the foot is flat on the treadmill surface (times T1 to T2) in both gaits. During this time the ankle is plantar flexing and the whole muscle tendon unit (MTU) is also shortening (Fig 4.3).

During walking, the fibres then act isometrically (showing very little length change) until the heel leaves the ground (T3). However, across the muscle measurement sites the fibres are at statistically different lengths at all of the times measured during the stance phase (T1-T3) ($P < 0.05$). During this time, the distal muscle fibres are at shorter lengths (appoximately 48mm) compared to both the proximal and midbelly fibres (approximately 52 and 53 mm respectively). The fibres also undergo very little change in pennation angle during this time. As the ankle begins to plantar flex, during the push-off phase of the gait cycle, fibres at all levels shorten by 9-18% from proximal to distal sites. As the foot leaves the ground for the swing phase (T4-T5) the fibres continue to shorten until midway through the swing phase when they lengthen back to their starting length. The shortening of the muscle fibres during this period also corresponds to the shortening of the whole muscle tendon unit (Fig 4.3). The shortening and lengthening of the muscle fibres during the swing phase (T4-T5) is also accompanied by, initially, an increase in

pennation angle followed by a rapid decrease in pennation angle at the end of the swing phase.

In contrast to walking, during running the muscle fibres shorten throughout the entire stance phase (T1-T4). The highest rates of shortening occur from T1-T2 and T3-T4, where muscle fascicle lengths shorten at approximately 0.94 muscle lengths per second as opposed to 0.58 muscle lengths per second from T2-T3. The muscle fibres shorten by approximately 23% from T1-T4, however only 40% of this length change occurs during the period when the whole foot is planted on the surface (T2-T3). This shortening of the fibres is also accompanied by increases in the pennation angle throughout the stance phase. Once the foot leaves the ground (T4) there is further shortening of the fibres (and increases in pennation angle). During running, the muscle fibres shorten to approximately 35mm at foot off from 55mm at foot on, which is a 5mm (9%) shorter minimum length than during walking. Again the muscle fibres begin to lengthen midway during the swing phase, when the knee begins to extend and the ankle dorsi-flexes.

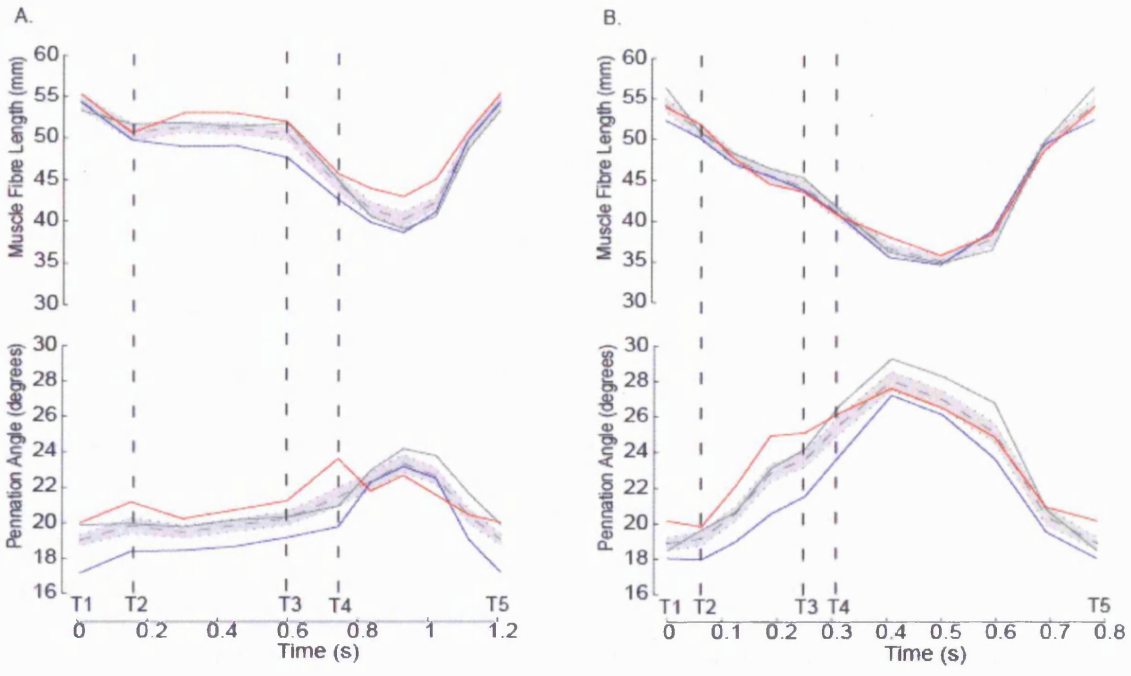

Figure 4.2

Average length and pennation angle of muscle fibres across one complete stride (heel on to next heel on) during walking (**A**) and running (**B**) for each of the three ultrasound sites (distal = blue; medial = green; proximal = red). The dashed line represents the average muscle fascicle length and pennation angle across all three sites and the 95% confidence interval of the pooled data across all three measurement sites (as calculated with a general linear model) is demonstrated by the shaded area. The stride is divided up into the following specific events averaged from the kinematics: T1-Heel strike; T2 – Foot flat; T3 – Heel off; T4 - Toe off; T5 – Heel strike.

The results of the repeated measures ANOVA show a significant difference in both fascicle length and pennation angle between the three sites of measurement across the whole gait cycle ($P = 0.003$, $P < 0.001$ for walking fascicle length and pennation angle respectively and $P = 0.045$, $P < 0.001$ for running). However the post hoc univariate ANOVA shows that most of this difference occurs during the stance phase of walking, where the distal fibres are shorter than the proximal and midbelly fibres, and during the swing phase of both walking and running. It is apparent that differences in the change in fascicle length and angle exist between the measurement levels, however the fibres do

perform similar actions regardless of site; fibres follow the same shortening and lengthening trajectory. The averaged trajectory is shown in Fig 4.2, along with the 95% confidence interval of the pooled data, assuming that each measurement site is subject to the same variation. Each of the measurement sites lies close to the confidence interval of the average and the effect of the difference is small.

Fig 4.3 demonstrates the change in GM MTU length across the gait cycle as participants changed from walking to running. During both walking and running the ankle initially plantar flexes before dorsi-flexing throughout the weight bearing period of stance phase. However it is apparent that during running the ankle begins in a more dorsi-flexed position (closer to 90 degrees) and undergoes a greater degree of dorsiflexion through the stance phase; approximately 20 degrees more (T2-T3). In walking the knee stays relatively extended during this period, only flexing a small amount (< 10 degrees). In contrast however, the knee bends by up to 40 degrees more during the stance phase in running. Therefore, the change in gait from walking to running is accompanied by both an increase in ankle dorsi-flexion and an increase in knee flexion. This results in a longer MTU throughout stance (T1-T3) during running (Fig 4.3), where the MTU extends up to 6 mm longer during the stance phase in running.

As the heel leaves the ground the ankle plantar flexes rapidly in both gaits. During walking this is accompanied by flexion of the knee, whereas the knee is still extending the running gait. In both cases, the result is a rapid shortening of the MTU during the push off phase (T3-T4). During walking the maximum shortening speed at this period is up to 6 muscle fascicle lengths per second, whereas it is only 4.5 muscle lengths per second in running. During the swing phase the MTU shortens synchronously with ankle plantar flexion and then begins to lengthen during the ankle dorsiflexion movement. During

walking the MTU is lengthened back to its starting length by 60% of the swing phase, whereas this occurs later in running (approx 70%).

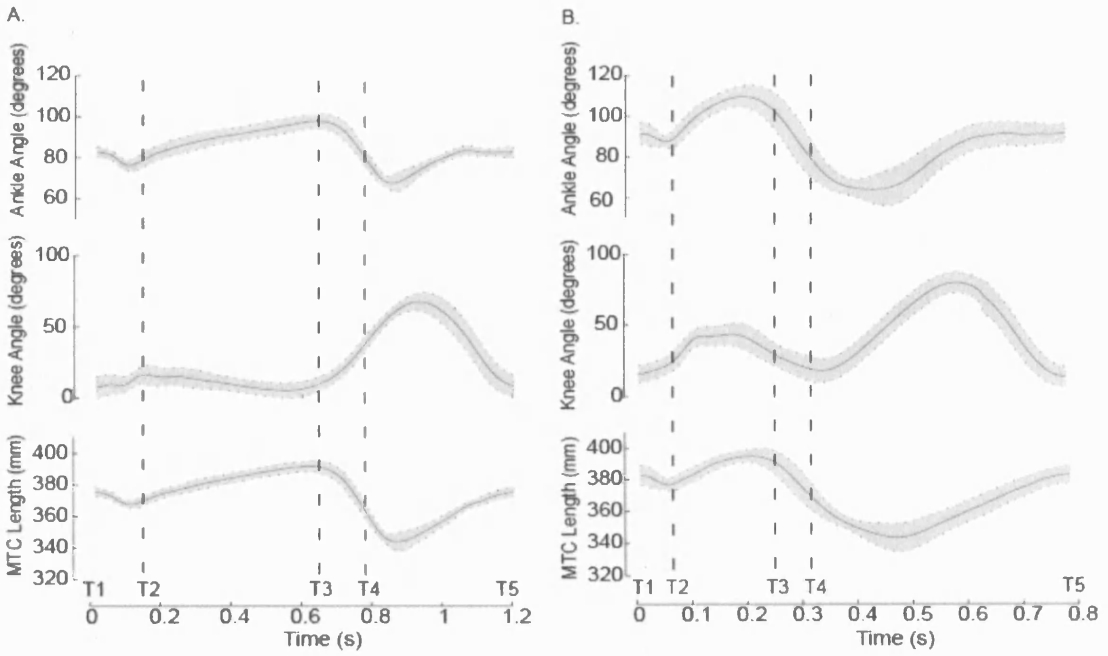

Figure 4.3

Average ankle and knee angles for one complete stride and the corresponding estimation of gastrocnemius muscle tendon unit length for walking (**A**) and running (**B**). The shaded area represents the 95% confidence interval. The stride is divided up into the following specific events averaged from the kinematics: T1-Heel strike; T2 – Foot flat; T3 – Heel off; T4 - Toe off; T5 – Heel strike.

The calculated SEE elongation for each of the three measurement sites and the elongation calculated using the averaged muscle model are shown in Fig 4.4 relative to the gait cycle for walking (4A) and running (4B). During the first portion of the walking stride, when the ankle is plantar-flexing and not weight bearing (T1-T3), it is apparent that the SEE has a negative elongation. This corresponds to the SEE being 'slack', however the absolute zero length is not accurately known. During the weight bearing portion of walking stance (T2-T3), there was a gradual increase in the SEE length, peaking at an average calculation of 17.5 mm elongation using the three measurement

sites. In contrast, during running the SEE was longer at heel strike and possibly already stretched. During the first portion of the gait cycle (T1-T2) it shortens towards its zero length before rapidly elongating to 23.5mm of stretch during the weight-bearing phase (T2-T3).

Throughout the push-off phase (T3-T4) the SEE rapidly shortens in both walking and running to be slack within 0.12 seconds in both cases. It continues to 'shorten' throughout the early stages of the swing phase before lengthening again in the final half of the swing phase back to its initial length in the gait cycle.

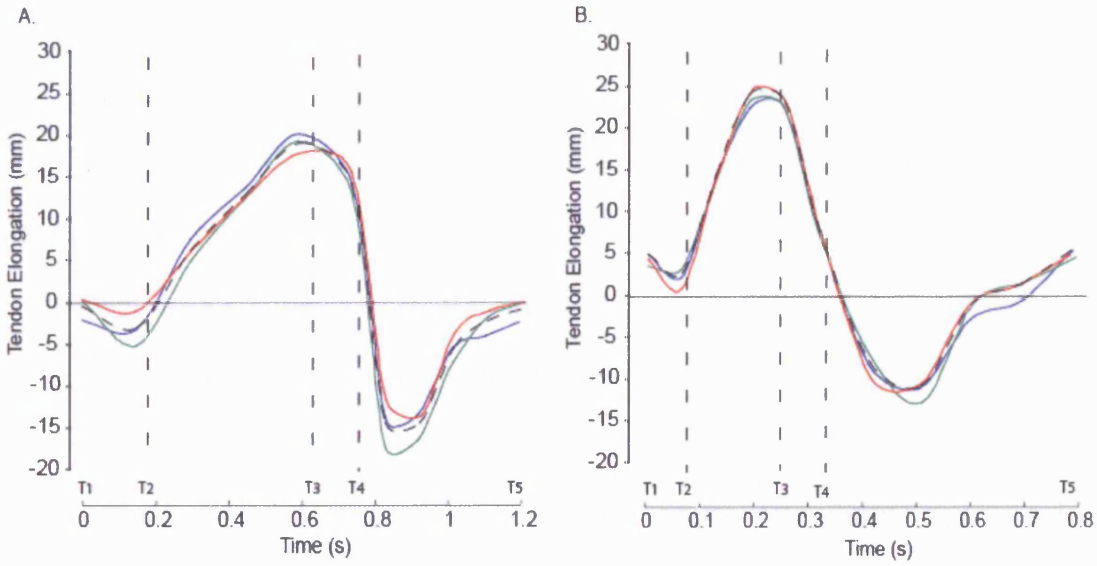

Figure 4.4

Calculated SEE elongation during the gait cycle for walking (A) and running (B) using each of the three ultrasound sites (distal = blue, midbelly = green, proximal = red) and the average muscle fascicle length change (dashed line). The stride is divided up into the following specific events averaged from the kinematics: T1-Heel strike; T2 – Foot flat; T3 – Heel off; T4 - Toe off; T5 – Heel strike. The length of zero strain (or zero length) was approximated from the length of the tendon at 10% through the swing phase; a time when zero force should be applied through the tendon.

The three measurement sites do differ in their predictions of SEE elongation, however it is apparent that the midbelly is a relatively good approximation of the SEE elongation calculated from using the average from all three sites .The largest discrepancies occur during the initial period of foot contact (T1-T2) and also during the swing phase, times when the loading of the SEE is small.

The individual subject variation in muscle fascicle length and length changes through the running stride cycle are shown (Fig 4.5A) along with the resultant calculation for individual tendon elongation (Fig 4.5B). During the stance phase it is apparent that each individual does indeed shorten their GM fibres, however by varying amounts. One participant had notably longer muscle fibres than the other participants, and this

participant's fibres act relatively isometrically during the stance phase. The SEE elongation also demonstrates that some participants stretch their tendons more than others and that the trajectory in time may also differ. Two participants stretched their SEE by up to 20 mm more than the others, while one participant doesn't undergo a period of SEE shortening during initial foot contact. However, all participants showed a substantial stretch of the SEE during the stance phase and a rapid shortening phase during the push-off phase.

The individual variation in muscle-tendon mechanics is further highlighted in a plot of the fascicle length change against the tendon length change (Fig 4.5C) during running. This figure may be thought of as a 'work loop' (a graph of muscle force *versus* muscle length), assuming that the SEE has a relatively linear relationship between length and force. Negative SEE elongations are assumed to produce zero force. It is apparent that in the majority of participants (with the exception of participant 6), the muscle fibres shorten only a small amount as the force rises. Most of the shortening then occurs during the decline of force, however the trajectory of this length change varies greatly between subjects.

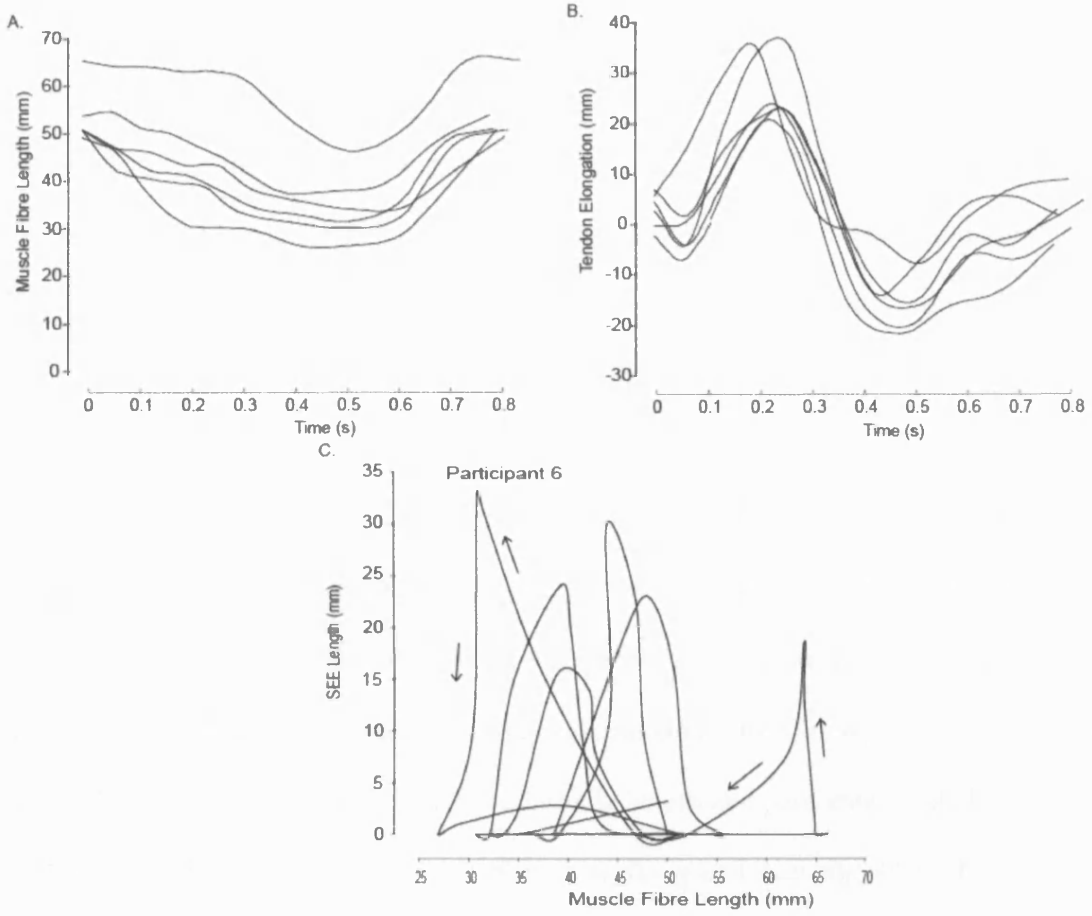

Figure 4.5

A. Average individual variation in muscle lengths across a complete running cycle for each of the 6 participants. Data for each of the three probe positions was pooled for each individual. **B**. Calculated individual SEE elongation for each of the 6 participants during a complete running cycle. In both figures the same colour corresponds to one individual. **C.** SEE length vs muscle fascicle length for each of the 6 individuals (with participant 6 marked) using the average SEE length change calculated from all three sites during the stance phase only (T1-T4). The loops go counter-clockwise, as indicated by the arrows on two examples. Negative values of SEE length (below that of the slack length) are ignored as these correspond to zero force.

Discussion

Using ultrasound to analyse muscle-tendon unit interaction during different gaits has provided valuable insights into real life muscle mechanics. The results of this study have shown that muscle fibres perform the same actions along the length of the human GM

muscle during locomotion, regardless of speed or gait. However, they do not act totally homogenously along the muscle's length; the distal fibres tend to shorten more and act at greater pennation angles than the more proximal fibres. The effect of the difference on calculation of SEE strain is minimal. There is also a difference in the action of the muscle fibres during running compared to walking, where the muscle fibres shorten more to produce the greater amount of work required during the stance phase of running.

The results of this investigation have demonstrated that the pennate GM muscle fibres act in a similarly along the length of the muscle throughout the gait cycle for both walking and running. This supports the isometric data of Maganaris (1997) from the same muscle. However, statistically significant differences in their length changes do occur at various times in the gait cycle in both walking and running within the population analysed. The biggest variation in muscle fascicle length and pennation angle between the sites occurred during the swing phase of both walking and running; when the muscle is typically unloaded. These variations are likely to be due to local stresses placed on the muscle fibres by connective tissue which can transmit forces from other muscles and skeletal structures (Maas *et al.*, 2003) and from internal pressures resulting from the change in shape of the muscle itself (Otten, 1988; Van Leeuwen and Spoor, 1993).

During walking there was a difference in muscle fascicle length at each level during the stance phase, although at all sites the muscle fibres acted almost isometrically. The difference in length change is again likely to be due to differences in the local stresses applied to the muscle fibres and also the internal pressure (Van Leeuwen and Spoor, 1993). For instance, the distal fibres are likely to have shortened by a greater amount than the central fibres which will have greater internal pressure placed on them as the muscle shortens and becomes fatter around the midbelly. The architecture of the muscle also dictates that the distal fibres are likely to be at a shallower angle to the line of

action of the tendon throughout the contraction. In addition, it is possible that greater measurement error is associated with measurements at the distal and proximal probe positions, where shape changes of the muscle distort the images due to movement of the muscle fibres out of the plane of the ultrasound probe.

The measurement of muscle fascicle length from the ultrasound data assumed that the muscle fibres ran in parallel straight lines from the upper fascia to the lower fascia. Experimentally it has been shown that the muscle fibres in fact experience a degree of curvature during muscular contraction that can significantly affect their measured length (Muramatsu *et al.*, 2002b). That study also demonstrated that curvature increases with force (or level of contraction) therefore it is possible that the length changes measured in this study during running (where forces are higher) underestimate the length of the muscle fibres by up to 6% of the fascicle length. This would mean that the length change and muscle fascicle shortening velocity that is measured is also slightly overestimated here. However, this does not affect the calculation of the SEE strain from these measures, which are only concerned with the linear length change of the tendon resulting due to the shortening of muscle fibres in that axis.

Applying a muscle model to determine the SEE strain (including the Achilles tendon and associated aponeurosis) during walking and running revealed that the SEE does indeed stretch throughout the stance phase so that it can recoil rapidly and achieve high power output at the end of stance (T4 in Fig 4.4). This allows the muscle-tendon unit to shorten at high speeds. These data are in agreeance with the data of Fukunaga and colleagues (2001), however it also demonstrates that the SEE continues to strain further with the change in gait. It is encouraging that the elongation of the SEE corresponds to the typical shape of the ankle plantar flexion moment measured with inverse dynamics and the forces measured directly at the Achilles tendon during walking and running

(Komi, 1990; Novacheck, 1998). Given the relatively linear force-length relationship of tendon and the fact that the Achilles tendon is the major tendon responsible for plantar flexion, this result supports that the Achilles tendon strains I have measured are realistic. However it is impossible to distinguish from this model as to where the majority of strain occurs, in the Achilles tendon or other SEE's such as aponeurosis, and which muscles of the *triceps surae* contribute most to stretching the SEE. It has been suggested that the aponeurosis does indeed strain significantly during gastrocnemius contraction (Muramatsu *et al.*, 2002a) and this must be considered along with the Achilles tendon. More direct measures, either using surgically implanted strain gauges at different sites of the elastic structures or by direct ultrasonographic measurement of the length changes, are required to determine these individual strains during locomotion.

The strains predicted by this model are at the higher end of the acceptable strains before tendon rupture as measured *ex vivo*, despite the running speed being extremely slow compared to the participants' physiological maximum running speed. Here we have measured the length change of the SEE, which consists of numerous elastic elements within the muscle, therefore perhaps the GM serial connective tissue can strain to these values. The length change of the SEE reported here is consistent with that of numerous other investigators during both dynamic activities and isometric contractions. Using the same muscle model has yielded estimates of up 20mm of stretch (~10% strain) during dynamic counter movements and up to 9mm during slow walking (~5% strain) (Kawakami *et al.*, 2002; Fukunaga *et al.*, 2001). However, these models depend highly on the definition of the point of zero strain and co-contraction of the *tibialis anterior* muscle can cause an underestimation of the point of zero strain. More direct measures of Achilles tendon strain which don't rely on this model also agree that during isometric contractions, the Achilles tendon can stretch by up to 15mm (Maganaris and Paul, 2002). Therefore,

perhaps the accepted estimates of tendon compliance based on *ex vivo* material testing of this tendon need to be revisited.

The unique architecture of the Achilles tendon must also be considered in combination with changes in shape of both heads of the gastrocnemius muscle. Material testing on the Achilles tendon and other such compliant 'anti-gravity' tendons is commonly done on the distal part of the tendon where the cross-sectional area of the tendon is greatest. In this region the tendon has an elliptical cross-sectional area. As the tendon moves more proximally it begins to fan out to attach to the two heads of the gastrocnemius muscle and the soleus muscle. During contraction of the gastrocnemius muscles, both muscles tend to become shorter and fatter in the middle and narrower at the end to conserve their volume and hence it is difficult to tell where strain in the SEE might occur.

Energetically it seems more expensive to have to shorten the muscle fibres during running. However it is apparent that the muscle fascicle never exceeds a shortening velocity of above 1.5 lengths per second even during running. In fact, at the point of peak tendon stretch (peak force) the velocity of the muscle fibres doesn't exceed 0.54 lengths per second at all levels of the muscle. This is a very slow speed for muscle to contract at considering that the maximum velocity of muscle contraction is about 10-13 lengths per second (Zajac, 1989). A muscle produces maximum power output at around 30% (Woledge *et al.*, 1985) of its maximum shortening velocity (V_{max}) and maximum efficiency at around 15% V_{max} (Hof *et al.*, 2002b). Therefore the muscle is in fact acting at a relatively optimal level (15% V_{max}) to produce high forces with small amounts of work and high efficiency. In contrast to the velocities of muscle fascicle shortening, the work done on the tendon allows MTU shortening velocities of up to 6 muscle fascicle lengths per second to be achieved during recoil of the tendon and shortening of the

muscle at take-off. Therefore the complex interaction between the muscle fibres and the attached tendon allows the muscle to operate with more optimal conditions. This is in agreement with the data turkey ankle extensor data of Roberts and colleagues (1997).

The results of the study also indicated that a great deal of individual variation exists with regards to muscle mechanics during running. Running styles can be classified relative to the kinematics, where people are often grouped into such categories as heel landing runners and fore-foot landing runners. The difference in running technique undoubtedly varies the length profile of the GM muscle and hence the muscle fibres are likely to act differently to produce the required force throughout the stance phase. These differences are highlighted in Fig 4.4, where muscle fibres of some subjects act almost isometrically, while others shorten a great deal during stance. However it is also apparent that there is individual variation in the peak Achilles tendon stretch achieved between participants. Recent studies have indicated that the stiffness of the Achilles tendon may indeed adapt to the athletic requirements made of it and that large variation in Achilles tendon stiffness may exist (Fukunaga *et al.*, 2000; Hof, 1998). Although the population group from the present study was too small to be able to speculate on the reasons for such variation, it is possible that athletic performance may have a role in adapting the mechanical properties of the Achilles tendon for optimal performance. The effect of running speed was also beyond the scope of this study. The running speed used here was slow, with increasing speed peak limb, and tendon, force would be higher which would result in greater stretch of the SEE which may result in a greater difference between sites. This would increase rather than decrease the overall difference between walking and running.

Conclusions

In summary, the results of this study suggest that the GM muscle fibres act similarly along the length of the muscle during locomotion, although significant differences in both length and pennation angle do occur (particularly under low force conditions such as walking). There are differences in both the length change trajectories of both the muscle fibres and also the whole muscle tendon unit when comparing between gaits, and these differences allow the SEE to stretch so that a greater force can be produced during running (equivalent to greater stretch) and the timing of the length change is comparable to the shape of typical ankle joint moments during these gaits. The compliance of the SEE allows the muscle fibres to shorten at a much slower speed, more concomitant with their optimal speed for maximal power output and efficiency, with high velocity shortening during take off in both walking and running achieved by recoil of the SEE. High strains that may be thought dangerous for elastic tissues such as tendon were estimated in this study, therefore further investigation into the nature of the stretch of the SEE and where this occurs is required.

Chapter 5: *In vivo* mechanical properties of the human Achilles tendon during one-legged hopping

This chapter has been accepted for publication to the Journal of Experimental Biology with co-author Alan Wilson. All work has been written originally by Glen Lichtwark.

In earlier chapters, I identified the importance of the interaction of the contractile element (CE) of a muscle with that of the series elastic element (SEE) in producing efficient and powerful muscular contractions. The ultrasound method for analysing muscle fascicle length changes provides a technique for measuring the CE of the muscle-tendon unit. In this Chapter, a method for analysing length changes of one component of the SEE is discussed, which allows for an approximation of the material properties of the tendon to be made.

Introduction

Muscles attach to the skeleton via tendons which transfer forces to the skeleton and the environment. Tendons consist primarily of a collagenous matrix that has elastic properties. This enables them to transmit force relative to the amount of the stretch that they experience (Koob and Summers, 2002). This mechanical property allows them to store and return elastic strain energy during locomotion and other movements (Griffiths, 1991; Fukunaga *et al.*, 2001; Roberts *et al.*, 1997; Alexander, 1988). In particular, the compliance of a tendon is critical in determining the timecourse of power output of the muscle (Roberts, 2002; Lichtwark and Wilson, 2005). There have been few studies that have been able to directly determine tendon strain and energy storage in human tendons during real-life movements (Fukunaga *et al.*, 2001; Hof *et al.*, 2002b). Here I apply a

novel technique to determine the *in vivo* mechanical properties of the whole human Achilles tendon (AT) during a high strain movement.

The mechanical properties of tendon have been shown to be relatively uniform across a range of vertebrate animals (Bennett *et al.*, 1986; Pollock and Shadwick, 1994). Many *ex vivo* mechanical tests have been carried out on tendons to determine how much energy it can store and return, its ultimate tensile strength and how repetitive loading affects the tensile strength (Bennett *et al.*, 1986; Ker *et al.*, 2000; Wang and Ker, 1995; Ker *et al.*, 1986). However, much of this work has been carried out on cadaveric animal material which may have undergone material changes as a result of the preservation process (Smith *et al.*, 1996).

In vivo measurements of mechanical properties of the AT have demonstrated mixed results compared to those measured *ex vivo*. Measures of the mechanical properties of the AT have demonstrated that there is variation in tendon stiffness and elastic modulus between individuals (De Zee and Voigt, 2001; Hof, 1998; Maganaris, 2002; Maganaris and Paul, 2002). Ultrasonography and magnetic resonance imaging (MRI) studies have recently reported strains of the AT ranging from 5-10% at forces below the maximum possible force during dynamic movements (Muramatsu *et al.*, 2001; Ishikawa *et al.*, 2005a; Ishikawa *et al.*, 2005b; Finni *et al.*, 2003; Maganaris and Paul, 2002). It has previously been thought that such high strain would cause tendon rupture and failure; however real-life activities such as one-legged hopping can induce much larger stresses and strains on the AT without inducing acute rupture (Komi, 1990; Ishikawa *et al.*, 2005b).

I seek to understand the amount of energy stored and returned from the AT under *in vivo* conditions where high strain is achieved. This will give an indication of the capacity for the AT to recycle mechanical energy during real life movements and

determine whether there is individual variation in the mechanical properties. I hypothesise that the AT acts like a classic energy storing spring which stores and returns a substantial proportion of the energy required for the hopping movement. In addition, I hypothesise that the high strain movement will provide further evidence for variation in AT stiffness amongst individuals due to the greater range of data available.

To test this hypothesis it is necessary to determine the length of the tendon and the force exerted during a dynamic activity that will induce large tendon strains. Therefore the aim of the experiment was to determine the *in vivo* AT length and force changes during one-legged hopping and hence the stress-strain relationships of individual ATs. I introduce a method that combines ultrasonography and motion analysis to make an estimate of the mechanical properties of tendons during the dynamic movement of one-legged hopping. This is a high force movement (Komi, 1990), due to the forward position of the ground reaction vector relative to the ankle joint centre, and will allow a greater range of the force-length properties to be explored. Although it is likely that differential strain patterns will occur along the tendon (Lyman *et al.*, 2004; Finni *et al.*, 2003), here I require the absolute force-length relationship during the high force activity of one-legged hopping.

Materials and Methods

Achilles tendon strain and elongation

Strain is fractional elongation of the tendon. To measure this, the tendon length must be measured along with the length that corresponds to zero force determined. The AT length was defined as the distance between the tendon insertion and the muscle-tendon (MT) junction. To determine this length change, I used the CODA active marker, motion analysis system and determined the accuracy of length measurement in the experimental

configuration to be better than 0.40 mm in 50% of cases. This is in line with manufacturer's specification.

The AT runs from the insertion on the calcaneous to its junction with the *triceps surae* muscle group, which is most proximal at the junction with the two heads of the *gastrocnemius* muscle (Fig 5.1a). The position of the insertion was tracked by attaching a CODA marker over the tendon insertion. In this position the LED attachment is within 4mm of the tendon insertion and the offset is orthogonal to the tendon elongation. The effect of skin movement on tendon length was determined in the direction of action of the tendon using B-mode ultrasound imaging. This was done by placing an echogenic marker on the LED attachment site and taking transverse ultrasound images of the heel of the foot whilst it underwent the full range of motion used during one-legged hopping.

The position of the MT junction and the calcaneous relative to the global coordinate system was determined by a combination of ultrasonography and motion analysis. The MT junction was imaged by ultrasound whilst synchronously determining the position and orientation of the ultrasound image. Therefore the position of the MT junction could be projected into three-dimensional space and the distance from this point to the calcaneous marker determined as the AT length (Fig 5.1b). Details of the methodology and potential sources of error of this method are discussed further below. Tendon strain at any time was determined by dividing the instantaneous length of the tendon by the length of the tendon at zero force (taken as 200 N).

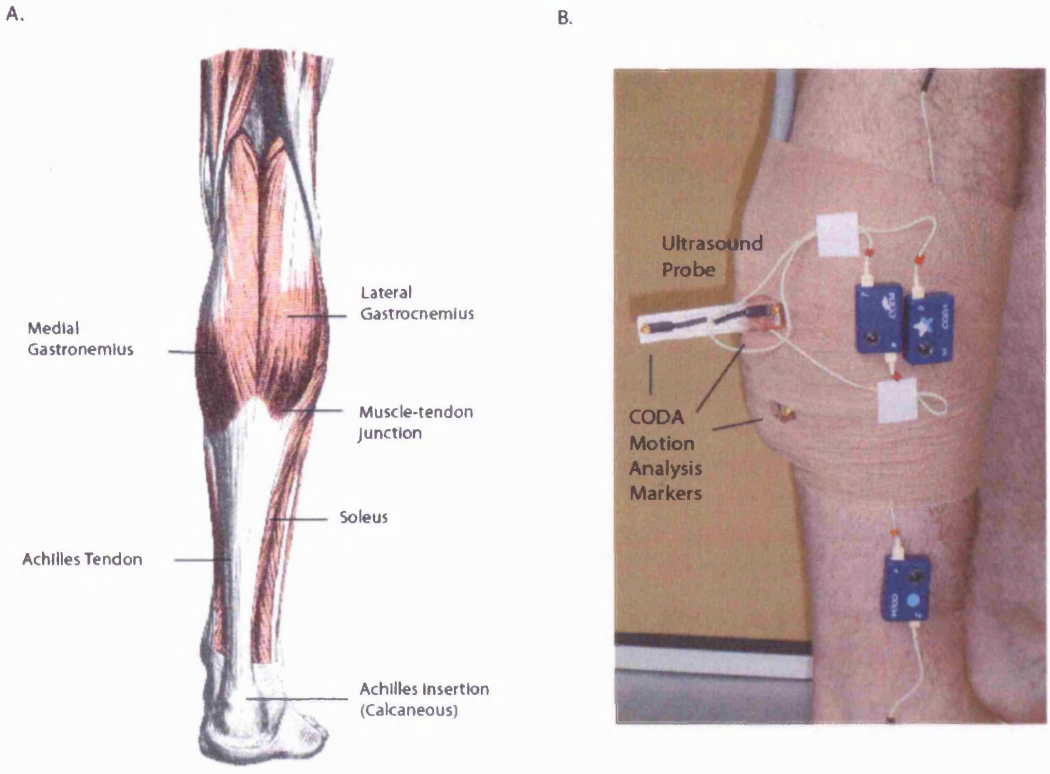

Figure 5.1

A. Anatomy of the *triceps surae* muscle group and the Achilles tendon (adapted from Gray's anatomy) **B.** Photograph of the attachment of the ultrasound probe to the leg. Three markers are rigidly attached to the probe by way of a fibreglass mould. This setup allowed for images of the gastrocnemius muscle tendon junction to be visualised in the sagittal plane of the leg (see Fig 5.2).

Determination of the muscle tendon junction position

Movement of the MT junction site was determined by ultrasound imaging. The same ultrasound setup as used in Chapter 4 was used to image the junction of the AT and the *lateral gastrocnemius* muscle fibres in the sagittal plane (Fig 5.2). The junction was imaged approximately 1cm laterally to the position where the *medial* and *lateral gastrocnemius* muscles join, which allowed for successful imaging of the MT junction. Images were again recorded at 25 frames/second and saved as a video file for further analysis. The position of the MT junction was tracked in the two dimensional image at

each frame (Fig 5.2). This was further spline interpolated to a frequency of 100Hz to match that of the CODA data.

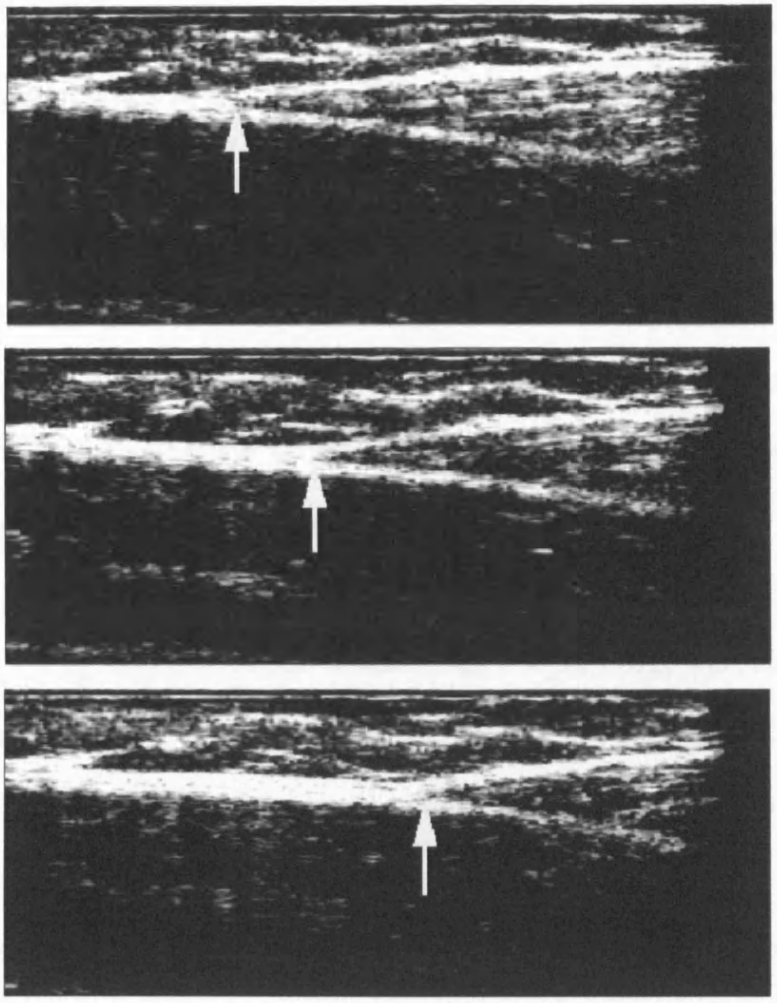

Figure 5.2

Images of the Achilles tendon junction with the *lateral gastrocnemius*. The tendon is the thick white structure to the left of the arrow, while the muscle fascia branches off this white structure to the right. The arrows represent the point that was tracked in the image for each frame during the hopping movement.

Synchronous motion analysis allowed the position and orientation of the ultrasound probe in the global coordinate system to be determined. This was achieved by attaching three markers to the probe such that two markers lay along the axis of the ultrasound probe and one in approximately the same plane as the image, a distance of approximately 70mm away from the line of the other two markers (Fig 5.1). The motion analysis data were synchronised with the ultrasound data as in Chapter 4.

The position of the ultrasound image relative to the probe coordinate system was required so measurements in the ultrasound image plane could be projected into the 3D global coordinate system. To do this the point of a metallic wand was tracked in 3D space using three CODA markers attached to the wand. The position of the wand tip relative to the three markers was first determined and the tip of the wand was then immersed into a water bath that was scanned by the ultrasound probe. Because metal is highly echogenic, it was possible to easily identify the point of the wand when it was in the plane of the images being scanned by the ultrasound probe. Three points (relative to the probe axis frame) in the plane of the image are required to translate the 2D coordinate data back into the 3D space. The average coordinate of three corners of the image were chosen to define the image plane relative to the three markers defining the probe axis system.

Points tracked in the 2D ultrasound image could then be embedded back into the laboratory frame of reference to get the 3D position relative to the laboratory. This was a two step procedure. First the coordinates measured in the 2D image were embedded into the corresponding probe axis system, which was fixed relative to the image. The marked 3D coordinates were then embedded into the laboratory reference frame.

Ultrasound Accuracy and Sources of Error

To determine the accuracy of the calibration and ultrasound measurements, I scanned a Perspex phantom located in the laboratory coordinate system that consisted of two Perspex sheets with grooves cut into them which corresponded to an approximate length and position of the muscle fibres relative to the skin (Fig 5.3). The phantom was immersed in a plastic container full of water so that the phantom grooves could be scanned from the outside of the container in a direction equivalent to the in which the MT junction is imaged on the leg (the X-Z plane of the laboratory coordinate system). The position of the bottom edge of each of the grooves relative to the laboratory was

determined by running the point of the previously used metallic wand along the grooves and tracking these points. A three-dimensional regression line was fitted through the data to represent the position of the grooves in the laboratory space. The phantom was then scanned with the ultrasound probe and the position of the image in the laboratory space was tracked synchronously using the previously mentioned methods. Visible points on the bottom edge of the grooves were marked in frames where the grooves where visible. These points were then embedded into the global coordinate space and a comparison between these points and the fitted regression line made.

To determine the effect of rotation of the probe on the length of the AT, the probe was manually rotated about the long axis of the leg and also around the medio-lateral axis of the leg. These rotations were chosen as they are likely to result in images of a different region of the MT junction and potentially cause measurement error. Rotation of the image plane was measured relative to a plane of the leg defined by the lateral malleolus, lateral head of the proximal fibula and lateral epicondyle of the femur.

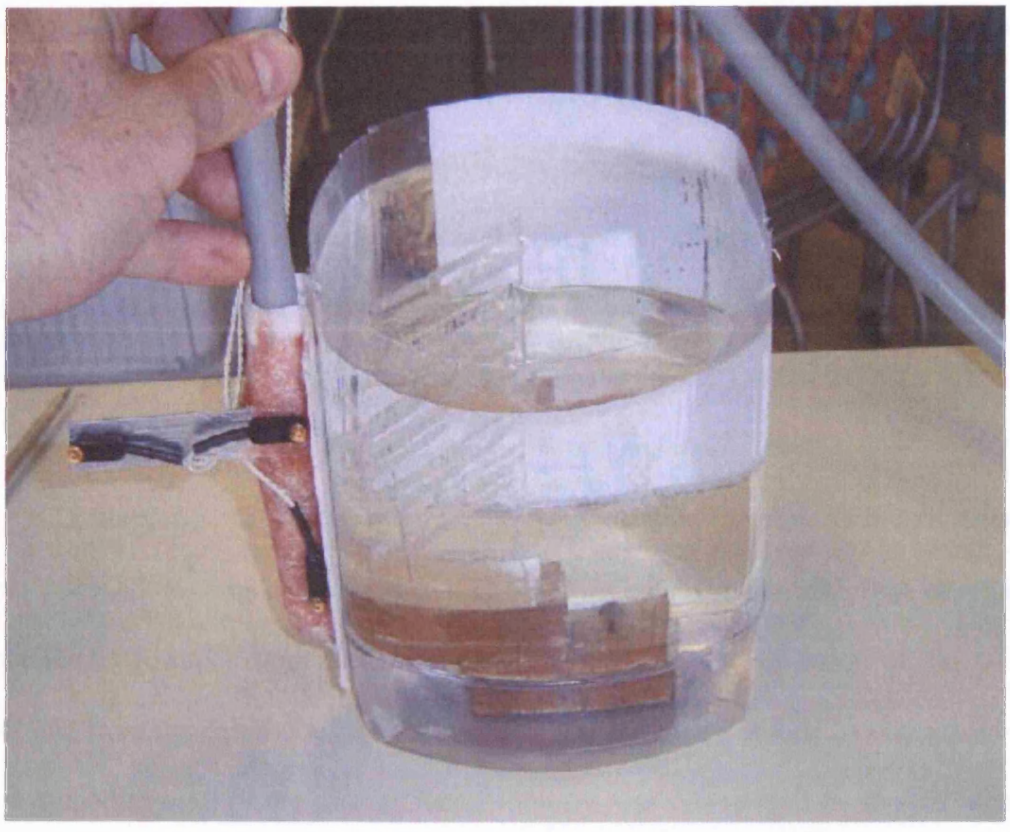

Figure 5.3

Photograph of the Perspex phantom emerged in water and imaged by the ultrasound probe (with rigidly attached markers). The position of the grooves relative to the laboratory were recorded by tracking the tip of a wand as it move along the grooves. The position of the grooves was also determined with the ultrasound probe using the technique described and a comparison between the two made.

Achilles Tendon Force and Stress

The three-dimensional ground reaction force was measured with a Bertec force plate (Bertec Corporation, Ohio, U.S.A.) and the motion analysis global coordinate system was aligned to the force plate so that the ground reaction vector could be transformed into it. The inertial properties of the foot segment as defined by (Plagenhoef *et al.*, 1983) were used in an inverse dynamics solution to calculate the ankle plantar flexor moment at the joint centre. This was defined as the moment about the axis perpendicular to the plane

defined by the calcaneous marker, the ankle joint centre of rotation and the insertion of the AT.

The ankle joint centre was estimated by creating a virtual point corresponding to an approximation of the centre of rotation of the ankle. This point was half the distance between the lateral and medial malleoli, perpendicular to the plane created by markers placed on the 5^{th} metatarsal, the calcaneous and the lateral malleolus. This effectively corresponds to a position midway between the lateral and medial malleoli.

AT force was calculated by dividing the ankle joint moment by the moment arm between the AT and the ankle joint centre. This was calculated at each time point as the perpendicular distance from the ankle joint centre to the line of action of the AT (the direct line from the calcaneous to the projected position of the muscle tendon junction). It was assumed that all of the plantar flexor moment was contributed by the AT structure and that co-activation of antagonists had only minor affects. Tendon stress was calculated for each individual by dividing the instantaneous force by the minimum cross sectional area (CSA) of the AT. CSA was measured by taking an ultrasound scan along the length of the tendon in the transverse plane and finding the minimum visible area.

Participants

Ten male participants, average age 30.9 (+/- 8.22) years, gave written consent to take part in the study, which was approved by a local ethics committee (RNOH JREC, 04/Q0506/11). The participants were asked to step onto the force plate and hop continuously on one leg on the spot at a frequency of approximately 2 Hz (average contact time = 0.32 s). An average of 45 hops were performed across three bouts with rest breaks between every 15-20 hops. Simultaneous force plate, 3D motion analysis and ultrasound data were collected and synchronised during the hopping periods as previously

described. One participant performed the experiment on three separate occasions so that the repeatability of the measures could be determined.

Marker Positions and Measurements

The instrumented ultrasound probe was attached to the leg with Coban™ tape (3M, Minnesota, USA) such that the lateral gastrocnemius muscle tendon junction could be imaged. Further active markers were placed on the following anatomical landmarks: head of the 5th metatarsal; proximal calcaneus (at the approximate insertion site of the AT); lateral malleolus; head of the fibula; lateral femoral epicondyle and on the ilotibial band (halfway between the greater trochanter and the lateral epicondyle).

Ankle and knee joint angles were calculated in two dimensions (in the plane of the hopping movement) using the markers previously mentioned. Total *gastrocnemius* muscle tendon unit (MTU) length was estimated from these angles by applying the equations of Grieve and colleagues (Grieve *et al.*, 1978). The length change of the muscle belly (including other series elastic structures like aponeurosis) was calculated by subtracting the measured AT length change from the MTU length change.

Data Analysis

Individual subject data were used to create an average force-length and stress-strain relationship. This was done by filtering the length data with a 4th order, 5 Hz low pass Butterworth filter and time interpolating the force and length measurements to 50 points across the period of foot contact (when the ground reaction force is above 0N) on each hop. The ground reaction force during hopping was symmetrical in time (i.e. the time course of force rise was similar to the time course of force fall), and therefore this method of interpolation means that the peak force (and strain) will occur at very similar times within the hop. The time point where the AT force was 200 N was taken as the zero

length (or slack length) of the tendon. Tendon stiffness (slope of the force-length curve) and the elastic modulus (slope of the stress-strain curve) of the tendon was determined by placing a linear regression through the averaged force length data for each individual. Hysteresis was calculated by dividing the difference between the area under the loading and the unloading curves by the area under the loading curve alone. This provides a measure of the energy converted to heat, an important feature of the mechanical properties of tendon.

To determine the amount of energy contributed to work of the hop, the energy recovered from the tendon was determined as the integral of the descending limb of the force length curve. The amount of work associated with each hop was determined as the maximum potential energy for the hop. This was calculated using the vertical ground reaction force measured with the forceplate using methods described in Cavagna (1979). The relative contribution of the AT recoil to the work of the hop was determined by dividing energy recovered from the tendon by the total work of the hop. This was averaged across all hops for each participant and a population average was determined from this.

Results

Ultrasound Accuracy and Sources of Error

The effect of skin movement on the predicted site of the insertion of the AT was found. The amplitude of the distance between the tendon insertion and the skin marker was measured in the direction of the tendon and average amplitude of skin movement across the range of movement was 1.9 mm. This corresponds to an approximate maximum strain error of 0.79% across the range of the movement.

A scan of the Perspex phantom with the ultrasound-motion analysis setup allowed for comparison between the predicted position of the grooves of the phantom and

regression lines fit to the position of these grooves (as measured by motion analysis) to be made. A three-dimensional reconstruction of the points measured with both techniques can be seen in Fig 5.4a, while a comparison in two dimensions for each Perspex sheet (in the plane of the sheet) is shown in Fig 5.4b. In three dimensions the error is less than 1.15 mm for 50% of the observations (Fig 5.4c), however much of this error is in the laboratory X-Y plane. In the X-Z plane, which is the plane where much of the length change in the AT length was measured, the accuracy was within 0.96 mm for 50% of the cases (Fig 5.4c).

Measurement of the AT length during manual rotation of the ultrasound probe resulted in a maximum error of 2.6 mm within the range of rotation recorded during the hopping activity (average range 22.9 degrees in the long axis and 0.8 degrees in medio-lateral axis). This corresponds to an approximate maximum error in the strain measurement of 1.08%. However most of the rotation occurs during the initial loading and final unloading of the tendon, which will affect the stiffness at these times only.

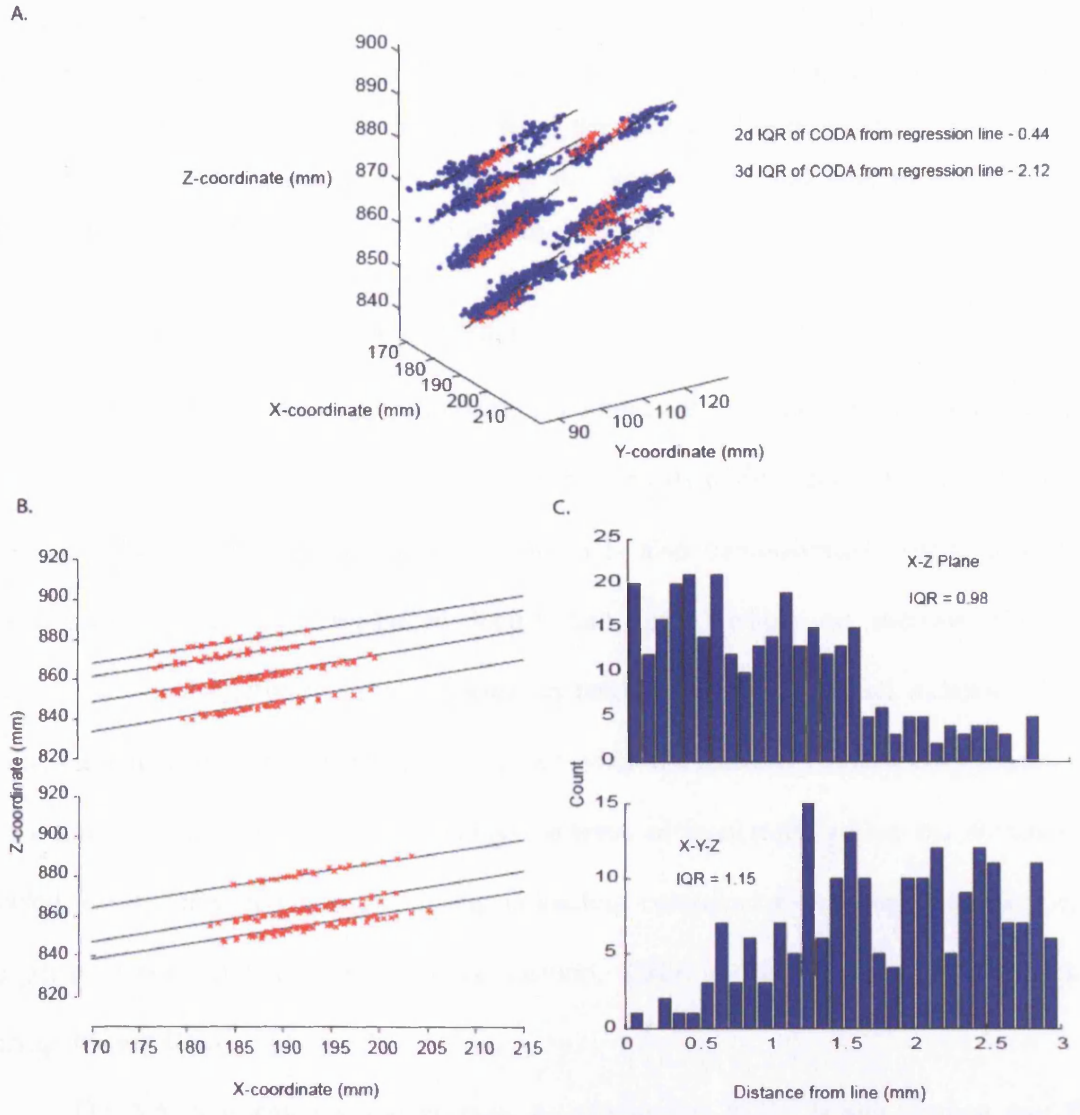

Figure 5.4

A. Three dimensional reconstruction of the position of the Perspex grooves of the phantom by tracking the tip of a wand with motion analysis (blue) and by embedding the position of the grooves when visualised by an ultrasound probe into the laboratory frame of reference (red). The line represents a 3D regression line placed through the motion anlysis data for each groove. The inter-quartile range (IQR) of the perpendicular distance of the motion analysis measured coordinates along the Perpsex grooves from the regression line in both 2D (X-Z plane) and the 3D were 0.44 mm and 2.12 mm respectively. **B.** Two dimensional comparison of the position of the grooves as determined by regression through the motion analysis data and the position determined by the ultrasound technique for each Perspex plate. This was measured in the same plane (X-Z) that was used to image the muscle tendon junction during the hopping experiments. **C.**

Histogram of the error of the ultrasound technique compared to the calculated regression line that represents the position of the phantom grooves in both two and three-dimensions. The IQR of the perpendicular distance from the measured coordinates of the grooves measured with the ultrasound technique to the linear regression line in both 2D X-Z plane) and 3D were 0.98 mm and 1.15 mm respectively.

Achilles Stiffness and Force-Length Properties

An example of the relationship between the instantaneous measurements of Achilles force and Achilles length for an individual during the periods of foot contact is shown in Fig 5.5. The effect of filtering the Achilles length is also demonstrated. There is a clear relationship between the measured length and force, where an increase in force corresponds to a relatively linear increase in tendon length. On initial increase of AT force, the length increases at a higher rate than when the tendon is almost fully loaded (at the highest forces) and generally displays patterns of hysteresis, where the Achilles is loaded less for any given length during unloading compared to loading. The force and length both rise and fall in a sinusoidal fashion, which is typical of a one dimensional spring mass system.

Fig 5.6 demonstrates the average *gastrocnemius* MTU length change and the Achilles length change for the population. This comparison reveals that the AT does not stretch as far as the whole MTU. It does, however, account for over 80% of the length change throughout the majority of the hopping cycle. Further length change must occur in the muscle belly, either in the muscle fibres or the aponeurosis and proximal tendon insertions of the gastrocnemius muscles.

The average force-length relationship for one individual participant on three separate occasions is shown in Fig 5.7. The change in length is measured from the zero force length and all three trials correspond closely with a stiffness of the tendon being 188, 187 and 170 Nmm^{-1} on each measurement occasion.

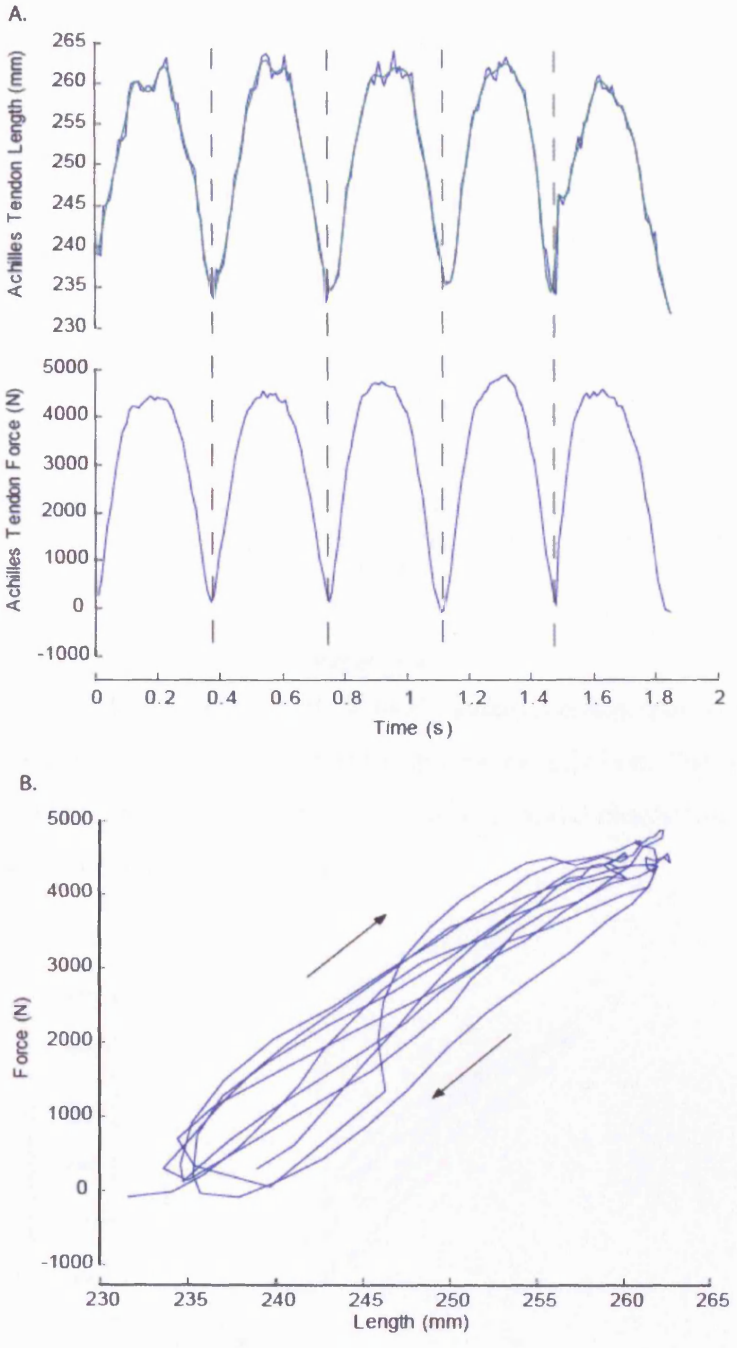

Figure 5.5

A. Achilles length and force measurements against time for five consecutive hops. Achilles length is shown in the raw form (blue) and after applying a 4th order, 5Hz low-pass Butterworth filter (green). Note that only periods of contact have been displayed and subsequent data during time off the ground were removed. **B.** Force against length for the same five trials as in A. Arrows represent the general trend for rise and fall of the force against length.

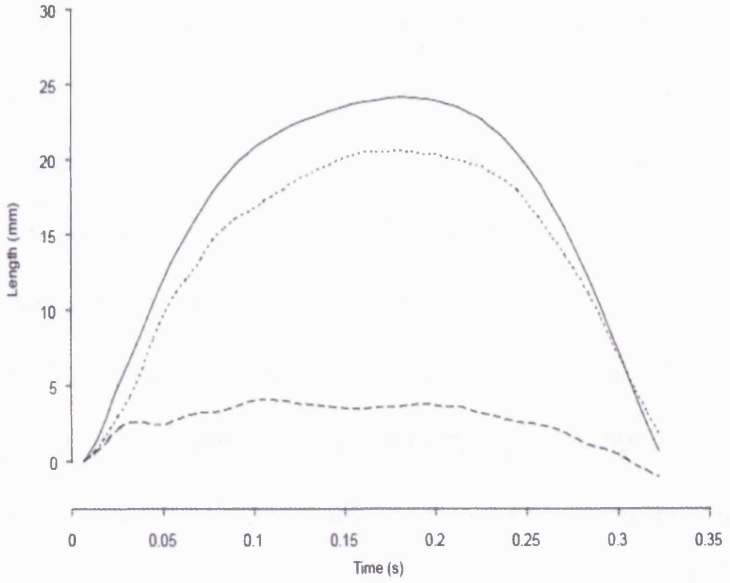

Figure 5.6

Average change in Achilles tendon length (dotted), gastrocnemius muscle-tendon length (solid) and approximate muscle length (dashed) during a single hop. The muscle length represents both the length of the fibres and the also other serial elastic tissues including the proximal tendon and aponeurosis.

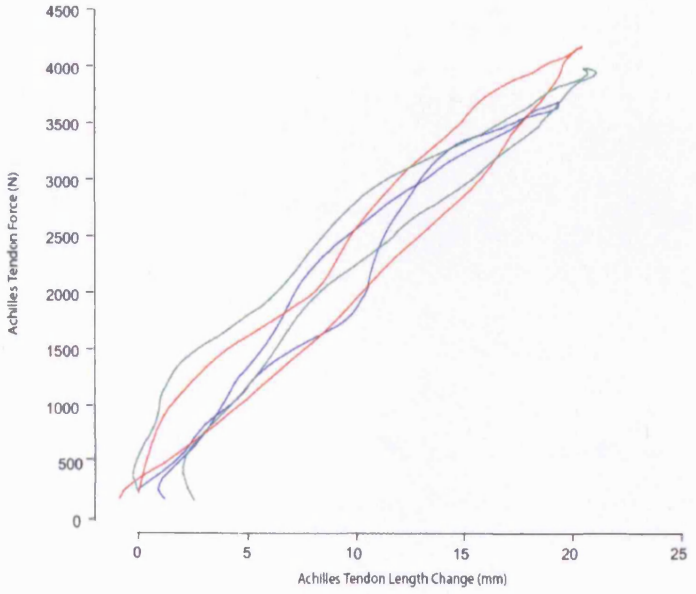

Figure 5.7

Average Achilles-tendon force vs the change in Achilles tendon length (relative to the length at 200N) for the same subject over three separate measurement occasions (Blue – Trial 1, Green – Trial 2, Red – Trial 3).

The force-length relationships for all nine subjects and the starting length adjusted force-length relationships are shown in Figs 5.8a and 5.8b respectively. There is a broad range of zero lengths for the AT across the small subject group, and the stiffness of the ATs (slope of the lines shown in Fig 5.8 is also variable between individuals. Generally the results suggest that the tendons don't display the classical toe region where the stiffness of the tendon should be lower during the initial loading. Instead the opposite is true for the majority of participants with an initially higher stiffness at low loads during loading. However, during unloading the stiffness is generally lower at smaller loads.

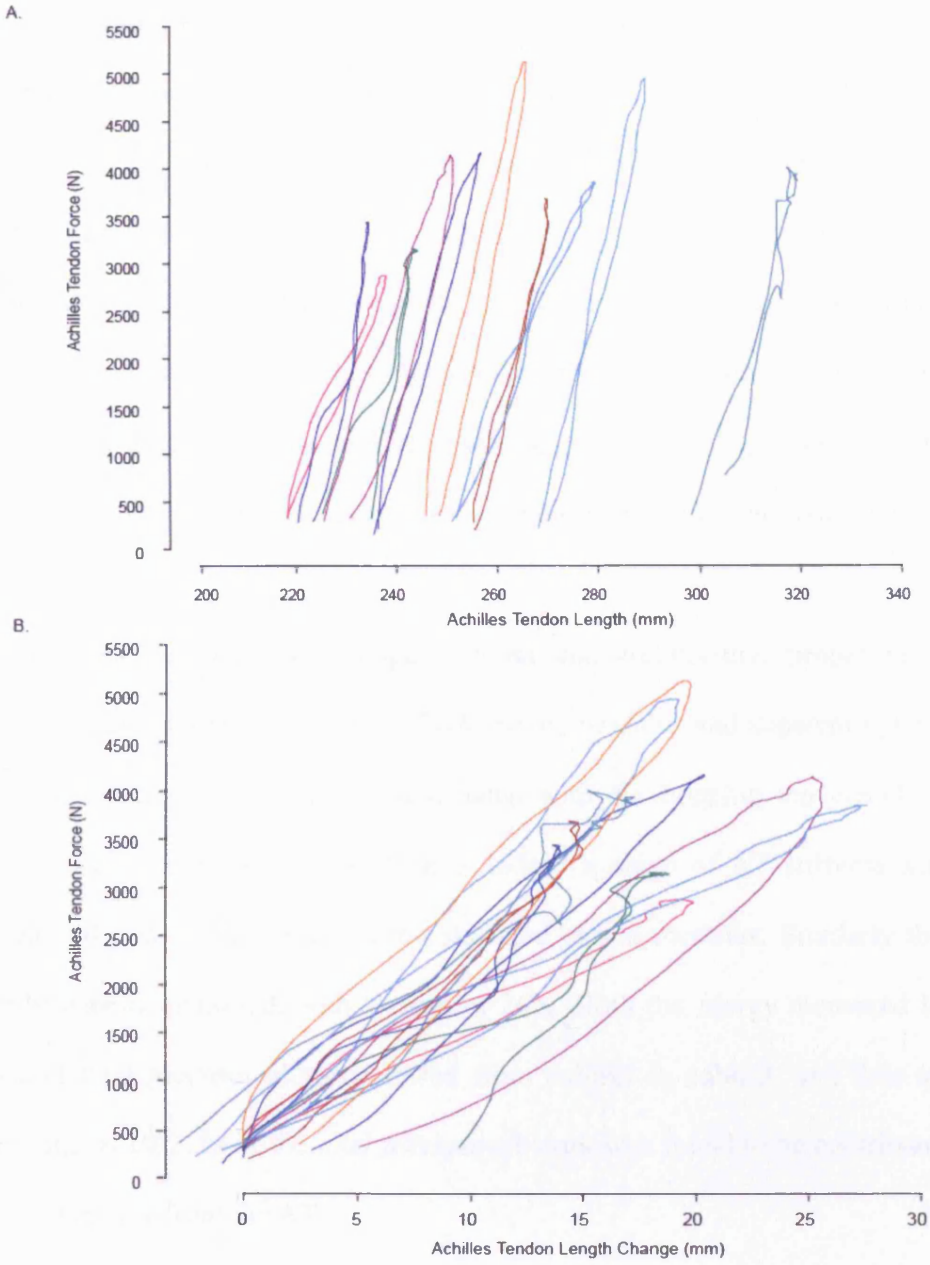

Figure 5.8

A. Average Achilles tendon force-length relationship for 10 individual participants. **B.** Average Achilles tendon force vs change in length (relative to the length at 200N) for each of the 10 participants.

Achilles Material Properties & Contribution to Work

The stress-strain relationships of three individuals representing the whole range of elastic moduli across the group is demonstrated in Fig 5.9a. A linear regression was performed

through each subject's average data and the elastic modulus recorded as the slope of this line. Due to interpolation with respect to the time for each individual hop and the sinusoidal loading pattern, more of the points acquired in each individual hop were recorded at high loads and strains. An average stress-strain relationship for all participants is demonstrated in Fig 5.9b. This figure also shows the standard deviation in both stress and strain measures during the hopping movements. The greatest deviation in strain measurement is apparent at lower stress values. An average hysteresis of 26% was recorded across all subjects, but these values varied greatly with the inter-quartile range being 17-35%.

Table 5.1 presents the average material and architectural properties of each individual's tendon, including stiffness, CSA, elastic modulus and apparent hysteresis. It also presents the average energetics associated with the hopping movement for each individual. These results show that there is indeed a range of AT stiffness across the population and this is also reflected in calculated elastic modulus. Similarly there is a range of hysteresis measured, with a mean of 26%. Both the energy recovered from the tendons and total mechanical work varied from subject to subject, and thus an inter-quartile range of 10-21% of the total mechanical work was found to be contributed to by the energy recovery from the AT.

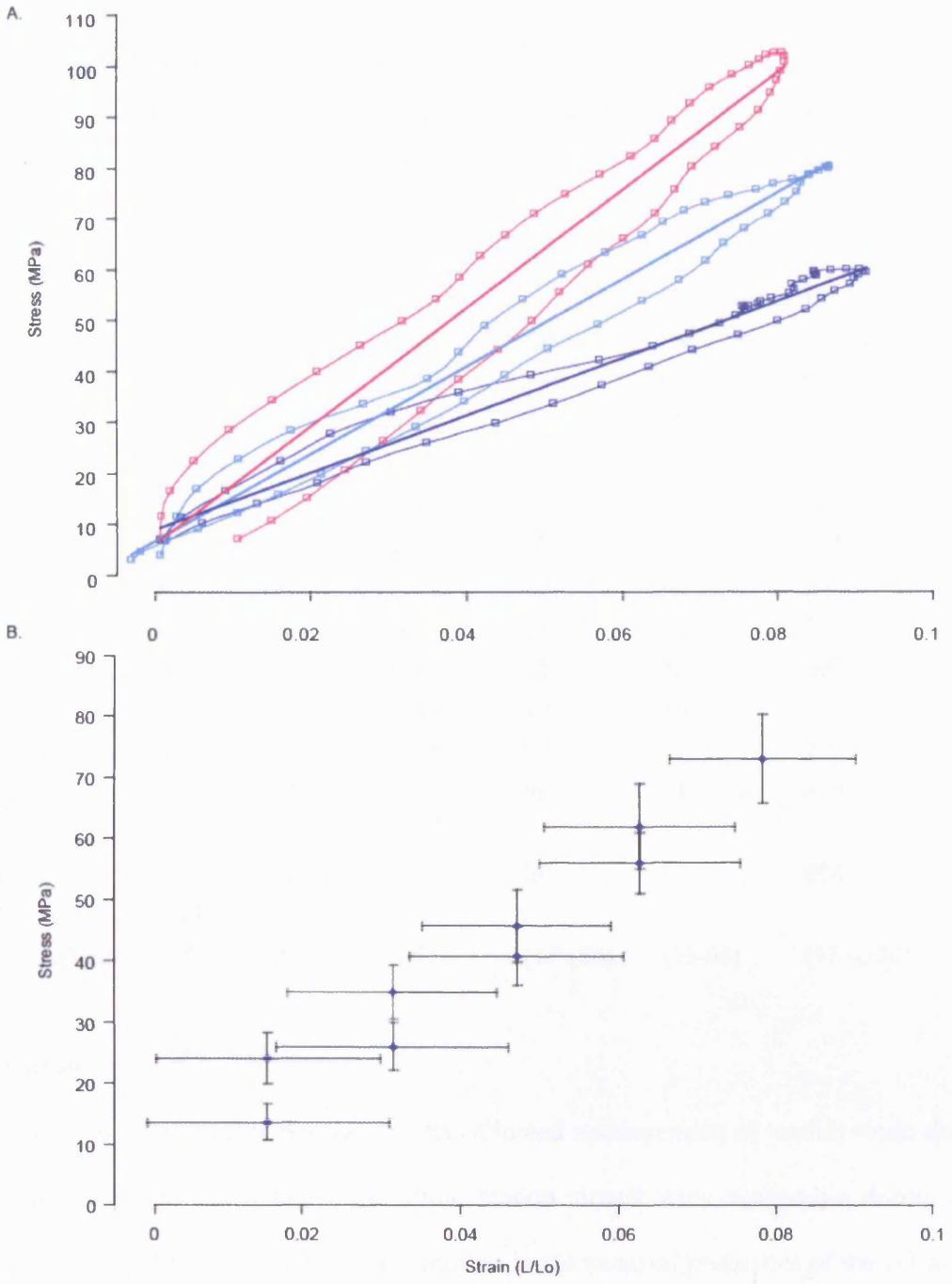

Figure 5.9

A. The average stress-strain relationship for three participants across the range of elastic moduli determined. The elastic modulus for each individual was determined by fitting a linear regression through the stress-strain data, as displayed. **B.** Group average stress-strain relationship at 5 points during both loading and unloading during the hopping movement and the standard deviation of stress and strain measurements (error bars indicate +/- one standard deviation).

Table 5.1

Average mechanical and architectural properties of the Achilles tendon for each participant and the average energy recovered from the tendon and its contribution to the total average work performed on the body for each participant. The population average and the inter-quartile range (IQR) are also shown.

Subject No	Weight (kg)	CSA (mm^2)	Stiffness (N/mm)	Elastic Modulus (GPa)	Hysteresis (%)	AT Energy Recovered (J)	Total Mechanical Work (J)	% AT Contribution
1	92	59	205	0.90	20	21	170	8
2	81	52	187	0.85	17	40	237	17
3	67	49	122	0.61	24	33	191	20
4	73	56	175	0.71	38	29	451	10
5	94	56	229	1.11	15	48	244	18
6	87	48	153	0.72	39	34	275	14
7	97	56	230	0.94	33	52	296	12
8	69	54	234	0.63	19	19	166	10
9	69	53	223	1.07	21	57	233	24
10	81	50	125	1.15	35	41	275	24
Average	81	53	188	0.87	26	38	254	16
IQR	(69-92)	(49.7-56.9)	(145-231)	(0.67-1.07)	(17 - 35)	(25-50)	(171-336)	(10-21)

Discussion

Here I have used a novel technique that has allowed measurement of tendon strain during very high strain movements. Large whole tendon strains were achievable during one-legged hopping. There was individual variation in the material properties of the AT across the group of participants assessed here, though the material properties were within the previously published range. The results indicated that the AT does indeed act like an energy storing spring by contributing a considerable amount of energy to the total mechanical work performed.

Achilles Tendon as an Energy Saving Mechanism

Combining traditional motion analysis with ultrasound imaging to determine whole tendon length changes during dynamic activities provides an ideal technique to study muscle-tendon unit interaction. The results of this study demonstrated the energy storing capabilities of the AT, whereby the tendon stretches in proportion to the force applied during the downward motion of the body and then recoils to release most of the energy stored (74%) during the upward movement. This provides a substantial amount of the total mechanical energy of the hop (16%). This mechanism has been thought to provide an energy saving mechanism during human walking, running and jumping (Alexander, 1988; Bobbert *et al.*, 1986; Fukunaga *et al.*, 2001) and has recently been suggested to account for up 6% of the total mechanical work produced during walking (Maganaris and Paul, 2002). This research therefore further shows the capacity of the body to utilise elastic stain energy and provides a valuable technique for quantifying tendon strain and energy storage capacity in further real-life movements such as running.

Most of the length change occurring in the MTU occurs in the AT (Fig 5.6), thereby the return of elastic energy during tendon recoil provides most of the shortening work required for take off. In contrast, the muscle (plus other series elastic structures such as the proximal tendon and aponeurosis) only stretch and shorten by small amounts during the hop, thereby reducing the work required by the muscle fibres. This is energetically efficient because it requires less work by the muscle fibres and reduces the heat produced from actively shortening the muscle fibres (Lichtwark and Wilson, 2005). The aponeurosis associated with the GM has also been found to be highly compliant and therefore some of the stretch and recoil occurring in the muscle fibres/aponeurosis complex may be elastic strain energy as well. This would allow the muscle fibres to act

almost isometrically which has been suggested to be the most efficient manner to operate (Roberts, 2002).

Achilles Tendon Material Properties and Strain

The strains measured here are at the higher end of those expected before tendon rupture based on *ex vivo* material testing. Typical tensile testing of tendinous material suggests that it should begin to fail at strains from 6-10% (Bennett *et al.*, 1986; Ker *et al.*, 1986), however here I have measured whole tendon strains of up to 10% without failure or injury. The activity performed here is a supra-physiological activity that should elicit high stress and strain and also there are major differences in what is actually measured between techniques. For instance, most *ex vivo* tensile testing is performed on sections of tendon, typically where the cross-sectional area is greatest. In contrast, here I have made a measure of whole tendon length. It is well documented that large strains can occur in tendinous material with some estimates of aponeurosis strain during contraction being as high as 50% (Zuurbier *et al.*, 1994). Therefore whole tendon strain is likely to differ from material testing on samples of tendon.

Nonetheless, the force-length and stress-strain properties of the AT measured are within estimates of animal tendon (Elastic modulus: 0.4-1.7GPa) (Zajac, 1989) and also *in vivo* measurements on the AT (Stiffness - 150Nmm^{-1}; Elastic Modulus - 1.16GPa) (Maganaris and Paul, 2002). In addition, the presence of hysteresis within the normal range (3-38%) is also encouraging. The average value of 26% is similar to that recently found to occur in the tibialis anterior and gastrocnemius tendons (19 and 18 % respectively) (Maganaris, 2002; Maganaris and Paul, 2002). This value of hysteresis may influenced by timing of contraction of other muscles in the *triceps surae* group, which may explain the large range of hysteresis values.

There are also measurement reasons why such high strains might have been measured. Firstly, it is likely that the measurement technique introduced some systematic errors in the calculation of the tendon length. The typical rotation of the probe has been shown to overestimate the Achilles strain by approximately 1.08%. Because this rotation occurs mainly during impact and take-off of the hop, then the estimate of slack length of the tendon may be incorrect. This may be partly responsible for the lack of toe-region in the force-length data for most subjects during the initial loading of the tendon. In addition, the muscle contraction under the skin may distort the junction and alter the results during muscle shortening on impact with the ground. Finally, a low sampling rate of 25 Hz in the ultrasound data means that approximately only 10 frames per hop could be determined, and this has been upsampled to 100Hz to match the CODA frame rate. This process is likely to affect the presence of a toe-region as will the presence of co-contraction of antagonist muscles, which would preload the tendon.

It is also possible that the three-dimensional structure of the AT allows high strains to be achieved. The structure of the AT varies dramatically along its length, from a uniform round cross-sectional area distally to a fan shape more proximally (Fig 5.1). It is possible that shape changes of the fan-shaped part of the tendon (particularly reducing the arc of the fan) during muscular contraction may allow for further linear strain without applying much stress to the structure. Also, because of the reduced cross-sectional area, the proximal part of the tendon may be allowed to strain further without reaching a failure point.

Numerous other studies have suggested that high levels of strain are possible in the AT and also other elastic structures. Recent ultrasonography studies during isometric and dynamic movements have reported that strains of the series elastic element (both the tendon and aponeurosis) can exceed 10% (Kubo *et al.*, 2002). These studies don't

however distinguish between distal tendon, proximal tendon or aponeurosis. A more direct ultrasound study also achieved strains of 5% (12mm) during an isometric contraction (Maganaris and Paul, 2002), however these contractions could only achieve small forces in the tendon compared to those during one-legged hopping (due to forward the position of the ground reaction vector relative to the ankle joint centre). Using phase-contrast magnetic resonance imaging, strains of approximately 4.7% were achieved during a 40% maximum isometric contraction (Finni *et al.*, 2003), therefore it does seem that the AT length is capable of large levels of strain without rupture. Taking these results into account as well as the strain records measured here, it is apparent that high AT strains are indeed achieved during human movement, although it is difficult to compare real-life activities with static postures due to different limb configurations and muscle lengthening conditions. The hopping movement is a particularly high force movement and therefore should elicit extreme strains, and prolonged one-legged hopping, which rarely occurs in everyday activities, may well begin to damage the AT.

Individual Variation

The individual tendon stiffness and elastic modulus show a relatively broad range across the subject group measured. Although broad studies of different animals suggests that there is little variation in the elastic modulus, there is some evidence that this can vary with training effects (Reeves *et al.*, 2003; Buchanan and Marsh, 2001). Therefore, with such a small group, the variation may be exaggerated. In addition, while the technique seems to be reproducible on one participant (Fig 5.7), there is still room for individual variability that is inherent to the technique. For instance, the protocol does not control for individual muscle architecture and also muscle activation during the movement. Individual muscle architecture could influence the force length relationship due to differences in probe rotation (as previously mentioned) and also the shape of the

tendon insertion relative to the orientation of the probe (and hence image plane). Muscle activation has also been suggested to influence the stiffness of the series elastic structures (Hof, 1998) and not controlling for this may influence the AT stiffness in some way. Also, co-activation of the antagonist muscles was not controlled for and may influence the strain pattern, particularly at low forces. Finally the contribution of the soleus and lateral gastrocnemius to the force which strains the AT may differ between participants and effect the measured whole tendon length change.

Conclusions

In conclusion, the current study has provided a new technique for the measurement of whole tendon length during dynamic activities. I have measured the length of the AT from the muscle-tendon junction to its insertion to the calcaneous using a combination of motion analysis and ultrasound. During the high strain movement of one-legged hopping, the elastic behaviour of the AT is highlighted, where a substantial amount of the mechanical energy required to produce the hopping movement is provided by elastic recoil of the AT. The majority of the strain occurs in the AT compared to the muscle contractile component and aponeurosis and this allows for rapid recoil of the muscle tendon unit during take-off. Synchronous measurement of AT force has shown that typically linear force length properties of tendons under high forces can be reproduced. The mechanical properties of the tendon are within the measured physiological range, despite high measures of whole tendon strain that result from the high forces. These high strains may be the result of the complex three dimensional fan shape of the AT, which may allow for such high whole tendon strains in the direction of muscle action due to shape change.

Chapter 6: Interactions between the human *gastrocnemius* muscle and the Achilles tendon during incline and decline locomotion.

I have now described two techniques developed to measure length changes specific parts of the muscle tendon unit; the *gastrocnemius medialis* (GM) muscle fascicles and the Achilles tendon. It is now possible to use these techniques under conditions which may require different power requirements from the muscle and determine how this done. In this Chapter I will apply these techniques during locomotion under different incline conditions to examine how the muscle fascicles interact with the tendon and other elastic materials and specifically how power output of the muscle might differ between conditions.

Introduction

The mechanics and energetics of both walking and running have been well documented in the past. Walking can be characterised by an inverse pendulum like gait where potential and kinetic energy are recycled throughout consecutive strides (Cavagna *et al.*, 1977). In contrast running employs a bouncing, spring like gait where elastic energy is stored and returned during each stride (Alexander, 1988; Farley *et al.*, 1993; Taylor and Heglund, 1982). In both gait types, elastic energy is thought to be stored within the elastic tissues of the muscle-tendon units that support the body and propel it upwards during the stance phase (Alexander, 1988; Fukunaga *et al.*, 2001; Ker *et al.*, 1987). To achieve versatility however, the amount of energy stored in the elastic tissues must be modulated by muscular contraction.

Although there are energetically optimal speeds for each type of terrestrial gait, animals need to perform these gaits under a wide range of conditions. These include differing speeds, accelerations and terrains. Each of these different conditions requires altered forces and moments at each joint to maintain steady locomotion (Roberts and Scales, 2004; Roberts and Belliveau, 2005). Therefore the muscles responsible for producing these forces are required to have a versatile mechanical function. Muscles must have the ability to either produce or absorb work at different periods of the stride depending on the conditions of locomotion. For instance it has been demonstrated that during downhill running, the turkey gastrocnemius muscle absorbs work and conversely is required to generate power during uphill running (Gabaldon *et al.*, 2004). Similarly, these muscles must produce more work in proportion to acceleration on level ground (Roberts and Scales, 2004).

As has previously between described in depth, the ability of a muscle to perform or absorb mechanical work is highly dependent on interactions between the muscles contractile component and the elastic structures that it attaches to. Compliant tendons and aponeurosis enable fascicle length changes to be uncoupled from that of the whole muscle-tendon unit (MTU) length (Griffiths, 1991; Fukunaga *et al.*, 2000). Numerous investigations on different terrestrial species, including those reported in humans in Chapter 4, have demonstrated that during locomotion, the ankle extensor muscles act nearly isometrically (constant length) or concentrically (shorten) whilst the whole muscle-tendon unit lengthens (Fukunaga *et al.*, 2001; Griffiths, 1991). This acts to stretch the relatively compliant tendon of this muscle group during the stance phase. Because tendon is an elastic material, energy is stored in the tendon whilst it is stretched and this energy is returned late in the stance phase when the tendon (and subsequently the entire muscle-tendon unit) shortens rapidly.

To better understand the mechanics and energetics of human muscle contraction it is important to distinguish the roles of the contractile components and also the elastic components. Here I have combined ultrasound imaging and motion analysis techniques to assess the length changes of the *gastrocnemius medialis* (GM) fibres, the entire series elastic element and the Achilles tendon during locomotion under different incline conditions and at different gaits (walking and running). These techniques allow us to assess the contribution of this muscle to force and power production or absorption during gait. By varying the grade of incline and the speed of locomotion (and the gait) I have varied the external mechanical work produced by the body (Gabaldon *et al.*, 2004) and hence been able to study the effect that GM muscle mechanics have on this change. I hypothesise that muscle power output will resemble the requirement for external mechanical work.

Methods and Materials

Participants & Protocol

6 healthy male participants, average age 28 years +/- 3.68 years, height 182 cm +/- 12 cm, and weight 82 +/ 12, gave written consent to participate in this study. The study was approved by a local ethics committee (RNOH JREC, 04/Q0506/11). No participants had any history of Achilles tendon pain and had a clinically normal gait pattern.

Participants were asked to walk (5km/h) and run (10km/h) on a treadmill at different grades while measurements were made. Participants walked at grades of -10, 0 and 10% (negative grades indicate decline/downhill) and ran at grades of 0 and 10%. A walking warm-up period of two minutes was initially used and a period of one minute was allowed at each condition for the participant to normalise their gait. This period preceded two ten second data collection periods for walking and one ten second collection period for running, which ensured that at least ten strides of good data were

collected for each individual. The order of the walking and running and the grades of incline were randomised between subjects. This protocol was applied twice in the same session so that muscle fascicle and tendon length measurements could be made using one ultrasound machine.

Kinematics & Muscle Activity

Active CODA light emitting diodes (LEDs) were again attached the same body landmark as in Chapter 4. The three dimensional (3D) position of these LEDs was determined at rate of 100Hz. Knee and ankle angles were determined in the sagittal plane as defined in Chapter 4. Simultaneous muscle activity was also measured using electromyography and collected with a sampling frequency of 2000Hz into the 16-bit A/D board of the CODA system.

Length changes of the GM muscle-tendon unit length were again estimated from the average joint angle data using the equations derived by Grieve and colleagues (1978), with shank length defined as the length of the lower length segment as defined above. A comparison was made between the estimations of this model and a generic human musculoskeletal model using the software package SIMM (Musculographics, California, USA) to confirm suitability of this model.

The vertical velocity of the calcaneus marker was used to determine when the foot contacted the ground. A consistent feature of this signal with respect to time was the minimum velocity (negative) for each cycle. This feature was automatically detected with respect to time and visual inspection of the stick figure relative to the treadmill was used to determine a time offset from this point in the gait cycle to foot contact. This varied for each participant and for each grade and speed, but was consistent across trials; therefore this process was done for each trial. The same technique was applied to estimate toe off, however the maximum velocity of was used as the consistent feature in the signal from

which an average time offset to toe off was found. This technique made for a consistent predictor of the time of foot on and foot off under the conditions of both walking and running.

The EMG was used to assess the muscle activity of the GM and its antagonist, the *tibialis anterior* (TA). Surface electrodes were placed on the muscle bellies of the GM and TA using round bi-polar electrodes (12mm diameter, 18mm spacing) with reference electrodes placed in between. The EMG signals were preamplified at the source with a frequency bandwidth of 20Hz-20 kHz (MA-310 - surface EMG, Motion Lab Systems, Inc, Los Angeles, USA) and synchronously collected with the motion analysis data at 2000Hz.

Ultrasound Measurement 1 - Muscle Fibre and Angle Measurement

Muscle fascicle length and pennation angle changes were determined at the midbelly position in the sagittal plane, as in Chapter 4. These measurements were made at 25 Hz.

Ultrasound Measurement 2 – Achilles Tendon Length

AT length was measured as the distance from the calcaneous marker to the projected 3D position of the GM muscle-tendon junction (MTJ). This was done by using the same techniques as described in Chapter 5. The Achilles tendon length change was measured relative to the slack length, which was defined as the average length of the tendon at toe off during walking on the level, 237.8 mm. Achilles tendon strain was calculated from the length change of the tendon divided by the slack length.

Series Elastic Element and Aponeurosis Length Measurement

The length of the series elastic elements (SEE) was determined by subtracting the length of the muscle fibres in the direction of the tendon from the change in whole muscle-tendon unit length –

$$L_{SEE} = L_{MTC} - L_{Fibre} \cdot \cos\alpha \quad (1)$$

where L_{SEE} is the length of the SEE, $L_{Fascicle}$ is the length of the muscle fascicle and α is the pennation angle. Length change of the SEE was reported relative to the average length of the SEE at toe off for each condition. This technique is appropriate to approximate the stretch of the elastic tissues (tendon, aponeurosis and other connective tissues) because the muscle fibres act relatively homogenously along the muscles length (see Chapter 4).

An approximation of the total stretch of both proximal tendon and the aponeurosis in series with the muscle was also made as follows –

$$\Delta L_{APO} = \Delta L_{SEE} - \Delta L_{AT} \quad (2)$$

where ΔL_{APO} is the length change of the aponeurosis plus the proximal tendon and ΔL_{AT} is the length change of the Achilles tendon using the previously described ultrasound method.

Data Analysis - Muscle Force, Work and Power

The timing of heel contact and toe off were determined and then the kinematic, whole muscle length and EMG data were divided into individual strides (from one heel contact to the next) for each participant. Three strides for each participant, for each condition were then chosen at random to analyse the muscle fascicle ultrasound data. The muscle fascicle length and pennation angle were measured at each frame of ultrasound across the selected strides and were interpolated to 100 points across the gait cycle. The interpolated data for each stride was then averaged across the gait cycle for each participant and pooled to determine an average muscle fascicle length and pennation angle throughout the gait cycle for each condition.

Knee and ankle angle as well as whole muscle length data were averaged across all strides recorded for all participants and each condition during trials where muscle

fascicle length was assessed (not trials where Achilles tendon length was determined). The EMG data was rectified and low pass filtered with a 4th order, 5Hz low pass Butterworth filter to create an EMG envelope. The data were then divided into individual strides and averaged across all participants for each condition.

The average muscle fascicle length ($L_{Fascicle}$), pennation angle (α) and whole muscle length (L_{MTU}) data across the gait cycle were used to calculate an average SEE length change as described above. A pooled standard deviation was calculated from the standard deviations of each measurement. The average SEE length change was also calculated for each individual participant.

The position of the GM MTJ was determined at each frame through the 10 s trial and the whole AT length was measured across each entire trial. There data were further divided into each individual full trial, interpolated to 100 points and averaged for each participant and also across the entire group. Strides with significant marker position errors (due to marker dropout) were disregarded.

An approximate Achilles tendon force (F_{AT}) was estimated using the length change of the Achilles tendon (ΔL_T) and the average stiffness of the Achilles tendon (k ~ 180N.mm^{-1}) as calculated in Chapter 5 (using the same method of length measurement).

$$F_{AT} = k_T \cdot \Delta L_T \quad (3)$$

The contribution of the GM to the total Achilles tendon force was estimated based on the physiological cross-sectional area (PCSA) of this muscle relative to all other plantar flexors. An average PCSA of 15.4% of the total PCSA has been estimated by Fukunaga *et al* (Fukunaga *et al.*, 1992) and therefore the force contribution of the GM (F_{GM}) was calculated as follows -

$$F_{GM} = 0.154 \cdot F_{AT} \quad (4)$$

The force applied by the muscle fibres ($F_{Fascicle}$) was then calculated in the direction of the muscle fibres as measured by the pennation angle (α) at each time instant and therefore the GM fascicle force were calculated as follows –

$$F_{Fascicle} = F_{GM} \cdot (\cos\alpha)^{-1} \quad (5)$$

Fibre length was then normalised (L_{Fo}) to a resting fascicle length of 60mm (mean fascicle length at foot on during walking trials) and fascicle force was normalised (F_{Fo}) to a maximum isometric force of 1200N, based on a physiological cross-sectional area of 42 cm^2 and an average pennation angle of 15° (Narici, 1996).

The instantaneous velocity of the muscle fascicles ($V_{Fascicle}$) was calculated by differentiating the relative fascicle length with respect to time ($L_{Fascicle}$ $.s^{-1}$). Muscle fascicle power output ($P_{Fascicle}$) was then calculated as the normalised fascicle force multiplied by the fascicle velocity.

$$P_{Fascicle} = F_{Fascicle} \cdot V_{Fascicle} \quad (6)$$

The total work performed by the muscle fibres during the stance phase (W_s) was then calculated as the integral of fascicle power with respect to stance time.

$$W_S = \int_{HeelStrike}^{ToeOff} P_{Fascicle} \quad (7)$$

Total muscle fascicle power during the stance phase (P_s) was defined as the total work performed during the stance phase divided by the stance time.

Results

Kinematics & Muscle Lengths

A comparison between the gastrocnemius MTU length estimated from the equations of Grieve *et al* (1978) and that estimated from a commercial musculoskeletal modelling package (SIMM, Musculographics, California, USA) is shown in Fig 6.1 for changes in

both ankle and knee angle. A high correlation between the two models was found for both the ankle ($R^2 = 0.99$) and knee ($R^2 = 0.99$).

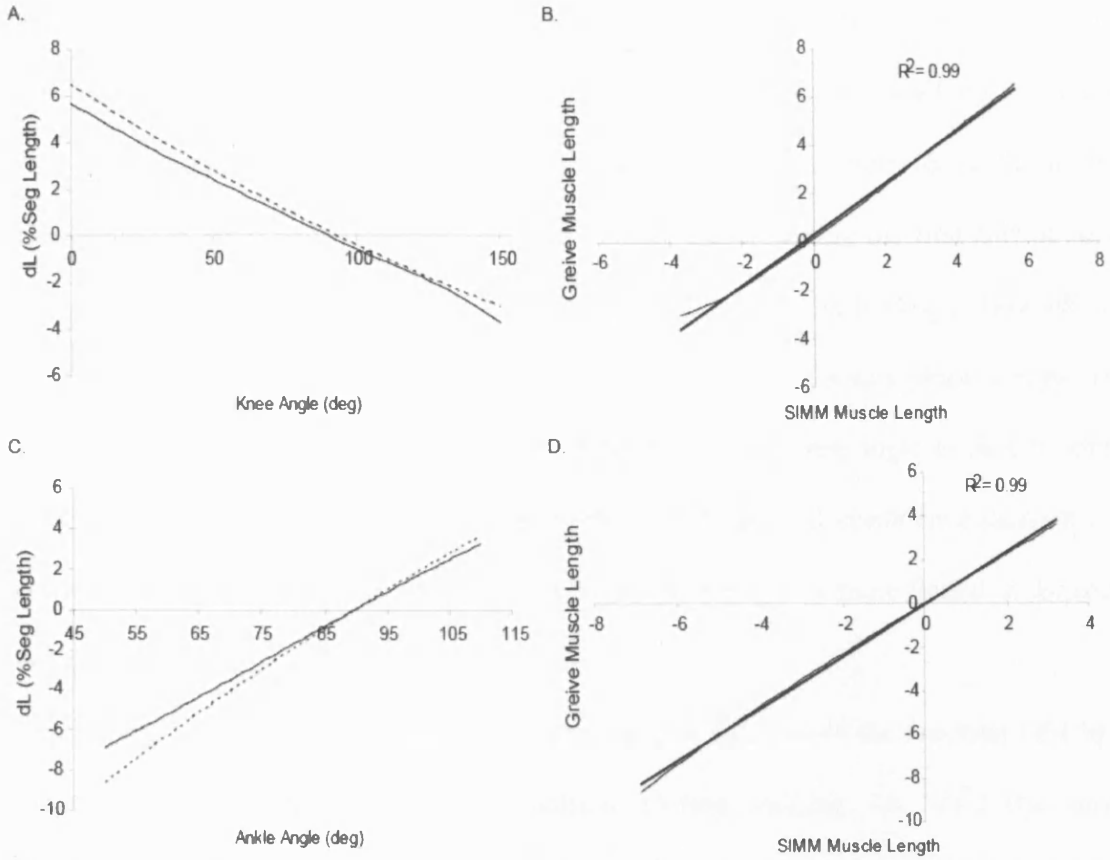

Figure 6.1

Comparison of the gastrocnemius MTU length estimated by the model of Grieve *et al* (1978) (dashed line) and a commercial musculoskeletal modelling package (SIMM) (solid line) with varying ankle (**A**) and knee (**C**) angle and the relationship between the models at the ankle (**B**) and knee (**D**). MTU lengths are represented as a change in length relative to the length of the MTU with the both the knee and ankle at 90°.

A comparison between the average kinematics and the calculated GM MTU length for each condition is shown in Fig 6.2. Although stance time varied slightly between incline conditions (Walking: 0.598 s (-10%), 0.610 s (0%), 0.627 s (+10%); Running: 0.300 s (0%), 0.288 s (+10%)), an average stance time for walking and running across all conditions is indicated by the grey shading. During both walking and running, the ankle is more dorsi-flexed throughout the majority of the stance phase, however at the approximate toe-off time the ankle angle is similar in each of the walking conditions and

each of the running conditions. In contrast, the ankle is a plantar flexed by approximately 10° more at take-off in the running conditions compared to the walking conditions. During walking, the knee angle differs throughout the gait cycle for each of three conditions. In the uphill condition, the knee is more flexed during the first half of stance phase, whilst it is more extended during the second half of stance, leading to take-off. The knee is also more flexed during downhill walking for all of the stance phase compared to the level walking condition. In running, the trajectory of the knee angle in time is similar in uphill walking compared to the level (within a 95% pooled confidence interval (two pooled standard errors) about the level condition); however it is more flexed in the initial period after landing.

The combination of the knee and ankle angles determines the resultant GM MTU length, which is different for each condition. During walking, the MTU was longer throughout the stance phase during the uphill condition and was 3 mm longer than during the level walking at the maximum length. In the downhill walking the MTU was 1.4 mm shorter at the maximum length than during the level walking. During the running conditions, the MTU is longer throughout the stance phase and is 2.3 mm longer at the maximum length compared to level running.

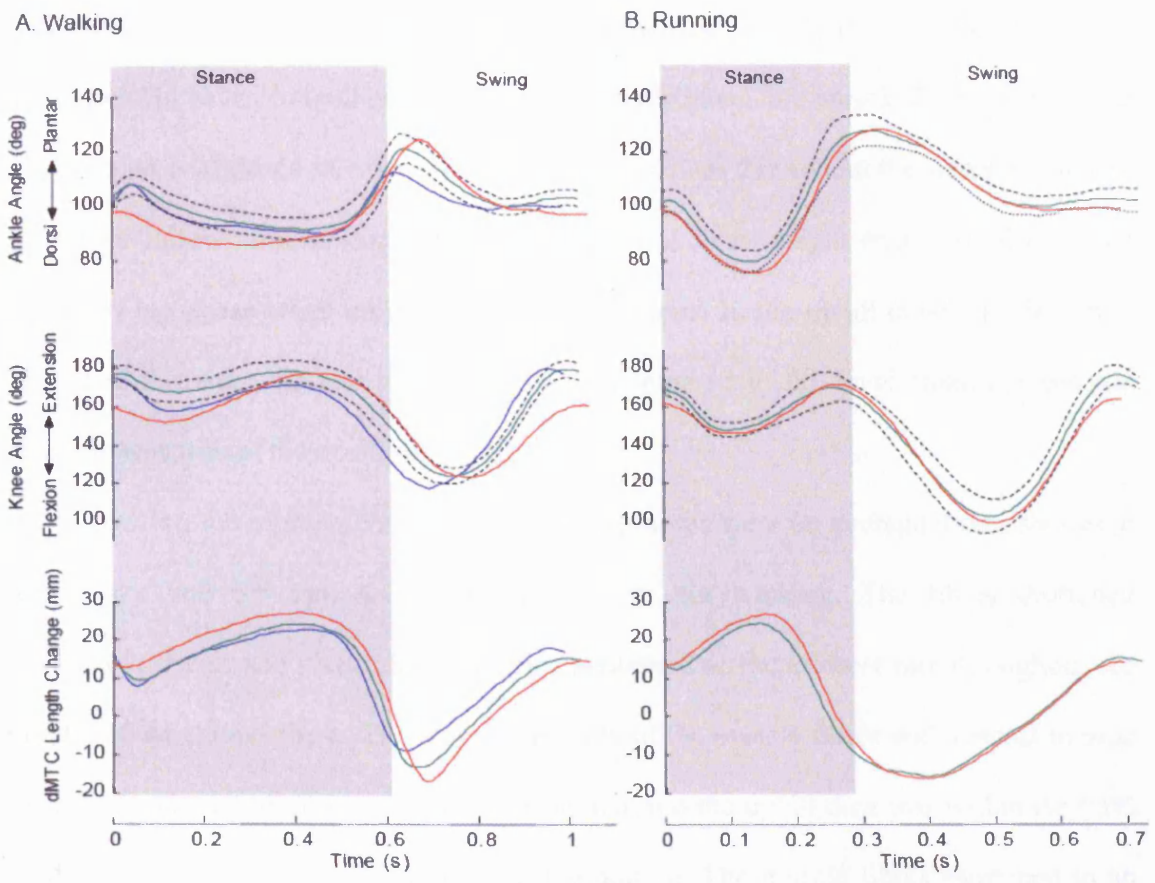

Figure 6.2

Average ankle and knee angle and GM MTU length changes with respect to time during walking (**A**) and running (**B**) for downhill (-10% - blue), level (0% - green) and uphill (10% - red) conditions. The average stance time across each condition is shown with the shaded area and the pooled 95% confidence interval (+/- two standard errors) across all grades for both walking and running is shown with respect to the level condition as the area within the dotted lines. The average standard error across each grade condition was equivalent.

Muscle Fibre Length, Pennation Angle and Activation

The average change in muscle fascicle length and pennation angle for each grade during both walking and running is shown in Fig 6.3. In all walking conditions the muscle fibres begin to shorten in the first period of stance and then remain relatively constant length until the final part of stance phase (the take-off phase) where the fibres begin to shorten again. The muscle fibres are shorter throughout most of the stance phase during the

downhill condition compared to the level condition and longer during the uphill condition. However, in both uphill and downhill conditions, the muscle fibres are within a 95% pooled confidence interval about the level condition throughout the stance phase and the fibres follow similar length change trajectories. Fibre length trajectory also varied during swing phase when comparing grade conditions. In the uphill condition the fibres shortened a greater amount during the swing compared to the level condition and the opposite was true of the downhill condition.

During the running conditions the muscle fibres were on average 4 mm shorter at heel strike and 6.5 mm shorter at toe-off than for walking. The fibres shortened throughout the stance phase; however they shortened at the slowest rate throughout the middle of the stance phase. The length trajectory of the muscle fibres with respect to time for both level and uphill running are very similar and the uphill data was within the 95% pooled confidence interval about the level condition. The muscle fibres shortened to an average of 41 mm during the swing phase for both running conditions, whilst the shortest average muscle length for the walking conditions was only 44 mm.

There was little variation in pennation angle with the change in grade for both walking and running. However the muscle fibres acted at a higher pennation angle during running than for walking. During walking at all grades the muscle fibres act at a relatively constant pennation angle throughout stance. In contrast, during running both on the level and uphill, the angle made between the fibres and direction of action of the tendon increases through stance and return to their initial pennation angle throughout the swing phase. The relationship between muscle fascicle length and pennation angle is shown in Fig 6.4. I found an inverse linear relationship between muscle fascicle length and pennation angle, however there were differences between shortening and lengthening of the muscle fibres and also some difference between walking and running conditions.

Fig 6.3 shows a comparison of the average muscle fascicle length and pennation angle changes relative to the length change of the entire GM MTU and the activation of the GM and *tibialis anterior* (TA) for all conditions. The results show that the GM muscle fibres actively shorten while the whole MTU lengthens during the first half of the stance phase. When the GM begins to deactivate, the muscle fascicle length trajectory reflects that of the MTU during the rest of stance phase and the swing phase for both walking and running. During walking in all conditions, the EMG signal from the GM increases throughout stance until the whole muscle length begins to shorten. However the GM is more active during the uphill condition than the level and less active in the downhill condition. In contrast, there is no difference between the amplitude of activation between level and uphill running. The TA signal shows some co-activation between it and the GM muscle at the beginning of the stance phase in both walking and running, and also at the end of the swing phase during running.

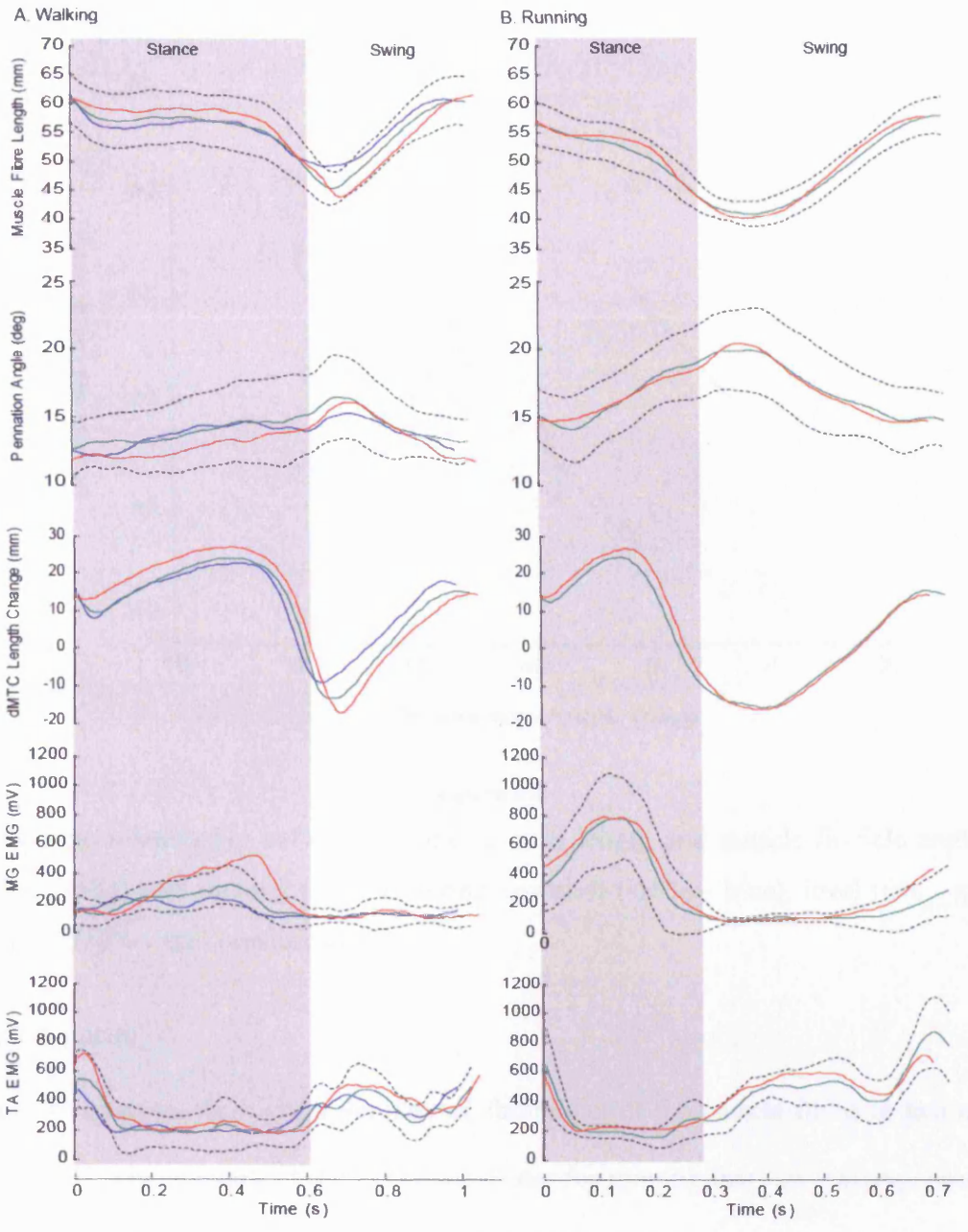

Figure 6.3

Average *gastrocnemius medialis* (GM) fascicle length, pennation angle, MTU length change and enveloped GM and *tibialis anterior* (TA) EMG signals with respect to time during walking (**A**) and running (**B**) for downhill (-10% - blue), level (0% - green) and uphill (10% - red) conditions. The average stance time across each condition is shown with the shaded area and the pooled 95% confidence interval (+/- two standard errors) across all grades for both walking and running is shown with respect to the level condition as the area within the dotted lines. The average standard error across each grade condition was equivalent.

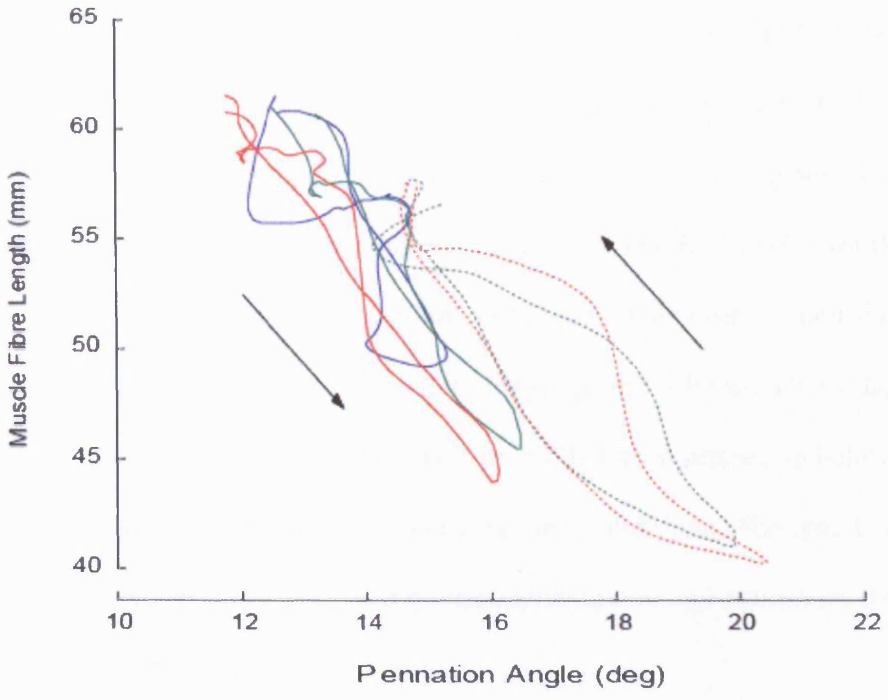

Figure 6.4

The average relationship between muscle fascicle length and muscle fascicle angle for walking (solid) and running (dotted) during downhill (-10% - blue), level (0% - green) and uphill (10% - red) conditions.

Muscle Velocity

Table 6.1 compares the highest velocity of shortening of the muscle fibres to that of the whole MTU. The velocity of the MTU was faster for running than for walking, however the change in grade in these conditions made little difference to the maximum MTU velocity. A similar effect is apparent in the muscle fascicle velocity data, with the uphill running condition achieving the highest muscle fascicle velocity. However the maximum shortening velocity of the muscle fibres was substantially lower than that of the MTU, being under 30% of the MTU shortening in all conditions.

Achilles Tendon and SEE Length Changes

The length change of the AT across the gait cycle for all conditions (Fig 6.5) shows that a greater stretch is achieved during running than walking. However in both gaits, the Achilles tendon stretches to a similar maximum length regardless of grade. The average maximum strain measured during the walking conditions was 4.6 % (10.9 mm), whilst it averaged 5.8 % (13.8 mm) during the running conditions. However the uphill conditions for both walking and running showed a longer length of the AT throughout the first half of stance phase compared to the level results. The AT length shortened to below the slack length before the approximate toe-off in both running conditions. The results also show that the AT was strained during the swing phase with an average maximum strain of 2.9 % during walking and 3.8 % during running.

Fig 6.5 also shows the estimated change in length of the SEE for each condition. The SEE stretched in a similar way to that of the AT, however the amplitude of the total length change was greater in the SEE. The maximum stretch for all grade conditions in both walking and running was similar, with a higher strain achieved during the running trials. The maximum length change estimated with the model was 23.4 mm during walking and 25.2 mm during running. This estimate is based on a zero length for each condition measured at toe-off, rather than a fixed zero length for the SEE. Subtraction of the AT length change from the overall SEE length change gave an estimate of other elastic strain (aponeurosis, proximal tendon, other muscle fascia), termed aponeurosis strain for simplicity. The estimated maximum length changes in the aponeurosis was similar for both walking and running, with an average maximum elongation of 13.8 mm and 12.8 mm respectively (Fig 6.5).

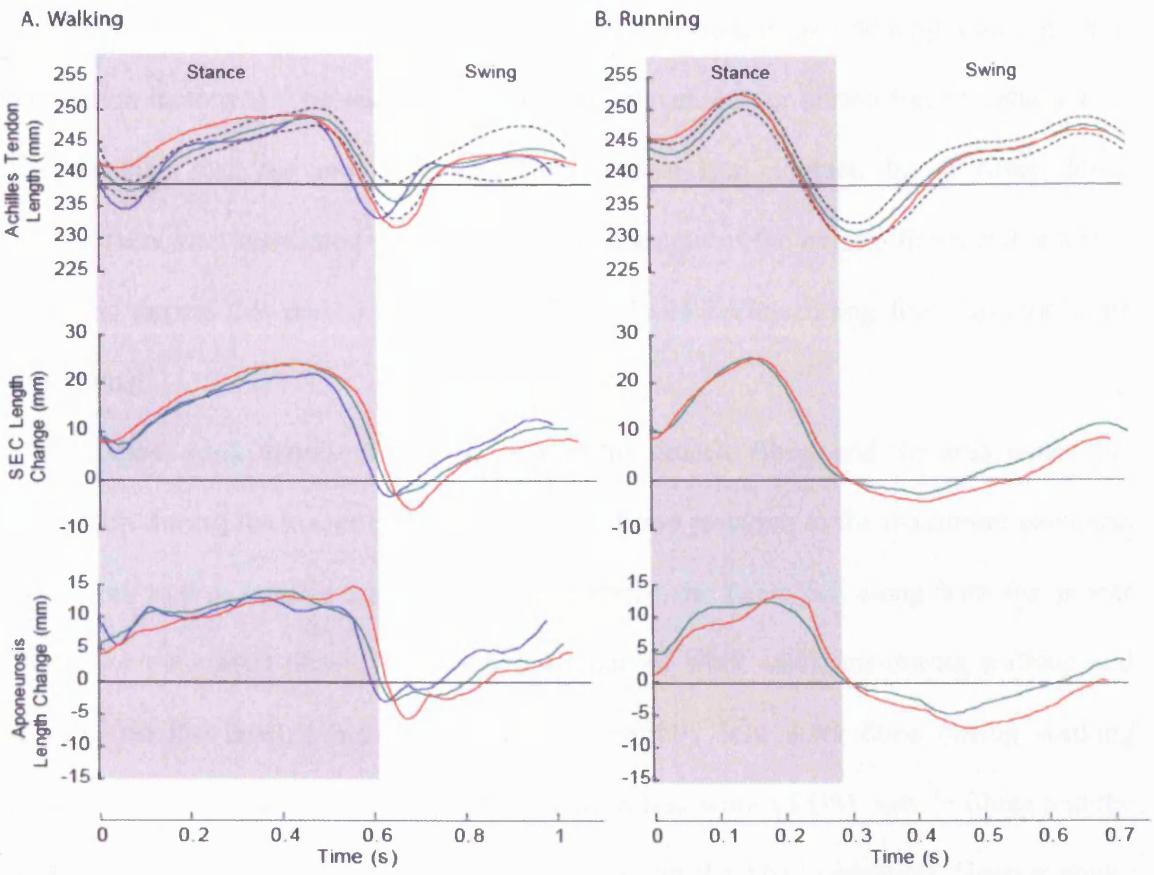

Figure 6.5

The average Achilles tendon length change measured directly using the projected MTJ measurement and the corresponding estimates of series elastic element (SEE) length change during walking (**A**) and running (**B**) for downhill (-10% - blue), level (0% - green) and uphill (10% - red) conditions. The AT slack length is estimated from the average length of AT during walking on the level at the average time of toe-off. The estimated aponeurosis length change (which includes the proximal GM tendon) is calculated as the difference between the AT length change (relative to the slack length) and the SEE length change.

Muscle Work and Power Output

The length change of the muscle fascicle relative to the length change of the tendon during the stance phase for each condition is shown in Fig 6.6. The approximate force applied by the muscle fibres, calculated using the stretch of the AT and equations 3-5, is also shown. The length of the muscle fibres during the rise of force was different for each

condition. As grade increased for both gait types, the muscle fascicle length during force production increased. The muscle fibres were however shorter during force production in running than walking and developed force before heel contact. In all cases, force development was associated with little change in length of the muscle fibres and is hence isometric during this period. Shortening of the fibres occurs during force decline in all conditions.

These plots represent a work loop of the muscle fibres and the area under this work loop during the stance phase for each condition (relative to the maximum isometric force and resting muscle fascicle length) is shown in Table 6.1 along with the power output for the stance phase. The greatest amount of work was done during walking and running on the level, whilst there was substantially less work done during walking downhill. Walking and running uphill resulted in less work of GM muscle fibres and the muscle fibres also generated less power than during the level condition. Greater power was generated during running compared to walking.

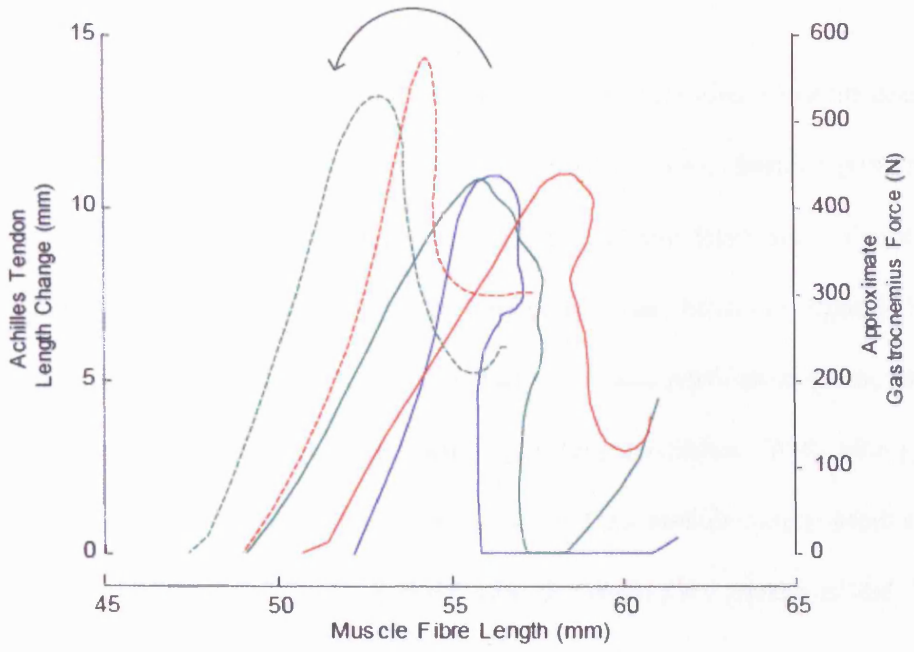

Figure 6.6

Average work loops for walking (solid) and running (dotted) during downhill (-10% - blue), level (0% - green) and uphill (10% - red) conditions during the stance phase of the gait cycle. Approximate GM fascicle force is calculated using equations 3-5.

Table 6.1

Average maximum GM muscle-tendon unit (MTU) velocity, maximum muscle fascicle velocity, relative work output (PoLo & J) and relative power output (PoLo/s & W) for the stance cycle for each condition. Po (Fmax) = 1200N, Lo (Resting Muscle Fibre Length) = 60mm.

	Walking (-10%)	Walking (0%)	Walking (+10%)	Running (0%)	Running (+10%)
Max MTU Velocity (Lo/s)	5.68	6.34	6.16	10.55	12.30
Max Fibre Velocity (Lo/s)	1.61	1.34	1.65	2.26	3.74
Muscle Fibre Work (PoLo)	0.029	0.059	0.055	0.060	0.054
Muscle Fibre Work (J)	2.09	4.25	3.96	4.32	3.89
Muscle Fibre Power (PoLo/s)	0.049	0.097	0.087	0.201	0.189
Muscle Fibre Power (W)	3.53	6.98	6.26	14.47	13.61

Discussion

The results of this study have shown that the human GM muscle power output does not necessarily mirror the requirement for external mechanical work. Similar power was produced by the GM fibres during walking and running on the level than is produced during uphill conditions. The power output of this muscle was however greater during running than walking. During downhill walking, less work was performed by the muscle fibres and hence the power output was reduced in this condition. With changes in locomotion conditions, there was a change in how the GM muscle fibres produce the power required, particularly the length and velocity at which they produced the forces required to support and propel the body during stance phase.

Mechanical function of the GM muscle in different conditions

Here I have demonstrated that when the MTU trajectory changes with change in grade and gait (speed), the muscle fascicle length trajectory also changes. In particular the length of the muscle fibres during force development varied as a function of grade and gait. As has previously been demonstrated, the muscle fibres act relatively isometrically during the stance phase of walking (Fukunaga *et al.*, 2001), and shorten during the stance phase of running (as demonstrated in Chapter 4). However, here I have found that there is an increase in muscle fascicle length associated with the increase in grade. This is likely to be due to the increase in whole MTU length occurring as a result of the increased dorsi-flexion throughout stance. The force-length properties of the muscle fascicle, including the contribution of parallel elastic elements, may therefore be important in determining the muscle power output.

The rate of energy storage in the Achilles tendon also varied between grade conditions. In both gaits, the Achilles tendon length was longer during the first half of the stance phase for the uphill condition compared to the level condition. This may be

associated with the requirement to produce positive propulsive forces in the horizontal direction, rather than braking forces during this period (Gottschall and Kram, 2005). This is associated with a requirement for the muscle to be activated more during this period so as to actively extend the elastic tissues. Alternatively the difference may just be a consequence of the slope changing foot angle and causing the MTU to be longer during uphill conditions and hence recruiting more parallel elastic structures and increasing the passive force. Interestingly, the length change of the SEE varies little with change of grade in both walking and running, compared to the AT length change. This maybe because the contribution to Achilles tendon length change (and hence force) is not consistent between muscles across the different grade conditions, i.e. the three muscles of the *triceps surae* are contributing different amounts to the total AT force depending on gait conditions.

In all conditions the Achilles tendon strain and hence force is developed with very little change in muscle fascicle length; the contractile element acts almost isometrically. This is both energetically efficient and is also advantageous in being able to produce high forces (Roberts, 2002). In all conditions it is apparent that the muscle produced most of the work during deactivation of the muscle (when the EMG signal strength begins to fall). During this period the muscle fibres shortened as the elastic tissues (Achilles tendon and aponeurosis) recoiled to shorten the whole muscle. The rate of muscle fascicle shortening increased with an increase in speed, however the rate of shortening was typically around 25-30% of the total MTU shortening speed. Therefore the elastic recoil of the tendon and aponeurosis contributes most of the MTU shortening.

Most of the work done by the muscle fibres was done during deactivation, when the elastic tissues were also recoiling and doing the majority of the work of the MTU. This raises the question as to why the muscles don't deactivate at a faster rate, remain

isometric, and allow the tendon to do all of the work whilst recoiling. Perhaps if the muscle were to relax too fast then the high forces would stretch the muscle and absorb some of the work of the whole MTU, which is an inefficient manner to perform whole muscle work. Also, perhaps the muscle must be able to maintain a short length during the swing phase so as to ensure foot clearance, and therefore the muscle fibres must be at a shorter length. Alternatively, this may be an efficient way to perform muscular work (Woledge *et al.*, 1985) or perhaps the neuromuscular system is unable to control such a precise method of deactivation.

During walking there was an increase in the muscle activation level (based on EMG) with an increase in inclination. However there was not an increase in muscle fascicle work or in the maximum force developed. Throughout the stance phase, however, the muscle fibres act at a longer length during force development as inclination increases. Therefore, perhaps the muscle moves along the descending limb of the force length curve here and requires more activation to produce the required force and stretch the Achilles tendon. However this is probably unlikely due to the effect of parallel elasticity. Alternatively, the muscle fibres also contract at a higher velocity in the uphill conditions which would require a higher activation to achieve the same force according to the force-velocity relationship of muscle. In contrast to walking, the running conditions showed a higher activation but this level was very similar between grade conditions. Again, the muscle fascicle lengths were much shorter and the contraction velocities were greater uphill running condition. However in the uphill condition there was a decrease in the amount of work performed by the muscle and the activation level may reflect this. The differences in activation level may also be due to variations the force sharing between the other muscles of the *triceps surae* (Arndt *et al.*, 1998).

During both walking and running there was some force developed in the Achilles tendon during the swing phase. During walking this occured during periods of inactivity in the GM muscle and is likely to be due to parallel elastic structures, other muscles or measurement errors in this portion of the stride (probe rotations etc). However in the running condition, where greater strain was developed and maintained throughout the heel contact period, the GM was co-activated with an antagonist, the *tibialis anterior*. This suggests that there is indeed some requirement for tension to be developed in the AT during foot contact. This may act to stabilise the ankle joint for impact with the ground. Activating the GM muscle before foot strike also alters the length of the muscle fascicle in preparation for force development during stance, and may optimise the length of the muscle for force production during stance.

Strategies for changing whole body mechanical work

Here I have shown that the power output of the biarticular GM muscle does not necessarily mirror that of the whole body, particularly when discussing the extra work required to facilitate uphill locomotion. During steady state locomotion on the level, the requirement for whole body work is zero across the period of a stride, however here I have demonstrated that the GM muscle does positive work even when travelling downhill. This is in contrast to the findings of Galaldon and colleagues (2004), who found that the work output of the *gastrocnemius lateralis* and *peroneous longus* muscles of the turkey more closely resemble that of the whole body work output. Perhaps the role of the human GM is dissimilar to that of the muscles examined in the turkey.

The *triceps surae* muscle group consists of two biarticular (*gastrocnemius*) muscles and one monoarticular (*soleus*) muscle attached to one common tendon; the Achilles tendon. During uphill running, where the power requirement of the whole body is greater than on the level, it is possible that the soleus contributes a greater proportion of

the power required than during level running. During uphill running, the results indicate that the GM muscle contributes less work with a similar activation level (from the EMG recordings) than in the level condition. Therefore the extra mechanical work required may come from the monoarticular soleus muscle. Previous research has suggested that whole body mechanical work is modulated by changing muscle recruitment rather than individual muscle function (Carlson-Kuhta *et al.*, 1998; Kaya *et al.*, 2003). Particularly, the relationship between the activation of the soleus of the cat has been shown to be influenced by contractile conditions such as length and velocity of the muscle and the relationship between activation of this muscle and the GM may vary depending on the MTU length trajectory (Kaya *et al.*, 2003).

In my estimates of muscle fascicle force, I have assumed that the three muscles of the triceps surae contribute a constant proportion to the whole tendon force based on their individual PCSA. This may not however be the case, and the contribution to whole tendon force may vary with difference conditions (as mentioned above). Direct measures of AT strain suggest that indeed the strain distribution of the muscles attaching to the tendon may not be equal and can cause differential strain patterns in the tendon (Finni *et al.*, 2003; Arndt *et al.*, 1998). Therefore the estimates of muscle fascicle work and power output may not represent the action of the fibres to the full extent and muscle recruitment may be critical in modulating whole body mechanical work and maintaining postural stability.

Previously it has been suggested that the primary function of biarticular muscles with opposite actions at each joint, such as the GM, is to transfer energy from the more powerful and proximal muscles of the knee and hip and hence may not be required to produce large amounts of work (Bobbert and Ingen Schenau, 1988; Neptune *et al.*, 2004). However the action at both joints must be considered in examining the amount of energy

that can be transferred. It has recently been demonstrated in human running, that although the maximum plantar flexion ankle joint moment does not vary between level and uphill running, the knee extensor moment actually decreases when running uphill (Roberts and Belliveau, 2005). Therefore the GM, which acts as a knee flexor, may produce less force in counteracting the knee extensors during uphill running.

This study has also demonstrated the importance of strain of other elastic tissues (e.g. aponeurosis) in producing muscular force. The large difference between the strain of the AT and the calculated SEE length (Fig 6.5) demonstrates that other tissues must be stretching. This has been shown experimentally by Magnusson and colleagues (2003), who have demonstrated that the aponeurosis strain is significant, although it appears to be stiffer than the AT. Hof and co-workers (1998) have also argued that series elastic tissue such as the aponeurosis may be selectively recruited based on muscle activation levels and that this may alter the entire stiffness of the elastic component. In essence, if fascicles act in parallel and each is attached to some elastic aponeurosis, only the elastic tissue that is attached to activated muscle fascicles will be recruited. This again would influence our estimations of fascicle force, work and power output. However, aponeurosis consists of a complex architecture to which muscle fascicles attach. As such it may be thought to act in both series *and* in parallel with the muscle fascicles which makes analysis of these length changes difficult and beyond the scope of this investigation.

Conclusions

In conclusion, the interaction of the GM muscle with the Achilles tendon and other elastic tissues varies with both gait and grade of inclination. Force is typically developed isometrically and work is done by the fibres during force decline, however the fascicle length at which force is developed varies with incline due to the change in force requirements and the change in whole MTU length trajectory resulting from kinematic

changes. To achieve this pattern of muscle contraction, the AT and other elastic elements are strained substantially, which allows the muscle fibres to act at velocities that maximise power output of the muscle. My results also indicate that the GM produces the most power in level walking and running conditions, which may be a result of the requirement for force production at both the knee and ankle or due to a change in force sharing between the three muscles of the *triceps surae*.

Chapter 7: Efficiency of the human gastrocnemius muscle: Effects of gait conditions and tendon compliance.

Under different gait and incline conditions, I have shown that the work and power output of the *gastrocnemius medialis* (GM) varies. However, in earlier chapters I was able to make a distinct connection between power output of muscle fibres and efficiency of those fibres by an understanding of how the contractile element interacts with the series elastic elements. Although at the whole muscle tendon unit level there are many levels of complexity, particularly in addressing the many levels where elasticity resides in both series and parallel with muscle fibres, the fundamental principles of muscle energetics from the fibre level will still apply at the muscle fascicle level. Hence it is possible to make some inference into how the muscle's efficiency may vary under these conditions where power output is changing. In this Chapter, I will use data from Chapter 6 and attempt to extrapolate further the active contractile element length changes from the passive and apply the energetic model described in Chapter 2 to make inference into the changes in efficiency under different gait conditions. I will also use this model to attempt to find an optimal stiffness of the series elastic component.

Introduction

Muscles are capable of producing force and power under a range of contraction conditions. However there is a relatively narrow range of contraction conditions where a muscle can produce near maximum power output and also maintain a high efficiency (Woledge *et al.*, 1985; Alexander, 1997). Therefore during cyclical movements such as locomotion, it is reasonable to suggest that a muscle might operate within such boundaries to optimise its power output and efficiency. If power output required by a

muscle is changed, however, are activation conditions adopted that achieve a near optimum efficiency or is the increased requirement for power detrimental to the efficiency of that muscle?

Recent studies have shown that during both human and turkey locomotion, the compliance of tendons and other series elastic elements (SEE) makes it possible for the muscle fibres to act at speeds more favourable for maximum power output and efficiency (Roberts, 2002; Lichtwark and Wilson, 2005). Muscles are however required to perform versatile actions, which require them to work across a range of contraction lengths and velocities. Subsequently, the instantaneous maximum power output and efficiency of the muscle is affected by the role of the muscle fibres in any movement. During locomotion under different conditions, such as at different speeds, grades and accelerations, it is necessary to modulate the power output of individual muscles to match the task (Gabaldon *et al.*, 2004) and hence efficiency may be compromised as a result.

I have previously demonstrated that during force development in the human *gastrocnemius medialis* (GM) in both walking and running, muscle fibres act relatively isometrically and thus produce very little work. During force decline the muscle fibres shorten and hence produce work during the period of elastic recoil of the tendon and aponeurosis. Therefore the periods of activation are accompanied with little shortening whilst the periods of fastest shortening occur during deactivation. A similar finding has been found in other anti-gravity muscles of a variety of animals (Griffiths, 1991; Roberts *et al.*, 1997). This pattern of work production is efficient because shortening occurs with lower activations (Woledge *et al.*, 1985).

The interaction between muscle fibres and the elastic tissues is crucial to determining muscle efficiency (Biewener and Roberts, 2000; Lichtwark and Wilson, 2005). Activation level, force output and length change trajectories of the muscle vary

under different gait conditions, therefore it is likely that the efficiency of a muscle will also change. Here I will apply the energetic model of muscle contraction described in Chapter 2, to muscle data collected under different gait conditions to determine the effect on muscle efficiency. I hypothesise that the efficiency of a muscle will vary little because the compliance of the Achilles tendon will allow the GM muscle fibres to continue to act at near optimal velocities under these changing conditions.

If the compliance of the elastic tissues is varied, one must change the way a muscle activates and subsequently shortens so that the required force output can be achieved (Ettema, 2001; Lichtwark and Wilson, 2005). I hypothesise that the series elastic tissues of the GM muscle have a compliance which allows the muscle to operate with optimal efficiency during normal walking and running. To test this hypothesis I will apply my muscle model to the experimental data to determine how varying the compliance of the elastic tissues (Achilles tendon and aponeurosis) would influence the efficiency of the GM muscle during locomotion.

Materials and Methods

Experimental Data

Average muscle fascicle length, Achilles tendon (AT) length and whole muscle tendon unit (MTU) length changes during a complete stride of level treadmill walking (5km/h) and running (10km/h) were accessed from Chapter 6. Walking conditions included grades of -10, 0 and +10% and running included 0 and +10%. The average data were taken across three strides from six male participants (data) for each condition. As in Chapter 6, the average force in the muscle during the stride was estimated from the strain of the Achilles tendon and the proportion of the Achilles tendon force assumed to be acting through the GM (15.4% of total force) (Fukunaga *et al.*, 1992).

Model of Muscle Efficiency

In Chapter 2, I showed that the heat produced by a muscle is highly dependent on the active state of the muscle and also on the length and shortening speed of the muscle (Fenn, 1924; Hill, 1938; Woledge, 1998). Therefore these states must all be considered in examining the relationship between power output of a muscle and its efficiency. Although my definition of efficiency is largely dependent on the work done by the muscle, it does not necessarily imply that the work done is useful in terms of external work done by the muscle-tendon unit.

Here I have applied a simplified version of the muscle model that predicts energy expenditure to the experimental data. However in this model, I will neglect the time dependent components of labile heat (excess heat associated with initial activation of a muscle that reduces exponentially with time). This is a reasonable simplification because during cyclical contractions the labile heat produced throughout each contraction should be relatively constant. Instead, I define the maintenance heat rate as follows –

$$\frac{dH_M}{dt} = \frac{1.4 \cdot V_{Max}}{G^2}$$

where dH_M / dt is the maintenance heat rate, V_{max} is the maximum shortening velocity of the muscle fibres and G describes the curvature of the force-velocity relationship (Woledge *et al.*, 1985). The constant value of 1.4 was chosen to represent a mean value of labile heat produced in a contraction (where labile heat can be as much as two to three times the maintenance heat initially in a contraction but decays exponentially to zero over a period of seconds (Aubert, 1956).

The relationship between velocity and force, power, heat rate and instantaneous efficiency at different activation levels (and optimum muscle length) from the current model is shown in Fig 7.1A-D. During lengthening (negative shortening velocity), muscle power output and efficiency are both negative. The current model also incorporated an

active force length relationship (Fig 7.1E) which is implemented into the energetic model of muscle contraction as described in Chapter 2.

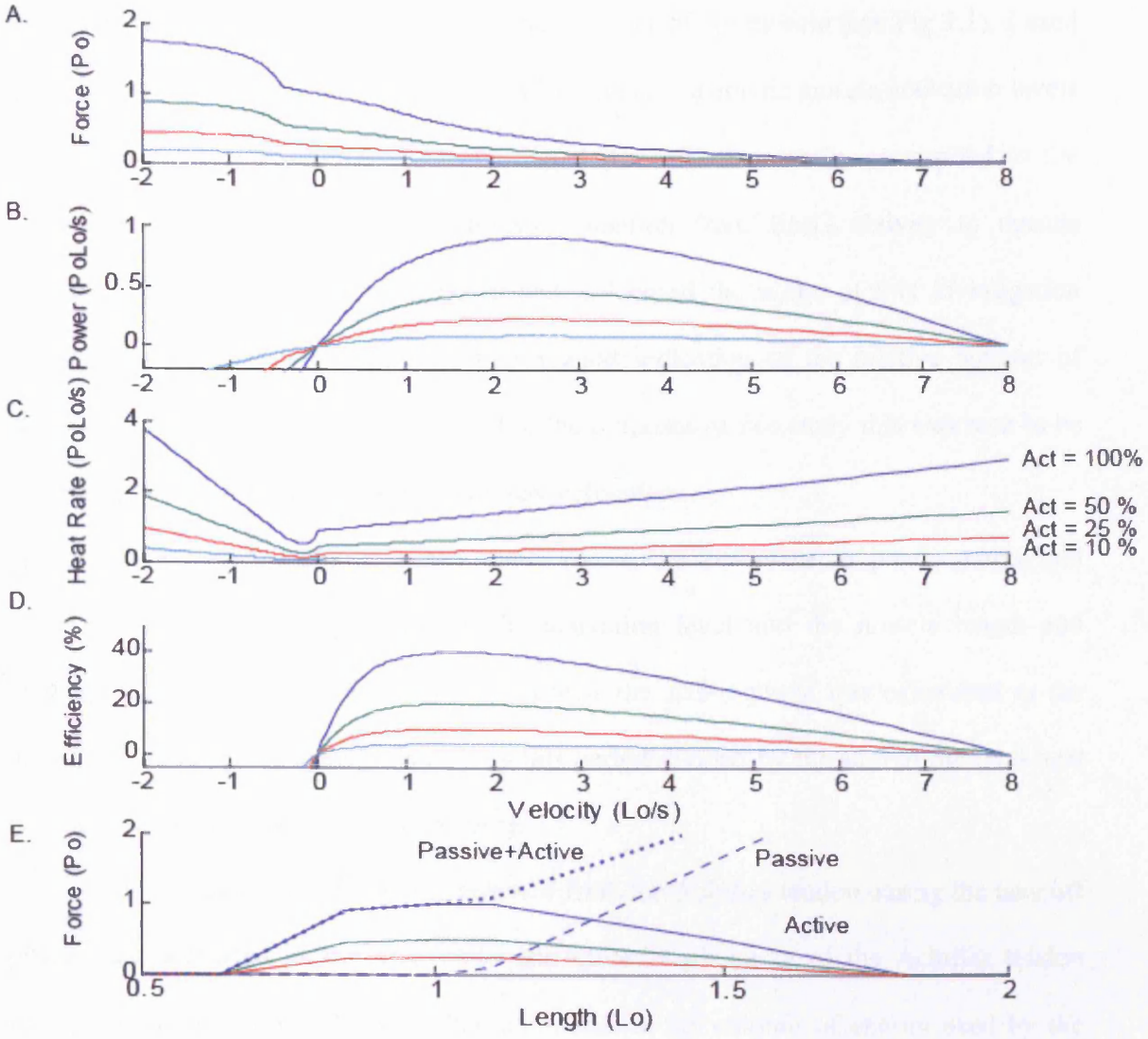

Figure 7.1

Modelled relationship between muscle fascicle velocity and force (**A**), power (**B**), heat rate (**C**) and efficiency (**D**) for a muscle with a maximum muscle fascicle velocity of 8 Lo/s. This relationship is scaled linearly with activation and activation levels of 100% (blue), 50% (green), 25% (red) and 10% (cyan) are shown. The force-velocity relationship is adapted from Curtin and Woledge (1998) and the heat-rate relationship adapted from Chapter 2. The relationship between force and muscle fascicle length (**E**) contains an active force length component (solid line) and a passive (dashed line) component which sum to give the overall force-length relationship (dotted line).

The model of muscle energetics requires an input of muscle activation. This activation level represents the number of bound cross-bridges and scales both the rate of heat production and the maximum isometric capacity of the muscle (see Fig 7.1). I used average enveloped electromyographic (EMG) signals to estimate muscle activation levels for each condition. Although the EMG signal does not necessarily correspond to the instantaneous activation level, the transfer function from EMG activity to muscle activation level in the GM is unknown and is beyond the scope of this investigation (Zajac, 1989). EMG does however give a good indication of the relative amount of activation between different conditions. For the purposes of this study this was seen to be the most practical method to estimate muscle activation.

Throughout the course of the stance phase, the instantaneous power output and efficiency will change depending on the activation level and the muscle length and velocity. Total muscle fascicle efficiency across the stance phase was calculated as the total work done by the muscle fascicle in this period divided by the sum of the total heat produced in this period and the work done.

The amount of elastic energy released from the Achilles tendon during the take off phase was calculated as the area under the force-length curve of the Achilles tendon during shortening only. This was then compared to the amount of energy used by the muscle fibres.

Modelling the effects of series elastic compliance on muscle efficiency

To model the effect that varying the series elastic stiffness might have on muscle efficiency, I calculated the SEE strain required to produce the muscle forces calculated to act on the GM fibres during level walking and running across a stiffness range of 0.25 to 4 times the measured stiffness of the Achilles tendon from Chapter 5 (~180 $N.mm^{-1}$). For instance, for the same muscle force the SEE must stretch twice as far if it has half the

stiffness. I have assumed that the GM contributes to 15.4% of the force straining the Achilles tendon at all times (Fukunaga *et al.*, 1992) Fig 7.2 shows the force-length relationship across the range of stiffness values.

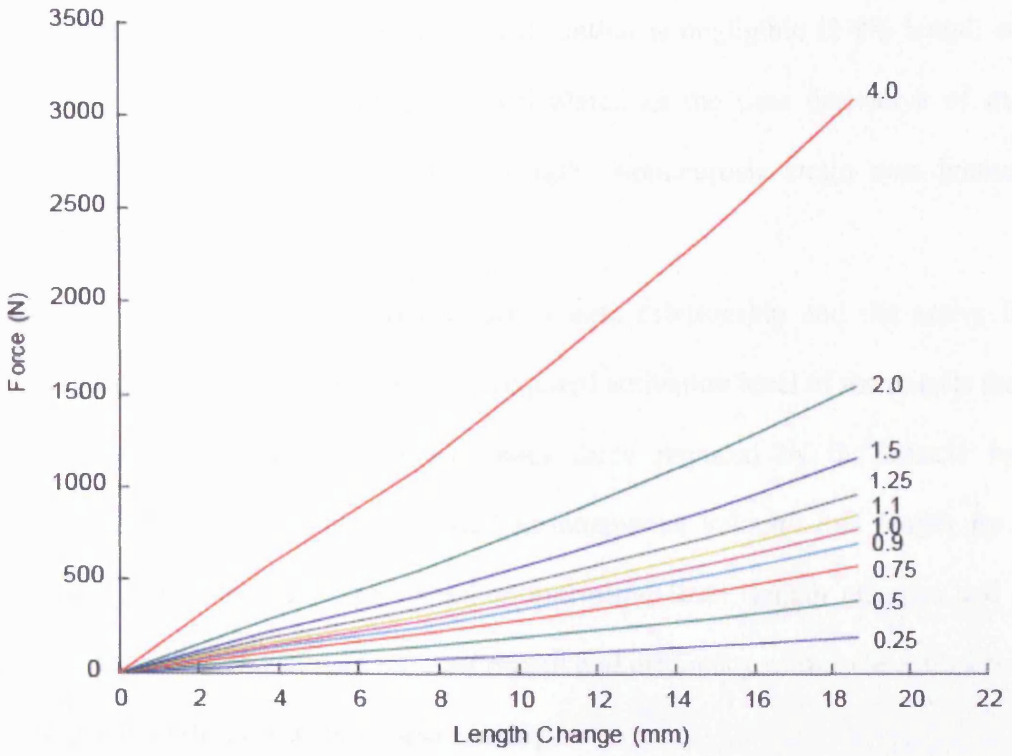

Figure 7.2

Force-length relationships for a stiffness range of 0.25 to 4 times the average measured Achilles tendon stiffness (180N.mm^{-1}). The measured Achilles tendon stiffness was scaled using the descending limb of the stress strain data from Chapter 5 and assuming a tendon CSA of 53 mm2 and a tendon slack length of 237 mm. The total force is scaled by 20 % to account only for the force applied by the GM.

The muscle was modelled as a 3-element Hill muscle model, with both a series and parallel elastic element. MTU resting length was assumed to be equal to the length of the contractile component (60 mm) plus the slack length (237 mm). Experimentally determined MTU strain was used to determine the modelled MTU length change

throughout the stance period. The difference between the MTU length and the predicted SEE length for each different tendon stiffness was calculated and this corresponded to the required muscle fascicle (contractile component) length. This calculation assumed that the muscle fibres act without pennation. According to the data from Chapter 6, pennation angles range between 10° and 25° throughout the stance phase, therefore the effect of pennation angle on muscle fascicle length calculation is negligible (2-9% length error). Normalised muscle fascicle velocity was calculated as the time derivative of muscle fascicle length normalised to its resting length. Aponeurosis strain was ignored to simplify the model.

Assuming an active plus passive force-length relationship and the active force-velocity relationship as shown in Fig 7.1, a required activation level of the muscle fascicle was estimated by dividing the instantaneous force required by the muscle by the maximum possible force at the estimated instantaneous velocity and length for each stiffness and each condition. The modelled activation level, length changes and force output were then used to estimate the heat output and efficiency of muscle contraction for each stiffness in both level walking and running.

Results

Muscle energetics and efficiency under varying locomotion conditions

The muscle fascicle force, fascicle length and muscle activation level and the estimated instantaneous heat and work output during the stance phase for gait each condition is shown in Fig 7.3. The total heat output was greater than the work output for all conditions in both walking and running. During running, less total heat was produced than that during uphill walking, whilst level and downhill walking appear to produce the least amounts of heat. However, the heat rate was highest during running, with peak heat rates of 0.62 PoLo/s (44 J/s) during level running compared to 0.35 PoLo/s (25 J/s) during

uphill walking. Walking produced the greatest heat rates in both gaits. During walking, total heat output increased with an increase in the grade. In contrast, the total heat output was similar during both level and incline running.

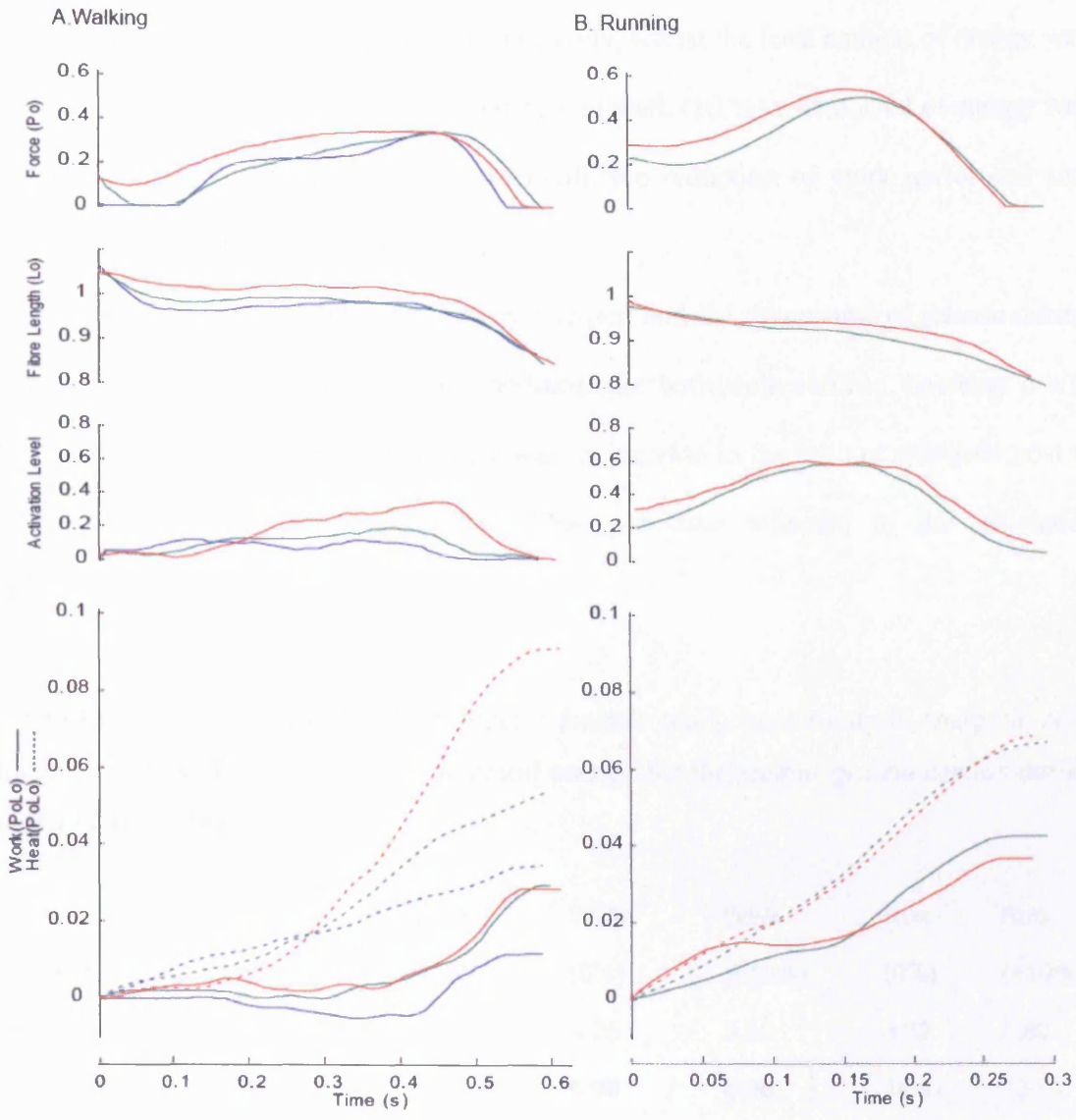

Figure 7.3

Average *medial gastrocnemius* muscle fascicle force, length and activation level for walking (**A**) and running (**B**) and the estimated work (solid line) and heat output (dotted line) calculated with the model for muscle energetics for downhill (-10 %, blue), level (0 %, green) and uphill (+10 %, red) treadmill walking. Heat is expressed relative to

maximum isometric force (1200N) x muscle fascicle length (60mm), where 1 PoLo = 72 J.

The relationship between muscle fascicle work and the energetic cost of doing this work is shown in Table 7.1. Muscle fascicle efficiency was highest on the level grade (0 %) at 37 % and 34 % for walk and run respectively, whilst the least amount of energy was consumed during the stance phase of the downhill walk (10 %) where 3.4 J of energy was consumed. In both walking and running uphill, the reduction of work performed also corresponded to a decrease in efficiency.

The amount of elastic strain energy released and the timecourse of release during recoil of the tendon was similar in all conditions for both walk and run, however it was apparent that during walking uphill, there was an increase in the ratio of energetic cost to elastic strain energy stored (Fig 7.4). This was also reflected in the efficiency calculations.

Table 7.1

Effect of gait and grade of incline on muscle fascicle work, power output, energetic cost, efficiency and Achilles tendon elastic recoil energy for the *medial gastrocnemius* during the stance phase only.

Gait and Grade of Incline	Walk (-10%)	Walk (0%)	Walk (+10%)	Run (0%)	Run (+10%)
Muscle Fibre Work (J)	2.09	4.25	3.96	4.32	3.89
Muscle Fibre Power (W)	3.53	6.98	6.26	14.47	13.61
Energetic Cost (J)	3.38	6.12	8.57	7.78	7.56
Efficiency (%)	26.8	37.4	25.8	34.9	30.8
Elastic Recoil Energy (J)	10.86	10.69	10.95	15.99	18.63

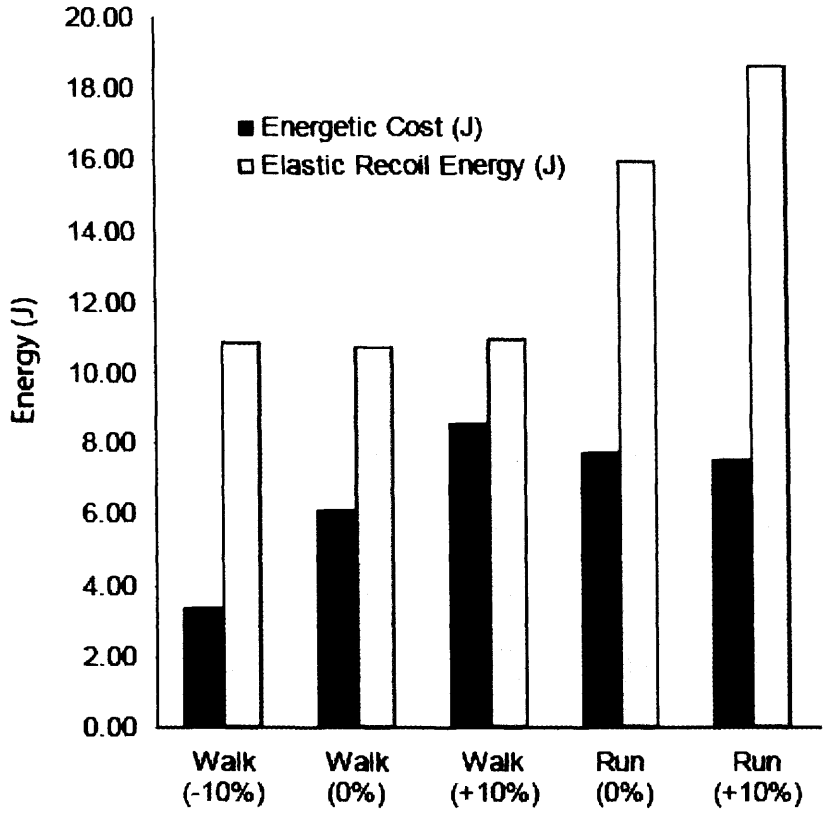

Figure 7.4

Average total Achilles tendon elastic recoil energy (grey) and *medial gastrocnemius* muscle fascicle energetic cost (heat + work, black) during the stance phase for different gaits conditions.

Muscle efficiency with varying series elastic stiffness

The model predictions for fascicle length trajectory, activation level and heat output for five different SEE stiffness values (0.25, 0.5, 1, 2 and 4 times the Achilles tendon stiffness) is shown in Fig 7.5. By varying the stiffness of the Achilles tendon the required shortening trajectory of the muscle fibres was altered substantially in both walking and running conditions. The stiffest condition (4 times the stiffness of the Achilles tendon) resulted in a muscle fascicle length change that resembles that of the MTU, as there was little length change of the SEE. In contrast, the most compliant SEE allowed muscle shortening to occur in both walking and running conditions. The length change therefore occurred in the SEE. The stiffness values that best resembled the fascicle length trajectory

measured experimentally (Fig 7.5) were in the range of 0.5-1.0 times the Achilles tendon stiffness.

The required activation levels at the lowest stiffness exceeded the maximum activation level (1.0) in both walking and running. During these periods the muscle fibres were at short lengths and needed high velocities (greater than V_{max}) which could not be achieved within the maximum activation level. During running, the higher stiffness values (above the Achilles tendon stiffness) also required a muscle activation level that exceeds the maximum level. During these periods, the muscle fibres are shortening at very high velocities.

The timing of peak muscle activation is altered with changes in SEE stiffness. The more compliant SEE require an early peak activation level, whilst the stiff SEE's require peak activation during the take-off phase when the MTU requires the highest shortening velocities. The activation levels that best represent those measured experimentally are obtained with a stiffness of 0.5 times the Achilles tendon stiffness in both walking and running.

The calculated heat output from the model suggests that during walking, the MTU with the most compliant SEE would produce the most heat, whilst all other conditions produce similar amounts of heat. During running, MTU's with stiffer SEE's (2 and 4 times Achilles tendon stiffness), produced the most heat across the stance phase.

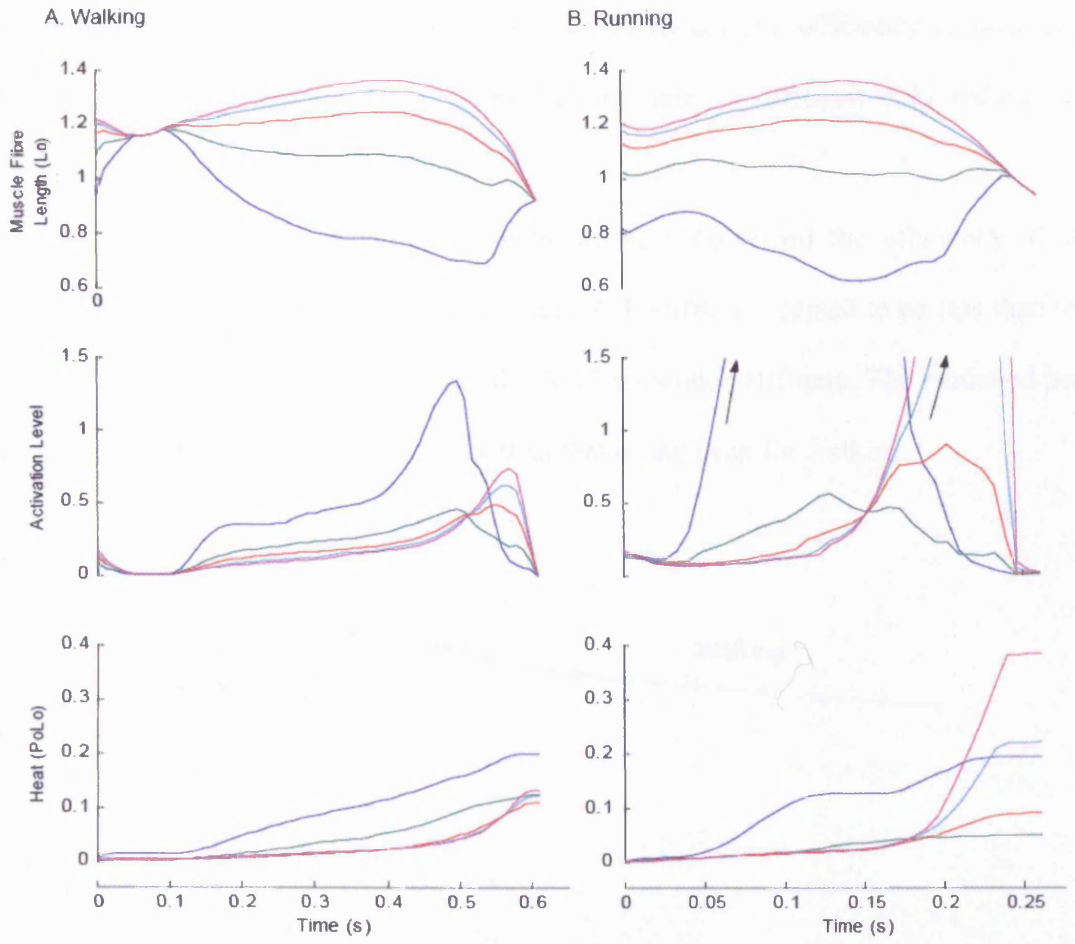

Figure 7.5

Modelled muscle fascicle length change, activation level and heat output required for walking (**A**) and running (**B**) with a series elastic element stiffness of 0.25 (blue), 0.5 (green), 1 (red), 2 (cyan) and 4 (pink) times the Achilles tendon stiffness. The muscle was modelled as a 3-element Hill muscle model, with a contractile component (optimum fascicle length of 60 mm), a series elastic element (slack length of 237 mm) and parallel elastic element (slack length of 60mm) with muscle properties from Fig 7.1. Heat output was estimated from the energetic model that was validated in Chapter 2 and muscle fascicle work is the same for each stiffness, therefore heat output is inversely proportional efficiency.

The relationship between SEE stiffness and efficiency is shown in Fig 7.6. It is apparent that during walking, the most efficient tendon stiffness was equivalent to the value measured experimentally in Chapter 5 (~180N.mm^{-1}). A more compliant SEE

(below 0.5 times Achilles tendon stiffness) would reduce the efficiency substantially, however higher stiffness (above 2 times Achilles tendon stiffness) only reduces the efficiency by 5%.

In contrast, during running a higher stiffness decreased the efficiency of the muscle fibres by more than 10%. The optimum SEE stiffness seemed to be less than that for walking, between 0.5 and 0.75 times the Achilles tendon stiffness. The modelled peak efficiency for running is also 7.5% lower than that of the peak for walking.

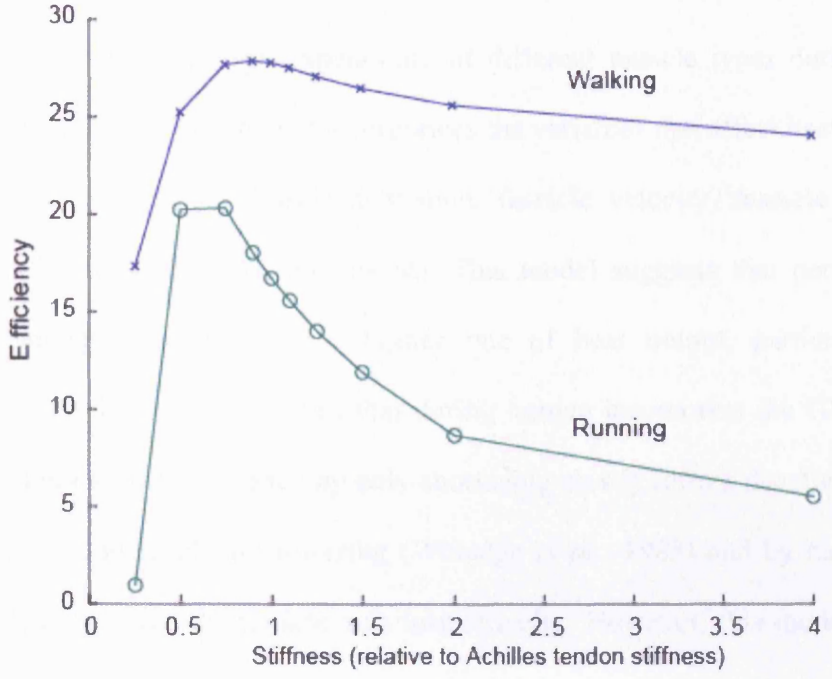

Figure 7.6

Modelled muscle fascicle efficiency for walking (5 km/h, blue) and running (10 km/h, green) on 0% incline across a range of SEE stiffness values (relative to the measured Achilles tendon in Chapter 5 – 180N.mm^{-1}).

Discussion

Muscle Power vs Efficiency

Here I have shown that with a change in the power output requirement of a muscle, there is also a change in the efficiency at which this muscle operates. Therefore, conditions exist in which a muscle can operate at its optimal efficiency. The results indicate that walking and running on level surfaces may be more energetically efficient than during both uphill and downhill running.

In the early chapters of this thesis, I developed a Hill-type muscle model to successfully estimate the energy expenditure of different muscle types during cyclical contractions (Chapter 2). This model incorporates the variables that affect heat production during muscular contraction: muscle activation, fascicle velocity, fascicle length and force produced (many of which are linked). This model suggests that periods of fast muscle shortening would produce a higher rate of heat output, particularly when activation is high. Therefore, it seems that during human locomotion the GM is indeed acting to maintain a high efficiency by only shortening slowly during deactivation (when the muscle activation levels are lowering (Woledge *et al.*, 1985) and by having higher levels of activation when the muscle acts isometrically. However, this model is a mere simplification which makes numerous assumptions about the linearity of force, power and efficiency with activation level and does not take into account that the MG is comprised of both fast and slow twitch fibres.

My data demonstrates that during the period of force decline, the rate of heat production changes very little from that of when the muscle is producing force. Hence when the muscle produces work at the end of the stance phase, there is very little change in the rate of heat production. However, the rate of heat production is highly dependent on the level of activation required to produce force, which is seen in the uphill walking

data where the activation level recorded with EMG is higher than other conditions, as is the total amount of heat produced.

There seems to be a higher level of heat production produced during the uphill walking compared to the level walking, despite very little difference in the predicted work output of the muscle fascicle. Therefore the efficiency of the muscle is lower during uphill walking compared to level walking. Perhaps this is due to variation in the contribution of the GM to total Achilles tendon force, as has previously been suggested (Arndt *et al.*, 1998). Here I have assumed that the GM contributes a constant 20% of the total force in the tendon. However in uphill walking the gastrocnemius may contribute more to the total muscle force, and hence it is required to activate more. If this were to be the case, then the GM muscle would be doing more work than I have estimated, however the heat calculations would remain relatively unchanged. Therefore the muscle efficiency may actually be higher in these conditions than predicted.

Experimental and modelling work have shown that humans and other animals choose to walk and run at speeds and grades that minimise whole body energy expenditure with respect to the work being done during locomotion (Minetti and Alexander, 1997; Hoyt and Taylor, 1981; Alexander, 2003; Minetti *et al.*, 2002). Perhaps the conditions for optimal GM efficiency are equivalent to those speeds (and slopes) where humans and other animals have been found to prefer to walk or run. My results suggest that level locomotion is indeed the most efficient and that there is a difference in efficiency between walking and running. Future studies might focus on a larger range of speeds and grades of incline, to determine whether optimal conditions for GM efficiency correspond to those of overall walking and running efficiency.

In all cases it is apparent that the muscle maintains a relatively high efficiency, despite performing different roles. The inclusion of a compliant Achilles tendon and

aponeurosis contributes to this. Fig 7.4 shows that the total energetic cost of the muscle contraction during stance is substantially smaller than that recovered from elastic recoil of the tendon. This supports the data of Roberts (1997), who suggested that 60% of the work done by a muscle tendon unit could be accounted for by elastic recoil. However, here I have shown that the energetic cost (not just muscle fascicle work) can increase depending on the gait conditions and how the muscle fibres interact with the attached tendons.

Elastic Effects on Efficiency

Using a simplified model of muscle contraction to model the effects of varying the compliance in the SEE of the GM, I have demonstrated that an optimal value exists to optimise muscle fascicle efficiency in different conditions. Varying the tendon compliance changes the required shortening pattern of the muscle fibres, and hence the energetics are greatly affected. The optimal value for stiffness in my model was equal to or slightly less than that previously measured for the Achilles tendon alone (Chapter 5) for both walking and running. However, differences in the optimal value for SEE stiffness were found to occur depending on the gait, and this result suggests that the SEE stiffness may affect the conditions under which an individual performs best.

During the walking gait, when overall MTU muscle shortening velocities are smaller than running, it is apparent that a high efficiency can be achieved across a range of stiffness values for the SEE. Only lower compliance values seem detrimental to the efficiency due to the high shortening velocity achieved whilst stretching the tendon to long lengths during force production. However, the importance of a more compliant tendon was more evident in the modelled running data, where SEE compliance above 1.25 times the Achilles tendon stiffness is unfavourable. Perhaps further studies could examine the effect of running at faster speeds and determine the optimal value for tendon stiffness in these conditions.

During the running gait then it seems that a more compliant SEE is required than that measured from the Achilles tendon to achieve maximum efficiency. However, the current muscle model did not include any additional source of series elasticity such as aponeurosis. Aponeurosis has been shown to contribute substantially to elastic strain energy (Magnusson *et al.*, 2001; Maganaris *et al.*, 2001), and I have shown, in Chapter 6, that during locomotion the aponeurosis is required to strain to achieve the measured muscle fascicle shortening. If two springs are placed in series, the equation for the overall stiffness for two springs in stiffness is as follows –

$$k_{eff} = \left(\frac{k_1 \cdot k_2}{k_1 + k_2} \right)$$

where k_{eff} is the effective stiffness, and k_1 and k_2 are the stiffness values for the two springs. Therefore having the Achilles tendon in series with a compliant aponeurosis will result in a reduced absolute stiffness. It is likely then that the SEE stiffness is less than that of the Achilles tendon and is somewhere closer to the value for optimum efficiency during running.

This reduction of the absolute stiffness due to the series effect of these two elastic tissues has been shown experimentally by Magnusson and colleagues (2003). That study showed that the aponeurosis of the GM has a higher stiffness than the free Achilles tendon and hence the SEE stiffness should be confined to 0.5 -1.0 times the Achilles tendon stiffness, which is the range for optimal efficiency for both walking and running. An opposite effect has been found in the *tibialis anterior* muscle (Maganaris and Paul, 2000b), however two elastic elements in series will always reduce the stiffness of the entire MTU. It has also been suggested that the amount the SEE stiffness can be varied by changing the activation level and hence the amount of aponeurosis that is strained (Hof, 1998). Therefore perhaps during walking and running, where the activation levels vary

substantially, the stiffness of the SEE can be adjusted to optimise efficiency of the muscle fibres further. This may also account for the difference in maximum efficiency predicted with the model between walking and running, which is less evident in the experimental results.

It has been previously shown by myself, and other investigators (Maganaris and Paul, 2002), that the structural properties of tendons can vary substantially between individuals, as can the force generating capacity of a muscle and the architecture of the muscle (Ichinose *et al.*, 1998; Fukunaga *et al.*, 2001; Kawakami *et al.*, 1998). Therefore the way a muscle interacts with the tendon will also change depending on architecture. Recent studies have suggested that Achilles tendon may be stiffer for people with greater muscle strength (Muraoka *et al.*, 2005) and hence the current model could be used to determine how muscle strength and tendon stiffness variations might affect muscle efficiency. However to perform such a study, one must also obtain better estimates of the force-length and force-velocity properties of muscle and the distribution of activation. In the current model, estimates commonly used in musculoskeletal models have been used, however these relationships may vary greatly amongst individuals, particularly when taking into account fascicle type and architecture differences.

The model predicts that to optimise muscle fascicle efficiency, an appropriate SEE stiffness must exist such that the muscle fibres can act relatively isometrically (walking) or shorten slightly (running). This is the result obtained from the experimental results and hence the simplified model of muscle contraction is a good tool for investigating muscle-tendon architecture. Also, it is encouraging that the muscle fascicle activation at the optimal SEE stiffness for walking and running resemble the estimated activation level from recorded EMG. However, further investigations into how muscle fascicle pennation

angle and aponeurosis strain affect muscle force, length and contraction efficiency are required.

Conclusion

In conclusion, we have demonstrated that muscles act at high values of efficiency by contracting at speeds which favour high efficiency and deactivating during periods of shortening. With changes in gait type and gait conditions, there seemed to be a change in the efficiency of muscles, suggesting that optimal conditions for locomotion do exist (zero incline conditions being demonstrated as optimal in this case). The compliant SEE structures provided much of the energy required during MTU shortening, however changing the properties of these structures would also affect the efficiency of a muscle greatly, with different optimal values for SEE during walking compared to running. We suggest that selective recruitment of SEE structures such as aponeurosis with changes in muscle activation can adjust the stiffness of the tendon and perhaps optimise muscle efficiency.

Chapter 8: Discussion and Conclusions

The results from the series of studies presented here have demonstrated the importance of elastic elements in producing normal muscle function. In addition, they have shown how both the theoretical and the real-life muscle tendon unit interactions affect both the power output and efficiency of muscle during movement. Briefly, I have shown that efficiency of a muscle can be determined through thorough measurements of muscular contraction and can then be applied to data collected from real-life movements. I have demonstrated that the effect of series elasticity largely influences the function of the contractile components and that this may increase both the power production capabilities and the efficiency of muscle as a whole. This can benefit the role of muscles in roles where the muscle both produces and absorbs work.

The role of muscle tendon unit elasticity in real life movements

The primary subject area of this thesis was concerned with how tendon and muscle elasticity affects the function of the contractile component (CC) of muscle during real-life movements. A series elastic element (SEE), even at the single fibre level, has been demonstrated to uncouple the length changes of the contractile component of muscle from that of the muscle and elastic tissue complex. In this way, I have demonstrated that a compliant tendon can be activated during lengthening to produce both optimal work and optimal power. My modelling research has shown however, that the activation conditions that achieve optimal power and efficiency differ and there is a complex relationship between muscle fibre power output and efficiency as a result.

These results have wide ranging implications for both control of movement and also development of muscle architecture. Although compliant tendons might benefit animals energetically by providing a mechanism for inexpensive rapid shortening, this requires activation during stretching of the muscle and therefore is best suited to muscles

which typically work against inertial loads, such as the anti-gravity and postural muscles. Here I have examined such a muscle, the *gastrocnemius medialis* (GM), but there are many muscles that are typically used for controlled movements that don't necessarily activate in this manner. For instance, many muscles of upper extremity are typically used for controlled and precise pointing movements where large amounts of SEE compliance might be detrimental to accuracy performance (Rack and Ross, 1984), and hence muscle power output and efficiency may not be the primary goal. Future studies might indeed examine how SEE compliance might influence control of movement and quantifying the relative compliance in these muscles. In addition, long term studies on how training and aging affect muscle tendon unit interaction and architecture would be valuable in understanding muscle function how the body optimises its structure for function.

A major result of this study was that during uphill walking and running, the power output of the GM did not increase from that of the level condition, however the muscle efficiency decreased. From these results, it was difficult to determine whether the reduction in GM muscle work relative to the stance time was a direct consequence of a reduction in muscle efficiency during these conditions, or whether there are other control issues which prevent the muscle from producing more power. The interaction between the bi-articular *gastrocnemius* muscle group the mono-articular *soleus*, and the load sharing between these muscles is key to understanding this problem. Indeed, this interaction between muscle groups may have influenced the measurements of muscle power output made here, as I have assumed a constant load sharing between the muscles. It is very difficult to distinguish how muscles share loads experimentally, however recent evidence suggests that there is differential strain along the tendon resulting from contributions of these muscle (Arndt *et al.*, 1998). These techniques of determining differential tendon strain along the length of the tendon may help us further understand the dynamics of

Achilles tendon and the interaction between the muscles of the *triceps surae* muscle group.

It was also suggested that perhaps the total series elasticity of a muscle might be able to be altered with different levels of activation. This suggestion was first suggested by Hof and colleagues (1998), whose measurements on SEE stiffness suggested that varying activation levels of the muscle might indeed correspond to variations in the compliance. My calculations suggest that the optimal tendon stiffness for walking and running vary, however walking muscle efficiency changed little except at very low stiffness values. The mechanism by which a muscle might change its overall SEE stiffness is yet to be fully explored, although the recruitment of aponeurosis is the likely candidate. In this thesis, I have suggested that aponeurosis strain (used as a collective term for all elastic structures that are not the Achilles tendon) could be estimated from difference between whole muscle length change, Achilles tendon length change and muscle fascicle length changes. Future studies might explore how this value of aponeurosis strain varies with different levels of muscle activation. However, thorough analysis should explore how the aponeurosis strains in three-dimensions to better understand this phenomenon.

Modelling muscle power and efficiency

The initial work from this thesis focussed on determining the relationship between power output and efficiency and determining if I can predict the heat and energy output of a muscle during dynamic contractions. I found that by applying the relationships between muscle lengthening rate and activation to heat output, that a reasonable prediction of efficiency of muscle could be made on a variety of muscle types. This type of model is of value to researchers in the field of both biomechanics and muscle physiology. The model allows us to use measurable muscle properties such as muscle fibre length (as done in this

thesis), and make reasonable estimations of muscle efficiency. It also provides criteria for modelling studies where the primary objective is to maximise efficiency (Anderson and Pandy, 2001).

Using such a model I was able to predict how variations in the SEE stiffness would affect the activation pattern of the muscle and also the maximum power output and efficiency (Chapter 3). In addition, in Chapter 7, I was able to apply this to experimental data to show efficiency might be influenced with varying tendon stiffness during walking and running. Although it is difficult to verify this data experimentally, similar simulations of the potential interaction between a muscle and its elastic elements and the influence this has on both movement and energetic consumption could be used to plan surgical or pharmacological interventions for patients with musculskeletal disorders (eg. Cerebral palsy). For instance forward dynamics simulations may be used to explore how varying the contractile or elastic properties affect the control of limb movement.

I also demonstrated that the relative stiffness of tendons varies across both species and also across different functional roles within the same species. Although I have been able to use a model to predict the effect that this has on both power output and efficiency of muscle for varying activation conditions, this approach is yet to be validated experimentally. Perhaps future experiments might try and artificially vary the series elastic stiffness on the same muscle type to determine whether or not the model predictions hold true under these conditions. If this is the case, then the modelling approach would provide for a powerful way to study muscle dynamics and energetics under different conditions.

However, as was discussed, the predictive powers of muscle models are susceptible to errors due to phenomenon not included in the model or not fully understood in the current literature. These included the phenomenon of shortening deactivation and

other possible history effects. The heat output resulting from these phenomenon are yet to be fully examined, although experimental work investigating the heat output during active lengthening does suggest that the model may need to be revised to account for increased heat rates (Linari *et al.*, 2003). However, my experimental results which focussed on a muscle that attaches to a compliant tendon, suggest that these types of muscles rarely actively lengthen, and therefore in these models this may be less critical. This may be due to complex control that would be required by the central nervous system to control such a muscular action (Rack and Ross, 1984).

Ultrasound: Limitations and future developments

Ultrasound, the key tool used here to assess muscle fascicle length changes *in vivo*, has been demonstrated to be a valuable tool for both physiological and biomechanical understanding of how muscles perform during movement. However, this tool is still in its infancy and further development may reduce its main limitations and drawbacks. For instance, currently measures of muscle fascicle length and also position of the muscle tendon junction is done manually and hence introduces a large degree of subjectivity. In the future, perhaps image analysis algorithms might be developed to automatically calculate muscle fascicle length and velocity trajectories. This may be achieved using cross-correlation techniques between images such that changes the image from one frame to the next might be statistically determined so that the relative motion of the image is assessed. The capture rate of the ultrasound might also be improved, as a rate of 25 Hz may not be fast enough to detect high speed fluctuations in fascicle length.

Ultrasound provides a relatively inexpensive and valuable tool for assessing musculoskeletal architecture and further development of techniques developed here are warranted. The technique used here to track the position and orientation of the ultrasound probe is analogous to other techniques which have been used to assess three dimensional

muscle architecture in both normal and spastic muscles (Fry *et al.*, 2004). Perhaps this technique might also be used to determine Achilles tendon architecture and particularly how this changes with contraction. As suggested in this thesis, the change in tendon shape may be key in understanding how large strains in the tendon are possible. However, this technique requires intensive computation to reconstruct muscle architecture. Instead, perhaps simple measures which assess only muscle and or tendon length might be adopted, whereby only the endpoints of these structures are measured (rather than combining a series of images).

Furthermore, the techniques applied here can be used to examine how MTU interaction varies with different musculoskeletal disorders such as muscle spasticity (resulting from disorders such as cerebral palsy, head trauma or spinal injury) or muscular dystrophy.

Recent advances in ultrasound technology has also made four dimensional ultrasound possible, where a three dimensional ultrasound volume is collected using a matrix ultrasound probe at consecutive time periods (up to 25 volumes per second). This advancement has great potential to better understand muscle contraction dynamics. One of the major limitations to the techniques used here is that images are restricted to one plane, whilst muscle fibres are likely to be moving in and out of this plane due to the change in three dimensional shape of the muscle during contraction. Currently, very little research has been able to successfully explain how a muscles shape change affects its function. Although some complex muscle modelling approaches have attempted to explain this (Van Leeuwen and Spoor, 1992; Van Leeuwen and Spoor, 1993), there is no strong experimental evidence to support this. New four dimensional ultrasound techniques may be the solution, providing accurate enough volumes could be collected.

This might also provide a technique to examine aponeurosis strain in three-dimensions as suggested earlier.

Conclusions

This thesis has demonstrated the mechanism by which different muscle types act to both produce and absorb work by interacting with series elastic elements. This interaction allows muscles to act with high efficiencies, although this is influenced by the power requirement of the muscle and function of the muscle during the movement performed. In the future, further research should be focussed on determining how muscles that perform different functions vary in material properties and architecture, how movement is controlled and force shared between muscles, how three-dimensional structure affects muscle performance and how ultrasound can be used as a tool to further understand muscle mechanics and energetics.

References

Abbot, B. C. and Aubert, X. M. (1952). The force exerted by active striated muscle during and after change of length. *J.Physiol* **117**, 77-86.

Alexander, R. M. (1974). The mechanics of jumping of a dog (*Canis familiaris*). *J.Zool.Lond.* **173**, 549-573.

Alexander, R. M. (1997). Optimum Muscle Design for Oscillatory Movements. *J.Theor.Biol.* 253-259.

Alexander, R. M. (2002). Tendon elasticity and muscle function. *Comp Biochem.Physiol A Mol.Integr.Physiol* **133**, 1001-1011.

Alexander, R. M. (1988). *Elastic mechanisms in animal movement* . Cambridge: Cambridge University Press.

Alexander, R. M. (2003). Principle of Animal Locomotion. pp. 101-145. Princeton, NJ: Princeton University Press.

Anderson, F. C. and Pandy, M. G. (2001). Static and dynamic optimization solutions for gait are practically equivalent. *J.Biomech.* **34**, 153-161.

Arndt, A. N., Komi, P. V., Bruggemann, G. P., and Lukkariniemi, J. (1998). Individual muscle contributions to the in vivo achilles tendon force. *Clin.Biomech.(Bristol., Avon.)* **13**, 532-541.

Askew, G. N. and Marsh, R. L. (1997). The effects of length trajectory on the mechanical power output of mouse skeletal muscles. *J.Exp.Biol.* **200**, 3119-3131.

Askew, G. N. and Marsh, R. L. (2001). The mechanical power output of the pectoralis muscle of blue-breasted quail (Coturnix chinensis): the in vivo length cycle and its implications for muscle performance. *J.Exp.Biol.* **204**, 3587-3600.

Askew, G. N. and Marsh, R. L. (2002). Muscle designed for maximum short-term power output: quail flight muscle. *J.Exp.Biol.* **205**, 2153-2160.

Aubert, X. (1956). *"Le Couplage Energetique de la Contraction Musculaire"* . Brussels: Arscia.

Barclay, C. J. (1994). Efficiency of fast- and slow-twitch muscles of the mouse performing cyclic contractions. *J.Exp.Biol.* **193**, 65-78.

Baylor, S. M. and Hollingworth, S. (1998). Model of sarcomeric Ca2+ movements, including ATP Ca2+ binding and diffusion, during activation of frog skeletal muscle. *J.Gen.Physiol* **112**, 297-316.

Bennett, M. B., Ker, R. F., Dimery, N. J., and Alexander, R. M. (1986). Mechanical properties of various mammalian tendons. *J.Zool.Lond* 537-548.

Biewener, A. A. (1998). Muscle-tendon stresses and elastic energy storage during locomotion in the horse. *Comp Biochem.Physiol B Biochem.Mol.Biol.* **120**, 73-87.

Biewener, A. A., Konieczynski, D. D., and Baudinette, R. V. (1998). In vivo muscle force-length behavior during steady-speed hopping in tammar wallabies. *J.Exp.Biol.* **201**, 1681-1694.

Biewener, A. A. and Roberts, T. J. (2000). Muscle and tendon contributions to force, work, and elastic energy savings: a comparative perspective. *Exerc.Sport Sci.Rev.* **28**, 99-107.

Bobbert, M. F., Huijing, P. A., and Ingen Schenau, G. J. (1986). An estimation of power output and work done by the human triceps surae muscle-tendon complex in jumping. *J.Biomech.* **19**, 899-906.

Bobbert, M. F. and Ingen Schenau, G. J. (1988). Coordination in vertical jumping. *J.Biomech.* **21**, 249-262.

Brown, N. A., Kawcak, C. E., McIlwraith, C. W., and Pandy, M. G. (2003). Architectural properties of distal forelimb muscles in horses, Equus caballus. *J.Morphol.* **258**, 106-114.

Buchanan, C. I. and Marsh, R. L. (2001). Effects of long-term exercise on the biomechanical properties of the Achilles tendon of guinea fowl. *J.Appl.Physiol* **90**, 164-171.

Carlson-Kuhta, P., Trank, T. V., and Smith, J. L. (1998). Forms of forward quadrupedal locomotion. II. A comparison of posture, hindlimb kinematics, and motor patterns for upslope and level walking. *J.Neurophysiol.* **79**, 1687-1701.

Cavagna, G. A. (1979). Force platforms as ergometers. *J.Appl.Physiol* **39**, 174-179.

Cavagna, G. A., Heglund, N. C., and Taylor, C. R. (1977). Mechanical work in terrestrial locomotion: two basic mechanisms for minimizing energy expenditure. *Am.J.Physiol* **233**, R243-R261.

Curtin, N. and Woledge, R. (1996). Power at the expense of efficiency in contraction of white muscle fibres from dogfish Scyliorhinus canicula. *J.Exp.Biol.* **199**, 593-601.

Curtin, N. A., Gardner-Medwin, A. R., and Woledge, R. C. (1998). Predictions of the time course of force and power output by dogfish white muscle fibres during brief tetani. *J.Exp.Biol.* **201 (Pt 1)**, 103-114.

De Zee, M. and Voigt, M. (2001). Moment dependency of the series elastic stiffness in the human plantar flexors measured in vivo. *J.Biomech.* **34**, 1399-1406.

Edman, K. A. (1979). The velocity of unloaded shortening and its relation to sarcomere length and isometric force in vertebrate muscle fibres. *J.Physiol* **291**, 143-159.

Edman, K. A., Elzinga, G., and Noble, M. I. (1978). Enhancement of mechanical performance by stretch during tetanic contractions of vertebrate skeletal muscle fibres. *J.Physiol* **281**, 139-155.

Epstein, M. and Herzog, W. (1998). *Theoretical Models of Skeletal Muscle* . Chichester: John Wiley & Sons.

Ettema, G. J. (1996a). Elastic and length-force characteristics of the gastrocnemius of the hopping mouse (Notomys alexis) and the rat (Rattus norvegicus). *J.Exp.Biol.* **199**, 1277-1285.

Ettema, G. J. (1996b). Mechanical efficiency and efficiency of storage and release of series elastic energy in skeletal muscle during stretch-shorten cycles. *J.Exp.Biol.* **199**, 1983-1997.

Ettema, G. J. (2001). Muscle efficiency: the controversial role of elasticity and mechanical energy conversion in stretch-shortening cycles. *Eur.J.Appl.Physiol* **85**, 457-465.

Ettema, G. J. and Huijing, P. A. (1989). Properties of the tendinous structures and series elastic component of EDL muscle-tendon complex of the rat. *J.Biomech.* **22**, 1209-1215.

Farley, C. T., Glasheen, J., and McMahon, T. A. (1993). Running springs: speed and animal size. *J.Exp.Biol.* **185**, 71-86.

Fenn, W. O. (1924). The relation between the work performed and the energy liberated in muscular contraction. *J.Physiol* **58**, 373-395.

Finni, T., Hodgson, J. A., Lai, A. M., Edgerton, V. R., and Sinha, S. (2003). Nonuniform strain of human soleus aponeurosis-tendon complex during submaximal voluntary contractions in vivo. *J.Appl.Physiol* **95**, 829-837.

Fry, N. R., Gough, M., and Shortland, A. P. (2004). Three-dimensional realisation of muscle morphology and architecture using ultrasound. *Gait.Posture.* **20**, 177-182.

Fukunaga, T., Kawakami, Y., Kubo, K., and Kanehisa, H. (2002). Muscle and tendon interaction during human movements. *Exerc.Sport Sci.Rev.* **30**, 106-110.

Fukunaga, T., Kubo, K., Kawakami, Y., Fukashiro, S., Kanehisa, H., and Maganaris, C. N. (2001). In vivo behaviour of human muscle tendon during walking. *Proc.R.Soc.Lond B Biol.Sci.* **268**, 229-233.

Fukunaga, T., Kubo, K., Kawakami, Y., and Kanehisa, H. (2000). Effect of elastic tendon properties on the performance of stretch-shortening cycles. In: *Skeletal Muscle Mechanics: From Mechanisms to Function* (ed. Herzog, W.), pp. 289-303. Chichester: John Wiley & Sons.

Fukunaga, T., Roy, R. R., Shellock, F. G., Hodgson, J. A., Day, M. K., Lee, P. L., Kwong-Fu, H., and Edgerton, V. R. (1992). Physiological cross-sectional area of human leg muscles based on magnetic resonance imaging. *J.Orthop.Res.* **10**, 928-934.

Gabaldon, A. M., Nelson, F. E., and Roberts, T. J. (2004). Mechanical function of two ankle extensors in wild turkeys: shifts from energy production to energy absorption during incline versus decline running. *J.Exp.Biol.* **207**, 2277-2288.

Galantis, A. and Woledge, R. C. (2003). The theoretical limits to the power output of a muscle-tendon complex with inertial and gravitational loads. *Proc.R.Soc.Lond B Biol.Sci.* **270**, 1493-1498.

Gordon, A. M., Huxley, A. F., and Julian, F. J. (1966). The variation in isometric tension with sarcomere length in vertebrate muscle fibres. *J.Physiol* **184**, 170-192.

Gottschall, J. S. and Kram, R. (2005). Ground reaction forces during downhill and uphill running. *J.Biomech.* **38**, 445-452.

Grieve, D. W., Pheasant, S., and Cavanagh, P. R. (1978). Preduction of gastrocnemius length from knee and ankle joint posture. In: *Biomechanics*, vol. VI-A (eds. Asmussen, E. and Jorgensen, K.), pp. 405-412. Baltimore: University Park Press.

Griffiths, R. I. (1991). Shortening of muscle fibres during stretch of the active cat medial gastrocnemius muscle: the role of tendon compliance. *J.Physiol* **436**, 219-236.

Herzog, W., Leonard, T. R., Renaud, J. M., Wallace, J., Chaki, G., and Bornemisza, S. (1992b). Force-length properties and functional demands of cat gastrocnemius, soleus and plantaris muscles. *J.Biomech.* **25**, 1329-1335.

Herzog, W., Leonard, T. R., Renaud, J. M., Wallace, J., Chaki, G., and Bornemisza, S. (1992a). Force-length properties and functional demands of cat gastrocnemius, soleus and plantaris muscles. *J.Biomech.* **25**, 1329-1335.

Hill, A. V. (1938). The heat of shortening and the dynamic constants of muscle. *Proc.R.Soc.Lond B Biol.Sci.* **126**, 136-195.

Hill, A. V. (1949). The abrupt transition from rest to activity in muscle. *Proc.R.Soc.Lond Ser.B.* **136**, 399.

Hof, A. L. (1998). In vivo measurement of the series elasticity release curve of human triceps surae muscle. *J.Biomech.* **31**, 793-800.

Hof, A. L. (2003). Muscle mechanics and neuromuscular control. *J.Biomech.* **36**, 1031-1038.

Hof, A. L., Elzinga, H., Grimmius, W., and Halbertsma, J. P. (2002a). Speed dependence of averaged EMG profiles in walking. *Gait.Posture.* **16**, 78-86.

Hof, A. L., van Zandwijk, J. P., and Bobbert, M. F. (2002b). Mechanics of human triceps surae muscle in walking, running and jumping. *Acta Physiol Scand.* **174**, 17-30.

Hoyt, C. R. and Taylor, C. R. (1981). Gait and energetics of locomotion in horses. *Nature* **292**, 239-240.

Huxley, A. F. (1957). Muscle structure and theories of contraction. *Prog.Biophys.Biophys.Chem.* **7**, 255-318.

Ichinose, Y., Kanehisa, H., Ito, M., Kawakami, Y., and Fukunaga, T. (1998). Relationship between muscle fiber pennation and force generation capability in Olympic athletes. *Int.J.Sports Med.* **19**, 541-546.

Ishikawa, M., Komi, P. V., Grey, M. J., Lepola, V., and Bruggemann, G. P. (2005a). Muscle-tendon interaction and elastic energy usage in human walking. *J.Appl.Physiol* **99**, 603-608.

Ishikawa, M., Niemela, E., and Komi, P. V. (2005b). Interaction between fascicle and tendinous tissues in short-contact stretch-shortening cycle exercise with varying eccentric intensities. *J.Appl.Physiol* **99**, 217-223.

Josephson, R. K. (1999). Dissecting muscle power output. *J.Exp.Biol.* **202 Pt 23**, 3369-3375.

Kawakami, Y., Ichinose, Y., and Fukunaga, T. (1998). Architectural and functional features of human triceps surae muscles during contraction. *J.Appl.Physiol* **85**, 398-404.

Kawakami, Y., Muraoka, T., Ito, S., Kanehisa, H., and Fukunaga, T. (2002). In vivo muscle fibre behaviour during counter-movement exercise in humans reveals a significant role for tendon elasticity. *J.Physiol* **540**, 635-646.

Kaya, M., Leonard, T., and Herzog, W. (2003). Coordination of medial gastrocnemius and soleus forces during cat locomotion. *J.Exp.Biol.* **206**, 3645-3655.

Ker, R. F., Alexander, R. M., and Bennett, M. B. (1988). Why are mamallian tendons so think? *J.Zool.Lond.* **216**, 309-324.

Ker, R. F., Bennett, M. B., Bibby, S. R., Kester, R. C., and Alexander, R. M. (1987). The spring in the arch of the human foot. *Nature* **325**, 147-149.

Ker, R. F., Dimery, N. J., and Alexander, R. M. (1986). The role of tendon elasticity in a hopping wallaby (Macropus rufogriseus). *J.Zool.Lond* 417.

Ker, R. F., Wang, X. T., and Pike, A. V. (2000). Fatigue quality of mammalian tendons. *J.Exp.Biol.* **203**, 1317-1327.

Komi, P. V. (1990). Relevance of in vivo force measurements to human biomechanics. *J.Biomech.* **23 Suppl 1**, 23-34.

Koob, T. J. and Summers, A. P. (2002). Tendon--bridging the gap. *Comp Biochem.Physiol A Mol.Integr.Physiol* **133**, 905-909.

Kubo, K., Akima, H., Kouzaki, M., Ito, M., Kawakami, Y., Kanehisa, H., and Fukunaga, T. (2000). Changes in the elastic properties of tendon structures following 20 days bed-rest in humans. *Eur.J.Appl.Physiol* **83**, 463-468.

Kubo, K., Kanehisa, H., and Fukunaga, T. (2003). Gender differences in the viscoelastic properties of tendon structures. *Eur.J.Appl.Physiol* **88**, 520-526.

Kubo, K., Kanehisa, H., and Fukunaga, T. (2005). Comparison of elasticity of human tendon and aponeurosis in knee extensors and ankle plantar flexors in vivo. *J.Appl.Biomech.* **21**, 129-142.

Kubo, K., Kawakami, Y., Kanehisa, H., and Fukunaga, T. (2002). Measurement of viscoelastic properties of tendon structures in vivo. *Scand.J.Med.Sci.Sports* **12**, 3-8.

Leach, J. K., Priola, D. V., Grimes, L. A., and Skipper, B. J. (1999). Shortening deactivation of cardiac muscle: physiological mechanisms and clinical implications. *J.Investig.Med.* **47**, 369-377.

Lichtwark, G. A. and Wilson, A. M. (2005). Effects of series elasticity and activation conditions on muscle power output and efficiency. *J.Exp.Biol.* ***Accepted.***

Lieber, R. L., Brown, C. G., and Trestik, C. L. (1992). Model of muscle-tendon interaction during frog semitendinosis fixed-end contractions. *J.Biomech.* **25**, 421-428.

Linari, M., Woledge, R. C., and Curtin, N. A. (2003). Energy storage during stretch of active single fibres from frog skeletal muscle. *J.Physiol* **548**, 461-474.

Lou, F., Curtin, N., and Woledge, R. (1997). The energetic cost of activation of white muscle fibres from the dogfish Scyliorhinus canicula. *J.Exp.Biol.* **200**, 495-501.

Lutz, G. J. and Rome, L. C. (1994). Built for jumping: the design of the frog muscular system. *Science* **263**, 370-372.

Lyman, J., Weinhold, P. S., and Almekinders, L. C. (2004). Strain behavior of the distal achilles tendon: implications for insertional achilles tendinopathy. *Am.J.Sports Med.* **32**, 457-461.

Maas, H., Jaspers, R. T., Baan, G. C., and Huijing, P. A. (2003). Myofascial force transmission between a single muscle head and adjacent tissues: length effects of head III of rat EDL. *J.Appl.Physiol* **95**, 2004-2013.

Maganaris, C. N. (2002). Tensile properties of in vivo human tendinous tissue. *J.Biomech.* **35**, 1019-1027.

Maganaris, C. N., Baltzopoulos, V., and Sargeant, A. J. (1998). In vivo measurements of the triceps surae complex architecture in man: implications for muscle function. *J.Physiol* **512 (Pt 2)**, 603-614.

Maganaris, C. N., Kawakami, Y., and Fukunaga, T. (2001). Changes in aponeurotic dimensions upon muscle shortening: in vivo observations in man. *J.Anat.* **199**, 449-456.

Maganaris, C. N., Narici, M. V., and Reeves, N. D. (2004). In vivo human tendon mechanical properties: effect of resistance training in old age. *J.Musculoskelet.Neuronal.Interact.* **4**, 204-208.

Maganaris, C. N. and Paul, J. P. (2000a). Hysteresis measurements in intact human tendon. *J.Biomech.* **33**, 1723-1727.

Maganaris, C. N. and Paul, J. P. (2000b). Load-elongation characteristics of in vivo human tendon and aponeurosis. *J.Exp.Biol.* **203 Pt 4**, 751-756.

Maganaris, C. N. and Paul, J. P. (2002). Tensile properties of the in vivo human gastrocnemius tendon. *J.Biomech.* **35**, 1639-1646.

Magnusson, S. P., Aagaard, P., Dyhre-Poulsen, P., and Kjaer, M. (2001). Load-displacement properties of the human triceps surae aponeurosis in vivo. *J.Physiol* **531**, 277-288.

Magnusson, S. P., Hansen, P., Aagaard, P., Brond, J., Dyhre-Poulsen, P., Bojsen-Moller, J., and Kjaer, M. (2003). Differential strain patterns of the human gastrocnemius aponeurosis and free tendon, in vivo. *Acta Physiol Scand.* **177**, 185-195.

Mai, M. T. and Lieber, R. L. (1990). A model of semitendinosus muscle sarcomere length, knee and hip joint interaction in the frog hindlimb. *J.Biomech.* **23**, 271-279.

Minetti, A. E. and Alexander, R. M. (1997). A theory of metabolic costs for bipedal gaits. *J.Theor.Biol.* **186**, 467-476.

Minetti, A. E., Moia, C., Roi, G. S., Susta, D., and Ferretti, G. (2002). Energy cost of walking and running at extreme uphill and downhill slopes. *J.Appl.Physiol* **93**, 1039-1046.

Muramatsu, T., Muraoka, T., Kawakami, Y., and Fukunaga, T. (2002a). Superficial aponeurosis of human gastrocnemius is elongated during contraction: implications for modeling muscle-tendon unit. *J.Biomech.* **35**, 217-223.

Muramatsu, T., Muraoka, T., Kawakami, Y., Shibayama, A., and Fukunaga, T. (2002b). In vivo determination of fascicle curvature in contracting human skeletal muscles. *J.Appl.Physiol* **92**, 129-134.

Muramatsu, T., Muraoka, T., Takeshita, D., Kawakami, Y., Hirano, Y., and Fukunaga, T. (2001). Mechanical properties of tendon and aponeurosis of human gastrocnemius muscle in vivo. *J.Appl.Physiol* **90**, 1671-1678.

Muraoka, T., Muramatsu, T., Fukunaga, T., and Kanehisa, H. (2005). Elastic properties of human Achilles tendon are correlated to muscle strength. *J.Appl.Physiol* **99**, 665-669.

Narici, M. (1999). Human skeletal muscle architecture studied in vivo by non-invasive imaging techniques: functional significance and applications. *J.Electromyogr.Kinesiol.* **9**, 97-103.

Narici, M. V., Binzoni, T., Hiltbrand, E., Fasel, J., Terrier, F., and Cerretelli, P. (1996). In vivo human gastrocnemius architecture with changing joint angle at rest and during graded isometric contraction. *J.Physiol* **496 (Pt 1)**, 287-297.

Neptune, R. R., Zajac, F. E., and Kautz, S. A. (2004). Muscle force redistributes segmental power for body progression during walking. *Gait.Posture.* **19**, 194-205.

Novacheck, T. F. (1998). The biomechanics of running. *Gait.Posture.* **7**, 77-95.

Otten, E. (1988). Concepts and models of functional architecture in skeletal muscle. *Exerc.Sport Sci.Rev.* **16**, 89-137.

Pappas, G. P., Asakawa, D. S., Delp, S. L., Zajac, F. E., and Drace, J. E. (2002). Nonuniform shortening in the biceps brachii during elbow flexion. *J.Appl.Physiol* **92**, 2381-2389.

Plagenhoef, S., Evans, F. G., and Abdelnour, T. (1983). Anatomical Data for Analysing Human Motion. *Research Quaterly for Excersie and Sport* 169-178.

Pollock, C. M. and Shadwick, R. E. (1994). Relationship between body mass and biomechanical properties of limb tendons in adult mammals. *Am.J.Physiol* **266**, R1016-R1021.

Rack, P. M. and Ross, H. F. (1984). The tendon of flexor pollicis longus: its effects on the muscular control of force and position at the human thumb. *J.Physiol* **351**, 99-110.

Rack, P. M., Ross, H. F., Thilmann, A. F., and Walters, D. K. (1983). Reflex responses at the human ankle: the importance of tendon compliance. *J.Physiol* **344**, 503-524.

Reeves, N. D., Narici, M. V., and Maganaris, C. N. (2003). Strength training alters the viscoelastic properties of tendons in elderly humans. *Muscle Nerve* **28**, 74-81.

Roberts, T. J. (2002). The integrated function of muscles and tendons during locomotion. *Comp Biochem.Physiol A Mol.Integr.Physiol* **133**, 1087-1099.

Roberts, T. J. and Belliveau, R. A. (2005). Sources of mechanical power for uphill running in humans. *J.Exp.Biol.* **208**, 1963-1970.

Roberts, T. J., Marsh, R. L., Weyand, P. G., and Taylor, C. R. (1997). Muscular force in running turkeys: the economy of minimizing work. *Science* **275**, 1113-1115.

Roberts, T. J. and Scales, J. A. (2002). Mechanical power output during running accelerations in wild turkeys. *J.Exp.Biol.* **205**, 1485-1494.

Roberts, T. J. and Scales, J. A. (2004). Adjusting muscle function to demand: joint work during acceleration in wild turkeys. *J.Exp.Biol.* **207**, 4165-4174.

Ruiter, C. J., Didden, W. J., Jones, D. A., and Haan, A. D. (2000). The force-velocity relationship of human adductor pollicis muscle during stretch and the effects of fatigue. *J.Physiol* **526 Pt 3**, 671-681.

Scott, S. H., Engstrom, C. M., and Loeb, G. E. (1993). Morphometry of human thigh muscles. Determination of fascicle architecture by magnetic resonance imaging. *J.Anat.* **182 (Pt 2)**, 249-257.

Scott, S. H. and Loeb, G. E. (1995). Mechanical properties of aponeurosis and tendon of the cat soleus muscle during whole-muscle isometric contractions. *J.Morphol.* **224**, 73-86.

Smith, C. W., Young, I. S., and Kearney, J. N. (1996). Mechanical properties of tendons: changes with sterilization and preservation. *J.Biomech.Eng* **118**, 56-61.

Sugi, H. and Tsuchiya, T. (1988). Stiffness changes during enhancement and deficit of isometric force by slow length changes in frog skeletal muscle fibres. *J.Physiol* **407**, 215-229.

Taylor, C. R. and Heglund, N. C. (1982). Energetics and mechanics of terrestrial locomotion. *Annu.Rev.Physiol* **44**, 97-107.

Tobalske, B. W., Hedrick, T. L., Dial, K. P., and Biewener, A. A. (2003). Comparative power curves in bird flight. *Nature* **421**, 363-366.

Umberger, B. R., Gerritsen, K. G., and Martin, P. E. (2003). A model of human muscle energy expenditure. *Comput.Methods Biomech.Biomed.Engin.* **6**, 99-111.

Van Leeuwen, J. L. (1999). A mechanical analysis of myomere shape in fish. *J.Exp.Biol.* **202**, 3405-3414.

Van Leeuwen, J. L. and Spoor, C. W. (1992). Modelling mechanically stable muscle architectures. *Philos.Trans.R.Soc.Lond B Biol.Sci.* **336**, 275-292.

Van Leeuwen, J. L. and Spoor, C. W. (1993). Modelling the pressure and force equilibrium in unipennate muscles with in-line tendons. *Philos.Trans.R.Soc.Lond B Biol.Sci.* **342**, 321-333.

Wakeling, J. M. and Johnston, I. A. (1998). Muscle power output limits fast-start performance in fish. *J.Exp.Biol.* **201**, 1505-1526.

Wang, X. T. and Ker, R. F. (1995). Creep rupture of wallaby tail tendons. *J.Exp.Biol.* **198**, 831-845.

Wang, Y. and Kerrick, W. G. (2002). The off rate of Ca(2+) from troponin C is regulated by force-generating cross bridges in skeletal muscle. *J.Appl.Physiol* **92**, 2409-2418.

Webber, S. and Kriellaars, D. (1997). Neuromuscular factors contributing to in vivo eccentric moment generation. *J.Appl.Physiol* **83**, 40-45.

Westing, S. H., Seger, J. Y., Karlson, E., and Ekblom, B. (1988). Eccentric and concentric torque-velocity characteristics of the quadriceps femoris in man. *Eur.J.Appl.Physiol Occup.Physiol* **58**, 100-104.

Westing, S. H., Seger, J. Y., and Thorstensson, A. (1990). Effects of electrical stimulation on eccentric and concentric torque-velocity relationships during knee extension in man. *Acta Physiol Scand.* **140**, 17-22.

Wickiewicz, T. L., Roy, R. R., Powell, P. L., and Edgerton, V. R. (1983). Muscle architecture of the human lower limb. *Clin.Orthop.Relat Res.* 275-283.

Wilson, A. M. and Goodship, A. E. (1994). Exercise-induced hyperthermia as a possible mechanism for tendon degeneration. *J.Biomech.* **27**, 899-905.

Woittiez, R. D., Huijing, P. A., Boom, H. B., and Rozendal, R. H. (1984). A three-dimensional muscle model: a quantified relation between form and function of skeletal muscles. *J.Morphol.* **182**, 95-113.

Woledge, R. C. (1961). The thermoelastic effect of change of tension in active muscle. *J.Physiol (Paris)* **155**, 187-208.

Woledge, R. C. (1998). Muscle energetics during unfused tetanic contractions. Modelling the effects of series elasticity. *Adv.Exp.Med.Biol.* **453**, 537-543.

Woledge, R. C., Curtin, N. A., and Homsher, E. (1985). Energetic aspects of muscle contraction. *Monogr Physiol Soc.* **41**, 1-357.

Yucesoy, C. A., Koopman, B. H., Baan, G. C., Grootenboer, H. J., and Huijing, P. A. (2003). Effects of inter- and extramuscular myofascial force transmission on adjacent synergistic muscles: assessment by experiments and finite-element modeling. *J.Biomech.* **36**, 1797-1811.

Zajac, F. E. (1989). Muscle and tendon: properties, models, scaling, and application to biomechanics and motor control. *Crit Rev.Biomed.Eng* **17**, 359-411.

Zuurbier, C. J., Everard, A. J., van der, W. P., and Huijing, P. A. (1994). Length-force characteristics of the aponeurosis in the passive and active muscle condition and in the isolated condition. *J.Biomech.* **27**, 445-453.

Zuurbier, C. J. and Huijing, P. A. (1991). Influence of muscle shortening on the geometry of gastrocnemius medialis muscle of the rat. *Acta Anat.(Basel)* **140**, 297-303.

Zuurbier, C. J. and Huijing, P. A. (1992). Influence of muscle geometry on shortening speed of fibre, aponeurosis and muscle. *J.Biomech.* **25**, 1017-1026.

Zuurbier, C. J. and Huijing, P. A. (1993). Changes in geometry of actively shortening unipennate rat gastrocnemius muscle. *J.Morphol.* **218**, 167-180.